



SKA1 SYSTEM BASELINE DESIGN

Document number SKA-TEL-SKO-DD-001
Revision 1
Author P.E. Dewdney
Date 2013-03-12
Status Released

| Name | Designation | Affiliation | Date | Signature |
|--|------------------------------|-------------|---------------------|---|
| Owned by: | | | | |
| P. E. Dewdney | SKA Architect | SKA Office | Peter E. Dewdney | Digitally signed by Peter E. Dewdney DN: cn=Peter E. Dewdney, o=SKA Organisation, ou, email=dewdney@skatelescope.org, c=GB Date: 2013.03.12 07:50:17 Z |
| Additional Authors | | | | |
| W. Turner, R. Millenaar, R. McCool, J. Lazio, T. J. Cornwell | | | | |
| Approved by: | | | | |
| Joseph Lazio | Science Director (Acting) | SKA Office | | |
| | | | | |
| Released by: | | | | |
| P. Diamond | Director-General | SKA Office | | |



DOCUMENT HISTORY

| Revision | Date Of Issue | Engineering Change Number | Comments |
|-----------------|----------------------|----------------------------------|------------------|
| A | 2013Mar01 | - | Unreleased Draft |
| B | 2013-03-01 | - | Further updates |
| 1 | 2013-03-12 | - | Released for RfP |
| | | | |

DOCUMENT SOFTWARE

| | Package | Version | Filename |
|---------------|----------------|----------------|--|
| Wordprocessor | MsWord | Word 2007 | SKA-TEL-SKO-DD-001-1_BaselineDesign.docx |

ORGANISATION DETAILS

| | |
|-------------------------|--|
| Name | SKA Program Development Office |
| Physical/Postal Address | SKA Organisation Jodrell Bank Observatory Lower Withington Macclesfield Cheshire SK11 9DL |
| Fax. | +44 (0)161 275 4049 |
| Website | www.skatelescope.org |

TABLE OF CONTENTS

| | | |
|----------|--|-----------|
| 1 | INTRODUCTION..... | 10 |
| 1.1 | Science Motivation | 10 |
| 1.2 | Purpose of the document | 11 |
| 1.3 | Scope..... | 12 |
| 2 | TOP LEVEL DESCRIPTION OF THE SKA1 BASELINE DESIGN | 13 |
| 2.1 | SKA1-low | 14 |
| 2.2 | SKA1-mid..... | 15 |
| 2.3 | SKA1-survey | 16 |
| 2.4 | Comparative Performance..... | 19 |
| 3 | PROGRESSION TO SKA2 | 20 |
| 3.1 | SKA-low | 20 |
| 3.2 | SKA-mid..... | 20 |
| 3.3 | SKA-survey | 20 |
| 3.4 | AIP Technologies | 21 |
| 4 | DESIGN CONSIDERATIONS | 22 |
| 4.1 | Sky Noise | 23 |
| 4.2 | Confusion Limits..... | 23 |
| 4.3 | Science Data Processing Capabilities | 24 |
| 5 | GLOBAL ASSUMPTIONS | 25 |
| 6 | SKA1-LOW | 25 |
| 6.1 | Key Design Requirements and Parameters..... | 26 |
| 6.2 | Aspects of the Array Configuration..... | 27 |
| 6.3 | Antenna Elements..... | 28 |
| 6.4 | SKA1-low with Log-Periodic Dipoles | 29 |
| 6.5 | Element and Station Properties | 29 |
| 6.6 | Configuration | 29 |
| 6.7 | Performance | 30 |
| 6.8 | Centres of Array Configurations | 33 |
| 6.9 | Fit to the MRO/Boolardy Site..... | 33 |
| 6.10 | Front-end Amplifiers and Receiver Noise | 34 |
| 6.11 | Digital Data Back Haul..... | 34 |
| 6.12 | SKA1-low Central Signal Processor | 35 |
| 6.13 | SKA1-low Science Data Processing | 37 |
| 7 | REFLECTOR ANTENNAS | 37 |
| 7.1 | Receiver Cryo-cooling and Noise | 38 |

| | |
|--|-----------|
| 8 SKA1-MID..... | 39 |
| 8.1 Key Design Parameters | 39 |
| 8.2 Array Configuration..... | 40 |
| 8.3 Receiver Bands..... | 44 |
| 8.4 SKA1-mid Overall Performance | 47 |
| 8.5 Digital Data Back-Haul..... | 54 |
| 8.6 SKA1-mid Central Signal Processor | 55 |
| 8.7 SKA1- mid Science Data Processing | 62 |
| 9 SKA1-SURVEY | 63 |
| 9.1 Key Design Parameters | 63 |
| 9.2 Antennas | 64 |
| 9.3 Array Configuration..... | 64 |
| 9.4 PAF Receiver Bands..... | 68 |
| 9.5 SKA1-survey Overall Performance | 68 |
| 9.6 Digital Data Back-Haul..... | 74 |
| 9.7 SKA1-survey Central Signal Processor..... | 74 |
| 9.8 SKA1-survey Science Data Processing..... | 76 |
| 10 DATA TRANSPORT FROM CSP TO SDP CENTRES | 76 |
| 10.1 SKA1-low and SKA1-survey – Australian site | 76 |
| 10.2 SKA1-mid – South African site | 76 |
| 11 SYNCHRONISATION | 77 |
| 11.1 Timing..... | 77 |
| 12 TELESCOPE MANAGER..... | 78 |
| 13 DATA PRODUCTS | 78 |
| 14 RFI MANAGEMENT ON BOTH TELESCOPE SITES | 81 |
| 15 INFRASTRUCTURE IN AUSTRALIA..... | 81 |
| 15.1 On-or-Near Site | 81 |
| 15.2 Off-site Infrastructure | 84 |
| 16 INFRASTRUCTURE IN SOUTH AFRICA..... | 84 |
| 16.1 On-or-Near Site | 84 |
| 16.2 Off-site Infrastructure | 88 |
| 17 REFERENCES | 89 |
| APPENDIX A: DESIGN FORMULAE | 92 |
| 17.1 Log-Periodic Array Design Relationships | 92 |
| 17.2 Log-Periodic Array Tradeoffs | 92 |
| APPENDIX B: CSP EQUIPMENT SIZE AND POWER DISSIPATION..... | 95 |

LIST OF FIGURES

| | |
|--|----|
| Figure 1 A schematic diagram of the SKA Observatory, showing the geographical locations of site entities (telescopes), the entities at regional centres (Host Country Headquarters and Science Data Processing), and entities that are globally located (Global Headquarters)..... | 14 |
| Figure 2: Sky Noise Temperature vs frequency for low radio frequencies..... | 23 |
| Figure 3 Cumulative collecting area as a function of core radius in the SKA1-low array..... | 30 |
| Figure 4 The SKA1-low configuration in the core (35-m diameter stations)..... | 30 |
| Figure 5 Sensitivity (Ae/Tsys and brightness temperature), resolution, and field-of-view of the core array as a function of frequency for the arrays consisting of log-periodic elements..... | 32 |
| Figure 6 SKA1-low configuration of stations (white dots) on a Google Earth image. The red dots are a potential configuration for SKA1-survey, incorporating ASKAP..... | 34 |
| Figure 7 SKA1-low Context Diagram - Central Signal Processing..... | 35 |
| Figure 8 SKA1-Low Correlator Functional Architecture | 36 |
| Figure 9 SKA1-mid array configurations for dishes at 100 km (left) and 20 km scales (right). SKA dishes are shown in red; MeerKAT dishes in blue. Top panels: The generic SKA1 configuration with clumped spiral arms. The red dots beyond a radius of 2.5 km are clusters of 5 antennas. The blue line is a spiral “generator” line. Bottom panels: An SKA1 configuration in which the clumps in the spiral arms have been replaced by evenly spaced (in the logarithmic sense) antennas..... | 41 |
| Figure 10 Distribution of baselines for SKA1-mid. The purple line is from the configuration containing 250 and clumped spiral arms. The blue line is for a configuration containing 190 antennas and logarithmically distributed antennas on the spiral arms..... | 42 |
| Figure 11 <i>u-v</i> coverage for SKA1-mid. In general these antenna positions are representative, and not optimised. In particular, the <i>u-v</i> coverage would improve if the maximum baseline were 100 km instead of 200 km. The very strong emphasis on core density enables a sensitive pulsar survey to be done, but results in patchy <i>u-v</i> coverage, especially for short, narrow-band (spectral line) observations at medium and long baselines. On the other hand, as is demonstrated in Figure 10, the <i>u-v</i> coverage out to about 6 km is very dense. | 42 |
| Figure 12 The generic SKA1-mid configuration superimposed on the site topology. No attempt here has been made to adapt to the landscape or other mask components. The black dots are SKA dishes; blue are MeerKAT dishes. The black dots are drawn from a 250-dish configuration and represent an over-density in the core..... | 43 |
| Figure 13 The generic SKA2 configuration with the SKA1 configuration embedded in a position in which the antenna densities of the two configurations are matched. Red dots are SKA1; blue are MeerKAT; black are SKA2 antennas. | 44 |
| Figure 14 Receiver bands for SKA1-mid (solid and dash-dot), shown with the planned receiver bands for MeerKAT (dashed). SKA1 bands are numbered 1-5. The band-edge frequencies are provided in Table 6. | 47 |
| Figure 15 SKA1-mid Context Diagram – Central Signal Processing..... | 55 |
| Figure 16 SKA1-Mid Correlator Functional Architecture | 56 |
| Figure 17 Figure-of-Merit used to select the optimum array diameter (~450 m) for pulsar searches. | 58 |
| Figure 18 SKA1-Mid Non-Imaging Processor Functional Architecture | 59 |

| | |
|---|----|
| Figure 19 Average DM vs Galactic latitude | 60 |
| Figure 20 The inner 400 km ² of SKA1-survey. The black dots are ASKAP antennas; the yellow ones are SKA1 core antennas; the blue ones are SKA1 antennas on spiral arms. The arms are connected by lines. Although the lines are included for clarity, they could become service corridors. The red dots are nearby SKA1-low stations. | 65 |
| Figure 21 The array configuration for SKA1-survey. The spiral arm SKA1 antennas are shown as white dots. The SKA1 antenna core and ASKAP antennas are not shown. The red dots represent the SKA1-low stations, which are on the same site..... | 66 |
| Figure 22 The distribution of fractional physical collecting area from the centre of the SKA1-survey array out to a radius of 4 km. | 67 |
| Figure 23 <i>u-v</i> coverage corresponding to the antenna layout in Figure 20 and Figure 21. In general these antenna positions are representative, and not optimised. Brightness temperature sensitivity is determined mainly by the coverage in the core, which is quite dense. | 67 |
| Figure 24 Receiver bands for SKA1-survey. The ASKAP band is shown as a dashed line, slightly offset for clarity, but is designed to overlap PAF Band 2 completely. The dotted lines are potential future bands. | 68 |
| Figure 25 SKA1-survey Context Diagram – Central Signal Processing | 74 |
| Figure 26 SKA1-survey Functional Architecture | 75 |
| Figure 27 Classification of data levels for time-series processing. | 79 |
| Figure 28 Classification of data levels for imaging..... | 80 |
| Figure 29 : SKA1/ASKAP site infrastructure shown in relationship to the SKA1-survey and ASKAP antennas. The yellow dots are additional core antennas in a quasi-random array. The blue dots connected by lines are the SKA1 antenna spiral arms. Grid lines are centred on ASKAP antenna 1, and are at 1000-m intervals. | 82 |
| Figure 30 MeerKAT power distribution network, showing potential positions of SKA1-mid antennas, shown as red dots. Miniature sub-stations are depicted as red triangles, and power lines are red and green lines. Roads are indicated by grey lines. | 86 |
| Figure 31 Routing of fiber of the MeerKAT site | 87 |

LIST OF TABLES

| | |
|--|----|
| Table 1 Parameters for Comparable Telescopes | 18 |
| Table 2 SKA1-low – Log-Periodic Dipoles..... | 30 |
| Table 3 Key System Performance Factors for Log-Periodic Dipoles | 32 |
| Table 4 Correlator Parameters for SKA1-low..... | 37 |
| Table 5 Subset of Dish Performance Requirements | 38 |
| Table 6 SKA1-Mid Array | 48 |
| Table 7 Key System Performance Factors for SKA1-mid Array..... | 49 |
| Table 8 Combined SKA1-mid Array | 52 |
| Table 9 Key System Performance Factors for Combined SKA1-mid Array | 53 |
| Table 10 Correlator Parameters SKA1-mid | 56 |
| Table 11 Central Beamformer Parameters SKA1-mid | 58 |

| | |
|---|----|
| Table 12 Pulsar Search Regions | 61 |
| Table 13 Pulsar Survey Parameters SKA1-mid Array | 61 |
| Table 14 Pulsar Timing Parameters SKA1 | 62 |
| Table 15 SKA1-Survey Array..... | 70 |
| Table 16 Key System Performance Factors for SKA1-survey Array | 72 |
| Table 17 SKA1-Survey Correlator Parameters | 75 |
| Table 18 Data Transport: Boolardy Correlation Centre to Perth | 76 |
| Table 19 Data Transport: Karoo Correlation Centre to Cape Town..... | 77 |
| Table 20 Data Rates (In and Out) for a Typical 12 Hour Observation..... | 80 |
| Table 21 SKA1-low Central Beamformer Equipment Estimates | 95 |
| Table 22 SKA1-mid Correlator Projected Equipment Estimates | 96 |
| Table 23 SKA1-mid Central Beamformer Equipment Estimates..... | 96 |
| Table 24 SKA1-Mid Non-Imaging Survey Equipment Estimates | 96 |
| Table 25 SKA1 Pulsar Timing Parameters | 97 |
| Table 26 SKA1-survey Central Beamformer Equipment Estimates | 98 |

LIST OF ABBREVIATIONS

| | |
|---------------|---------------------------------------|
| AA | Aperture Array |
| AIP..... | Advanced Instrumentation Programme |
| CoDR | Conceptual Design Review |
| CPU..... | Central Processing Unit |
| DAA..... | Dense Aperture Array |
| DRM..... | Design Reference Mission |
| EoR | Epoch of Reionisation |
| FLOPS | Floating Point Operations per second |
| FoV..... | Field of View |
| HPC..... | High Performance Computer |
| Hz..... | Hertz |
| K..... | Kelvin |
| Km..... | kilometre |
| LNA | Low Noise Amplifier |
| m | metre |
| OTPF..... | Observing Time Performance Factor |
| PAF | Phased Array Feed |
| PrepSKA | Preparatory Phase for the SKA |
| RFI | Radio Frequency Interference |
| s | second |
| SEFD..... | System Equivalent Flux Density |
| SKA..... | Square Kilometre Array |
| SKADS | SKA Design Studies |
| SPDO | SKA Program Development Office |
| SSEC | SKA Science and Engineering Committee |
| SSFoM | Survey Speed Figure of Merit |
| T..... | Temperature |
| TBD | To be determined |
| WBSPF | Wide Band Single Pixel Feed |

1 Introduction

1.1 Science Motivation

These headline science programs are outlined below of the larger SKA Science Case, which is highlighted by Key Science Projects (KSPs). These KSPs represent unanswered questions in fundamental physics, astrophysics, and astrobiology that the SKA will play a key role in addressing [29], [30].

- *Probing the Dark Ages and the Epoch of Reionization.* When did the first stars form? By observing the highly redshifted hyperfine spin-flip (21 cm) transition from neutral hydrogen, the SKA will track the changes in the Universe as the first stars and galaxies form and begin to ionize their surroundings. As neutral hydrogen is the raw material for formation of the first stars, the SKA will provide a unique deep into this fundamental epoch in the Universe.
- *Strong Field Tests of Gravity Using Pulsars and Black Holes.* Was Einstein wrong? General relativity is a powerful theory that has passed all tests to date and forms an integral part of everyday life. Yet, it is also a classical theory, not consistent with quantum mechanics. By conducting high precision pulsar timing observations, the SKA will probe into extreme environments, such as orbiting neutron stars, orbiting black holes, and potentially even neutron star-black hole systems, to test the limits of Einstein's Theory of General Relativity.
- *Galaxy Evolution, Cosmology, and Dark Energy.* How do galaxies get their gas and form stars? What is the fate of the Universe? Hydrogen is the fundamental baryonic component of the Universe, and the SKA will have sufficient sensitivity to the 21-cm hyperfine transition of neutral hydrogen to detect galaxies to redshifts $z > 1$. Conducting both wide and deep surveys of galaxies, the SKA will track how galaxies accumulate gas, merge, and form stars. Using the galaxies as tracers of the Universe, the SKA will also be able to test the properties of the mysterious dark energy that is causing the expansion of the Universe to accelerate.
- *The Origin and Evolution of Cosmic Magnetism.* How do cosmic magnets work? While a common and everyday force, the cosmic origins of magnetism are shrouded. With large surveys, the SKA will track how cosmic magnetism has been generated and grown over cosmic time in both galaxies and clusters of galaxies.
- *The Cradle of Life.* Are we alone? The existence of life elsewhere in the Universe has been a topic of speculation for millennia. The SKA will image nearby stellar nurseries, searching for orbiting disks of material in which planets are forming, perhaps not unlike how the Earth formed around the Sun nearly five billion years ago. The SKA will also search for complex, prebiotic molecules in interstellar space, to understand how planets might acquire the raw materials for life, and, in scanning the skies, the SKA will search for the whispers from other civilizations.

Finally, much of modern astronomy arose from observations at radio wavelengths. The design of the telescope is being developed to allow for "Exploration of the Unknown," allowing for evolution of its capabilities. This philosophy is essential as many of the outstanding questions of the 2020–2050 era—when the SKA will be in its most productive years—are likely not even known today.

1.2 Purpose of the document

This document provides a baseline technical starting point and system decomposition (baseline design) for eventual construction of the two radio astronomy systems to be located in Australia and Southern Africa, extensible to the full SKA.

This document describes the first baseline for SKA1. The baseline design contains a plausible estimate of the performance of SKA1, lays the foundation for further technical development, and will be used to obtain capital/operation cost estimates and to estimate science capability. A baseline is a formal artifact of the SKA project that allows development at the sub-system (referred to as Element) level to proceed simultaneously. Specifically, the decomposition into Elements will enable further technical work to be carried out by institutions and companies representing the sponsoring agencies of the SKA. The baseline will also outline the incorporation of the Precursor telescopes, ASKAP and MeerKAT, into SKA1-survey and SKA1-mid, respectively. It is anticipated that future baselines will be established by the project following system wide reviews.

The system decomposition into Elements will form the basis for a Request for Proposals (RfP) to carry out design work at the Element level (first high level design, followed by detailed design). The work will be carried out by consortia, which will assemble to provide responses to the RfP.

In addition to being necessary for the RfP process, this document will provide sufficient performance information that the science capabilities of the baseline can be assessed through a series of “science assessment workshops”. The science remit is described in the Science Case and the Design Reference Mission (DRM). [8] The purpose of the workshops is to project the baseline design on to the science goals covered in these two source documents, supplemented in a few cases by more recent documents. This process will enable traceability to the science.

The authors have striven to produce an outline of a design that:

- Covers the SKA1 key science that has been the inspiration for the SKA for a long time,
- Is feasible technically,
- Is buildable for a reasonable cost, and
- Incorporates the SKA precursor telescopes into the design.

The baseline design is not the final design. Changes will be made as a result of the science assessments, the responses to the RfPs, and the design work by the consortia during preconstruction. The final design will result from the combination of these inputs and results of cost analysis, carried out as well considered trade-off decisions [42]. Thus all design choices in this document are in principle open to question. Some changes to design choices are of course expected as a result of the processes described above. Note, however, that major design changes will have to be extremely well motivated.

This baseline design document (or a subsequent revision) will be a companion document to the Concept of Operations and the DRM.

Sections 1 through 3 provide an overview of the baseline design and serve as a useful summary for those not engaged in detailed design or scoping work. Sections 6 and beyond provide the details that will be useful to Element design consortia.

1.3 Scope

1.3.1 Boundary Conditions

The SKA Board and Members have taken decisions that define a set of boundary conditions for the SKA. Other constraints are set by documents such as the DRM. These are discussed below.

- Based on recommendations from the SKA Site Advisory Committee in their report [6] and other considerations [7], the Members of the SKA Organisation have selected two sites for the SKA, one in Western Australia at the Murchison Radio Observatory near Boolardy Station and one in Southern Africa, centred in the Karoo Central Astronomy Advantage Area, but extending eventually to neighbouring countries in Southern Africa.
- Following from recommendations contained in [7], the Members have decided that the telescope facilities for SKA1 have been defined as SKA1-low, a low-frequency aperture array; SKA1-survey, a mid-frequency array of dishes equipped with Phased-Array Feeds (PAFs), both arrays to be built in Australia; and SKA1-mid, a mid-frequency array of parabolic reflectors (dishes) to be built in South Africa.
- The SKA1 Design Reference Mission (DRM) is now “baselined”. The document describing the DRM[8] is intended to establish a set of observations that define an “envelope” of requirements for the telescope.
- The SKA Board has required the incorporation of the Precursor telescopes, ASKAP and MeerKAT, into SKA1 so as to take advantage of as much of the investment in infrastructure and telescope equipment as possible, based on a feasibility and cost-benefit analysis.
- In order to move into the construction phase of SKA1, the SKA Board requires a “motivated cost cap”, based on a cost analysis of a representative SKA1 system consistent with achievable science capabilities.
- A recent review of the engineering process for SKA1 [10] has recommended that a Baseline Design be written, agreed and adopted by the Board, reflecting the basic architecture of the system, the site decisions and consideration of the Precursor telescopes as a prerequisite to continuing with pre-construction work.
- Consistent with good project management practices, satisfactory technical performance of SKA1 at both sites is expected for the implementation of all aspects of SKA2.

1.3.2 The Baseline Design

This document is the first version of the Baseline Design; it is expected to evolve over time but must continue to adhere to the boundary conditions outlined in the previous section. It includes the basic architecture for a 3-telescope, 2-site model in which there are as many common design approaches, common operational methods, and sharing of infrastructure as possible.

The final optimised system design will emerge from a more extensive, systematic study, which the SKA Element consortia will carry out. Such a study will involve an orderly decision-making process that trades-off technical requirements, derived from the user requirements (essentially the Design

Reference Mission (DRM)) and other sources, system performance and total cost of ownership. This process is needed to define the most cost-effective Phase 1 sub-set as well as SKA Phase 2.

The scope of the document contains as much specific information as needed to carry out the purpose (see previous section), but as little “arbitrary” information as possible, leaving as much freedom as possible for innovative solutions at the more detailed levels. However, the baseline design is conservative in the sense that it utilises the results of many years of investigation into enabling technology; nothing in the baseline design requires a completely fresh start in developing solutions. This is necessary in order for construction to proceed on the required timescales.

The scope includes a plausible estimate of the performance of each of the telescopes using standard radio astronomy measures of performance: frequency coverage, sensitivity, resolution (distribution of collecting area), and processing in the spatial (images and maps), spectral (spectra) and temporal (pulsars, variables, transients) domains.

In some areas (e.g. notably signal processing) more detailed analysis of potential solutions is needed to ensure reasonable feasibility and that assumptions of the use of infrastructure (e.g. existing space and power) are viable. These are representative designs, not final implementations.

Representative array configurations have also been described. Some features, such as maximum extent, have a large impact on other aspects of the design, and will have to be decided early. Other aspects, such as the individual placement of antennas/stations, are only representative.

Broad outlines of the extensibility to SKA2 (the full SKA) are described for SKA1-low and SKA1-mid.

In summary the document is to be used for the following:

- To guide system engineering work.
- To guide design work at the sub-system (Element) level.
- To inform operations considerations, particularly those specifically related to design.
- To obtain first-order capital/operation cost estimates.
- To enable assessment and traceability of science capability.

2 Top Level Description of the SKA1 Baseline Design

In this section we provide a condensed top-level description of this baseline design for SKA1. In reading this description, bear in mind that this is current baseline design and not the final design.

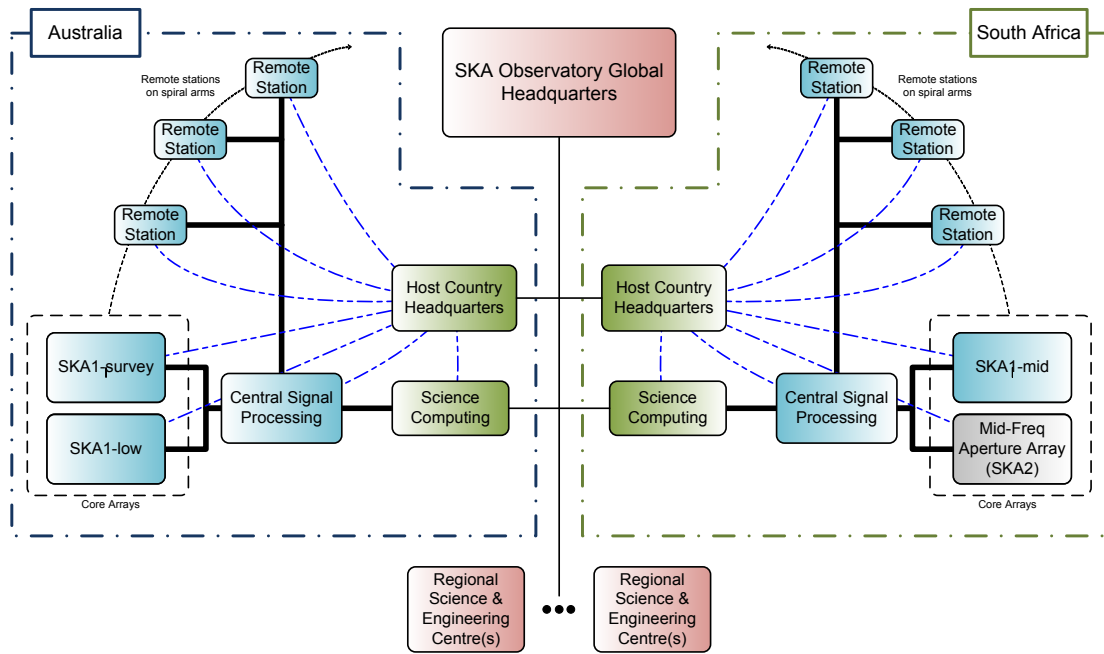


Figure 1 A schematic diagram of the SKA Observatory, showing the geographical locations of site entities (telescopes), the entities at regional centres (Host Country Headquarters and Science Data Processing), and entities that are globally located (Global Headquarters).

Figure 1 shows the major SKA Observatory entities: SKA1-low and SKA1-survey in Australia, SKA1-mid in South Africa. In each Host Country the Host Country Headquarters will be in Perth and Cape Town respectively, as will the Science Data Processing Centres. The Host Country Headquarters will be responsible for Operations and Maintenance. The thick flow-lines show the uni-directional transport of large amounts of digitised data from the receptors to the central signal processing facilities on the sites, and from the central signal processing facilities to the Science Data Processing Centres. The thin dash-dot lines show the bi-directional transport of system monitor and control data.

The Science Data Processor is envisaged to be a supercomputing facility. Sufficient on-site processing will be done to reduce to a manageable rate the data sent to the off-site science computing facility. The science data processor is where calibration of the data takes place, images of sky brightness are formed, and further analysis of time-domain effects are carried out. For current aperture synthesis arrays, algorithms for carrying out calibration and imaging are mature. However, the SKA is likely to require significant new developments in this area to handle the much larger amount of data, and to achieve dynamic range targets without continuous human input. Developments by the precursors and pathfinders are likely to be critical enabling technologies.

Some fraction of the processed data and data products will be delivered to the Regional Science and Engineering Centres, which will be globally distributed. The precise nature and volume of this data will not be defined until the telescopes are closer to operations, and even then may only be defined in a preliminary way.

2.1 SKA1-low

This telescope in the Observatory will primarily address observations of the highly redshifted 21 cm hyperfine line of neutral hydrogen from the Epoch of Reionization and earlier. It will also be well

suites for conducting low radio frequency observations of pulsars, magnetized plasmas both in the Galaxy and intergalactic space, radio recombination lines, and potentially extrasolar planets.

The telescope receptors will consist of an array of ~250,000 log-periodic dual-polarised antenna elements. Most of the elements will be arranged in a very compact configuration (the ‘core’) with a diameter of ~1 km, the rest of the elements will be arranged in stations about 35-m in diameter. The stations will be configured in three equally spaced spiral arms. The maximum radius of the configuration is ~45 km. The antenna array will operate from 50 MHz to ~350 MHz. Its sensitivity will be ~1000 m² / K at frequencies above 110 MHz at the zenith, assuming an instantaneous bandwidth of 250 MHz. The core will have a brightness temperature sensitivity of ~1 mK over the same frequency range at the zenith.

The elements will be grouped into 866 35-m diameter stations, whose elements will be beam-formed to expose a field-of-view of ~20 deg² in a single smooth beam. Possibilities exist for more elaborate beamformers in the core, if needed.

Signals from the beamformers will be transported to a central signal processing building, where they will be channelised and cross-correlated with each other. Output data from the correlator will be transported to the science data processing centre in Perth. Additional signal processing equipment may be warranted but is not included at present.

The required processing of the science data will be varied, and probably elaborate, and will likely include calibration, image-cube (i.e., spatial plus spectral) formation on various scales, and statistical analysis.

The entire array can be built within the boundaries of Boolardy station, and operated concurrently with the SKA1-survey telescope on the same property.

2.2 SKA1-mid

This telescope in the Observatory will primarily address observations of radio pulsars and observations of the 21-cm hyperfine line of neutral hydrogen from the local Universe, to moderate redshifts, as well as high sensitivity observations of continuum emitting objects. It will also be well suited for conducting observations of various spectral lines in addition to the 21-cm hydrogen line (e.g. OH-lines), many classes of radio transients, magnetized plasmas both in the Galaxy and intergalactic space, and potentially proto-planetary disks.

The telescope receptors will consist of array reflector antennas (‘dishes’). The array will be a mixed array of 64 13.5-m diameter dishes from the MeerKAT array and 190 15-m SKA1 dishes. The antennas will be arranged in a moderately compact core with a diameter of ~1 km, a further 2-dimensional array of randomly placed dishes out to ~3 km radius, thinning at the edges. Three spiral arms, a subset of the 5 equally spaced arms reserved for SKA2, will extend to a radius of ~100 km from the centre. In this baseline design, the SKA1 dishes will be clear-aperture, offset-Gregorian optics design, capable of handling five cryo-cooled receiver packages, each of which can be moved into the focal position. The SKA1 dishes will be capable of operations up to at least 20 GHz, although not equipped to cover this entire range for SKA1.

SKA1-mid will cover the continuous frequency range from 350 MHz to at least 3050 MHz in three receiver bands. Additional receiver bands for higher frequencies on the SKA1 dishes can be accommodated, depending on costs and science priorities. It is planned that MeerKAT dishes will be

equipped with X-band receivers (8 – 14.5 GHz). Lower frequency receivers will have a bandwidth of ~1 GHz and higher frequency receivers ~2.5 GHz in each polarisation.

Over much of the frequency range, optics and feeds have been designed for an expected aperture efficiency of 78%, and spillover-plus-sky noise of ~6K at the zenith. With additional noise contributions of 14 K (LNA, other losses) the SKA1 dish-sensitivity is expected to be $6.9 \text{ m}^2/\text{K}$. The combined array is expected to have a System Equivalent Flux Density (SEFD) of 1.7 Jy.

Signals from the dishes will be transported to a central signal processing building, where they will be divided into narrow frequency channels and cross-correlated with each other. Output data from the correlator will be transported to the science data processing centre in Cape Town.

The signals from the dishes will also be combined into a large number of array beams, the outputs of which will then be distributed to specialised pulsar search equipment. Pulsar candidates will be sent to the science data centre for further analysis. This equipment will also have some capability for detecting de-dispersed transients (rare or one-off, potentially extra-terrestrial radio-burst signals).

As for the other telescopes, the required processing of the science data will be varied, probably elaborate, and will likely include calibration, image-cube (i.e., spatial plus spectral) formation on various scales, time-domain analysis and statistical analysis.

The SKA1-dish array can be built essentially in the same location as the MeerKAT array, and the array can be expanded to a much larger SKA2 array from that location.

2.3 SKA1-survey

This telescope in the Observatory will primarily conduct surveys of large fractions of the sky, mapping the sky both for spectral lines and continuum. Primary surveys are likely to include the 21-cm hydrogen line from the Galaxy to moderate redshifts, continuum emitting objects (both in total and polarised intensity), and potentially various classes of radio transients.

Like SKA1-mid the telescope receptors will consist of array reflector antennas ('dishes'). The array will be a mixed array of 36 12-m diameter dishes from the ASKAP array and 60 15-m SKA1 dishes. The SKA1 antennas will be arranged in a core with a diameter of ~2 km, to add density to the existing ASKAP array in the core. Three spiral arms will extend to a radius of ~25 km from the centre, although space is available for ~50-km arms, if needed to suppress confusion noise.

In this baseline design, the SKA1 dishes will be clear-aperture, offset-Gregorian optics design, equipped with Phased Array Feeds (PAFs), similar or identical to those planned for the ASKAP antennas. Conceivably the optical surfaces for the PAF application will be optimised slightly differently from those used for SKA1-mid, while sharing all the other aspects. Although not actually equipped, positions for at least two additional positions for PAFs will be available, which would share the beamforming electronics. The dishes will be capable of operations up to at least 20 GHz.

SKA1-survey will cover the continuous frequency range from 650 MHz to 1670 MHz in a single dual-polarised PAF in a 500 MHz wide instantaneous bandwidth.

When illuminated by a Phased Array Feed, both the ASKAP and SKA1 dishes are expected to have aperture efficiencies of 80%, and system temperatures of ~30 K. The PAFs provide a constant Field-of-View of approximately 18 deg^2 in 36 beams at the highest frequency. The combined array is expected to have a Survey Speed Figure-of-Merit (SSFoM) exceeding $\sim 10^6 \text{ m}^4 \text{ K}^{-2} \text{ deg}^2$.

Signals from the PAFs will be transported to a central signal processing building where they will be formed into an array of beams covering the field-of-view, divided into narrow frequency channels and cross-correlated with each other. Output data from the correlator will be transported to the science data processing centre in Perth.

As for the other telescopes, the required processing of the science data will be varied, probably elaborate, and will likely include calibration, image-cube (i.e., spatial plus spectral) formation on various scales, time-domain analysis and statistical analysis.

The SKA1-survey array can be built within the boundaries of Boolardy station, and operated concurrently with the SKA1-low telescope on the same property.

Table 1 Parameters for Comparable Telescopes

| Table xxx: Parameters for Comparable Telescopes | | | | | | | | | | | | | | | |
|---|---|--------------------------------|--------------------|--------------------|-----------------------------|--------------------|--------------------|--------------------|---------------------|--------------------|--------------------|--------------------|--------------------|--------------------|--------------------|
| | eMERLIN | JVLA | GBT | GMRT | Parkes MB | LOFAR | FAST | MeerKAT | WSRT | Arecibo | ASKAP | SKA1-survey | SKA1-low | SKA-mid | |
| $A_{\text{eff}}/T_{\text{sys}}$ | m^2/K | 60 | 265 | 276 | 250 | 100 | 61 | 1250 | 321 | 124 | 1150 | 65 | 391 | 1000 | 1630 |
| FoV | deg^2 | 0.25 | 0.25 | 0.015 | 0.13 | 0.65 | 14 | 0.0017 | 0.86 | 0.25 | 0.003 | 30 | 18 | 27 | 0.49 |
| Receptor Size | m | 25 | 25 | 101 | 45 | 64 | 39 | 300 | 13.5 | 25 | 225 | 12 | 15 | 35 | 15 |
| Fiducial frequency | GHz | 1.4 | 1.4 | 1.4 | 1.4 | 1.4 | 0.12 | 1.4 | 1.4 | 1.4 | 1.4 | 1.4 | 1.67 | 0.11 | 1.67 |
| Survey Speed FOM | $\text{deg}^2 \text{ m}^4 \text{ K}^{-2}$ | 9.00×10^2 | 1.76×10^4 | 1.14×10^3 | 8.13×10^3 | 6.50×10^3 | 5.21×10^4 | 2.66×10^3 | 8.86×10^4 | 3.84×10^3 | 3.97×10^3 | 1.27×10^5 | 2.75×10^6 | 2.70×10^7 | 1.30×10^6 |
| Resolution | arcsec | $10\text{-}150 \times 10^{-3}$ | 1.4 - 44 | 420 | 2 | 660 | 5 | 88 | 11 | 16 | 192 | 7 | 0.9 | 11 | 0.22 |
| Baseline or Size | km | 217 | 1 - 35 | 0.1 | 27 | 0.064 | 100 | 0.5 | 4 | 2.7 | 225 | 6 | 50 | 50 | 200 |
| Frequency Range | GHz | 1.3-1.8, 4-8, 22-24 | 1 - 50 | 0.2 - 50+ | 0.15, 0.23, 0.33, 0.61, 1.4 | 0.44 to 24 | 0.03 - 0.22 | 0.1 - 3 | 0.7 - 2.5, 0.7 - 10 | 0.3 - 8.6 | 0.3 - 10 | 0.7-1.8 | 0.65-1.67 | 0.050 - 0.350 | 0.35-14 |
| Bandwidth | MHz | 400 | 1000 | 400 | 450 | 400 | 4 | 800 | 1000 | 160 | 1000 | 300 | 500 | 250 | 770 |
| Cont. Sensitivity | $\mu\text{Jy}\cdot\text{hr}^{-1/2}$ | 27.11 | 3.88 | 5.89 | 6.13 | 16.26 | 266.61 | 0.92 | 3.20 | 20.74 | 0.89 | 28.89 | 3.72 | 2.06 | 0.72 |
| Sensitivity, 100 kHz | $\mu\text{Jy}\cdot\text{hr}^{-1/2}$ | 1714 | 388 | 373 | 411 | 1029 | 1686 | 82 | 320 | 830 | 89 | 1582 | 263 | 103 | 63 |
| SEFD | Jy | 46.0 | 10.4 | 10.0 | 11.0 | 27.6 | 45.2 | 2.2 | 8.6 | 22.3 | 2.4 | 42.5 | 7.1 | 2.8 | 1.7 |

Notes to Table

| | | | | |
|-------------|---|---|---------------------------------|--------------------------------------|
| eMERLIN | Frequencies non-contiguous | | | |
| JVLA | Multiple antenna configurations | | | |
| GBT | Single dish | | | |
| GMRT | Frequencies non-contiguous | | | |
| Parkes MB | Multi-beam (13) | Frequencies non-contiguous | | |
| LOFAR | Parameters for all NL stations | Frequencies non-contiguous | | |
| FAST | Single dish | Under construction | | |
| MeerKAT | SKA Precursor | Under construction | | |
| WSRT | Frequencies non-contiguous | | | |
| Arecibo | Single dish | | | |
| ASKAP | SKA Precursor | Multi-beam (36) | Under construction | |
| SKA1-survey | Multi-beam (36) | Mixed 12-m & 15-m dishes | FoV based on 15-m dishes | Planned |
| SKA1-low | | | | Planned |
| SKA-mid | | Mixed 13.5-m & 15-m dishes | FoV based on 15-m dishes | Planned |
| Notes: All | Fiducial frequency: Most Parameters | $\Omega_{\text{FoV}} = (\pi/4)(66\lambda/D\text{dish})^2$ | Gray shading: <400 MHz capable | SEFD: System Equivalent Flux Density |
| (cont'd) | SEFD derived from $A_{\text{eff}}/T_{\text{sys}}$ | Sensitivity derived from SEFD & BW | System efficiency assumed 100%. | |

2.4 Comparative Performance

Part of the telescope design process is to ensure that astronomical performance will be a major step over currently available telescopes. The driving concepts for the SKA have been to develop high sensitivity as well as high “survey-speed” telescopes. Table 1 contains a list of performance parameters for radio telescopes, both currently available and those that are under construction or planned, including the SKA1 telescopes.

In the decimetre range of wavelengths, represented by a frequency of 1.4 GHz, SKA1-mid provides a major advance over existing instruments. Resolution, sensitivity and survey speed are an order of magnitude better in most cases, and in combination occupy a new region of performance.

SKA1-low covers a similar frequency to LOFAR and MWA but provides an overall sensitivity increase of more than an order of magnitude albeit being optimised for brightness temperature sensitivity – most of the collecting area in a very compact array.

SKA1-survey is comparable with the JVLA in SEFD, but the SKA1-survey PAF-enabled field-of-view, two orders of magnitude larger, provides a huge increase in survey speed.

SKA1-mid antennas will be capable of contiguous frequency coverage from 350 MHz to 20 GHz, although they may not be initially equipped with all the receivers. Noting that continuous frequency coverage was a major goal of the upgrade of the Very Large Array to the JVLA, this is a scientifically critical capability for a modern radio telescope.

In summary, the SKA1 designs outlined in this document will be a major step forward in astronomical performance, and their location in the Southern hemisphere will compliment similar telescopes in the North, as well as the very large optical/IR telescopes and ALMA in the South.

3 Progression to SKA2

This progression can be visualized either from the perspective of the introduction of new technologies currently being investigated or from the perspective of how the individual telescopes might be expanded or enhanced. It is beyond the scope of this document to review in detail the Advanced Instrumentation Programme (AIP), which has been widely documented [11]. The following sections are based on additional capabilities that have been planned for in SKA1 designs outlined herein.

3.1 SKA-low

There are multiple paths from SKA1-low to SKA2. The actual path will probably depend on the results from the scientific observations.

If imaging of the HI-line in emission becomes important and is seen to be feasible in the redshift range 2.5 – 6 (equivalent to the upper end of the ~200 – 400 MHz band), then it may make sense to build a second aperture array to target that range with much better brightness temperature sensitivity, and if possible higher resolution as well. This could also be a lower frequency version of dense aperture technology.

Also, if the HI-line associated with the EoR era is detected but perhaps not imaged, then an expansion at the low end of the band would be an important investment. Higher resolution imaging would involve a much larger, less compact array configuration.

3.2 SKA-mid

The original plan to expand the array to provide sensitivity (A_e/T_{sys}) of $\sim 10000 \text{ m}^2/\text{K}$ remains part of the vision of the full SKA. The array configuration needed for this is discussed in Section 8. In addition, equipping the dishes with a complete set of receivers will increase the frequency range, enabling observations of higher frequency spectral lines (red-shifted extragalactic and Galactic).

Equipping SKA2 antennas with PAFs is potentially a powerful technique for increasing the survey speed of SKA2. Since PAFs can operate at any frequency in the SKA band, the frequency range would be selected based on science priorities at the time.

Dense aperture array technology has been considered for the L-band (1-2 GHz) frequency range as well. If sufficient sensitivity were possible, then a multi-beam, high survey-speed telescope would enable very large surveys to be undertaken. This technology may also make sense for the ~350-700 MHz band, where a large-scale survey of the red-shifted HI-line in emission. This is already part of the original DRM for SKA2.

3.3 SKA-survey

SKA-survey could be equipped with at least two more PAF feeds, at adjacent-lower or higher frequency bands, for which all-sky surveys would open up new discovery space. Small, high frequency PAFs could be amenable to cryo-cooling, which would greatly increase their sensitivity.

3.4 AIP Technologies

Wide-band Single-Pixel Feeds (WBSPF): The development of feeds for SKA reflector antennas that can cover much wider bands than the current best feeds would greatly reduce system cost, enable simultaneous observations of multiple spectral lines, and increase continuum sensitivity. Active R&D is being carried on out on these feeds. They could be used in the future in place of several existing or planned feeds for SKA1-mid. Within limits, the design for SKA1-mid could be considered WBSPF-ready.

Dense Aperture Arrays: Dense aperture arrays are close-packed arrays of regularly spaced elements which form large filled apertures capable of forming multiple independent beams, in effect re-using the aperture for each beam. Large-scale prototypes have already demonstrated the principles [50], and plans are under way to scale these up further. Enormous fields-of-view are potentially possible, which could lead to “billion-galaxy” surveys of the radio sky.

Phased Array Feeds: This new feed technology for reflector antennas is already part of the SKA1 design.

4 Design Considerations

The performance of the SKA telescopes for science is determined mainly by five characteristics. These are the key factors in evaluating the capability of a particular design or implementation to carry out the SKA science programme.

- *Frequency Range:* The range of frequencies or wavelengths over which the telescope has significant sensitivity for astronomy applications.
- *Sensitivity:* The sensitivity is defined here as generalized survey speed, essentially the inverse of the time taken for the telescope to observe a set of objects of given minimum flux or an area of sky of given minimum brightness temperature. More precisely, it is the inverse of the length of time needed to carry out a well-defined observing programme. The sensitivity will depend on the nature of the limiting factors, namely: sky noise and instrument noise that reduce in proportion to the square root of the observing time for a particular observing direction, and systematic errors that do not reduce or reduce more slowly than in proportion to the square root of the observing time. Telescope sensitivity is evaluated differently for the following broad classes of observations:
 - Spectral Characteristics:
 - Continuum emission
 - Spectral line emission
 - Time dependent emission
 - Motion or apparent motion of compact objects
 - Repetitive changes in flux
 - Long-term flux variability
 - Short-term flux variability
 - Single or rare events or changes in flux
 - Spatial Characteristics
 - Spatially continuous emission
 - Widely separated compact objects
 - Large regions of sky

Although sensitivity is generally a function of frequency, distribution of collecting area, pointing direction and instantaneous field-of-view, not all these are applicable for a given observing programme.

- *Polarisation capability:* The capability to measure and image polarisation characteristics of radio emission, usually characterised as Stokes parameters, is fundamental to the science, in both continuum and spectral line observations. The SKA must be capable of doing so across the full fields-of-view. Polarisation characteristics are also used in calibration, removing ionospheric effects, etc.
- *Distribution of Collecting Area:* At a given frequency, the sensitivity of the telescope to components of the spatial spectrum. This is determined by the array configuration, and is a function of frequency. For observations of continuum emission sensitivity may be limited by confusion. This will likely determine the length of the longest baselines in the arrays .
- *Processing capability of the telescope along three dimensions:*

- Spatial processing: the capability to make images of the sky in a given frequency band in all four Stokes parameters (IQUV).
- Spectral processing: the capability to make spectra over a defined area of sky.
- Temporal processing: the capability to determine changes in the flux of emission from a defined area of sky over a given frequency band.

These performance factors are complex and exhibit strong interdependencies. Performance models based on these factors will be used to evaluate the capability of the telescope to carry out the SKA science programme. The complexity of models ranges from simple calculations to elaborate simulations. In this document simplified models will be used as much as possible.

4.1 Sky Noise

The component of system temperature originating as “sky noise” that will be used in this document is given in Figure 2, which also shows the approximation, $T_{\text{sky}} = 60\lambda^{2.55}$ used [12] at low frequencies. This approximation agrees with an “average” between those given for the Galactic pole and the Galactic Plane, and is valid up to ~ 450 MHz. For the purposes of determining collecting area, T_{sky} is assumed to be 500 K at 130 MHz ($z \approx 10$).

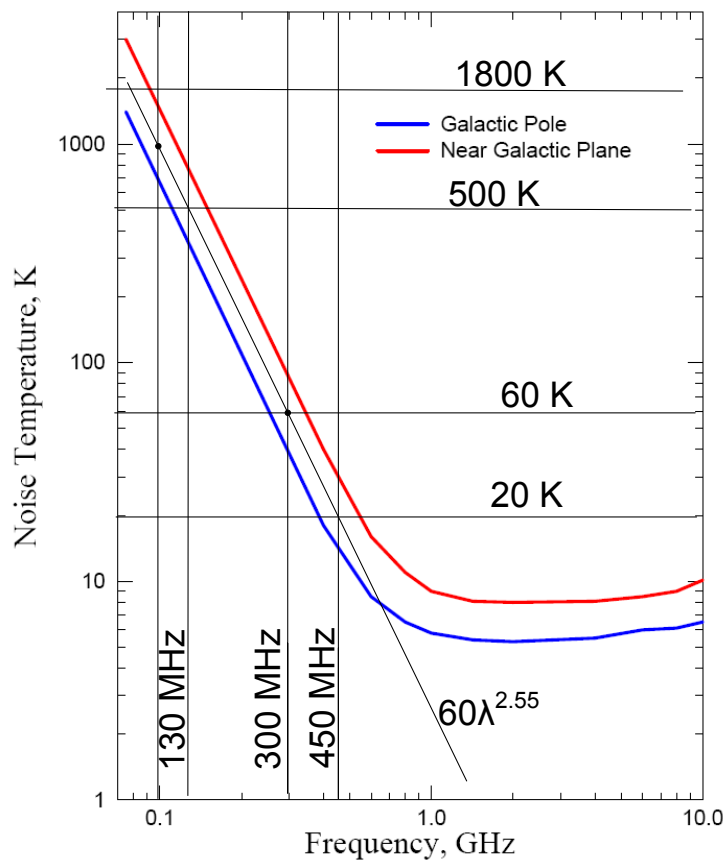


Figure 2: Sky Noise Temperature vs frequency for low radio frequencies.

4.2 Confusion Limits

Confusion is an important factor in determining the length of the longest baselines for SKA1. It has been best studied near 1.4 GHz, and is therefore directly applicable to SKA1-survey and SKA1-mid.

The analysis of Condon et al. [35] estimates the confusion noise due to faint sources to be:

$$\sigma_{conf} = 1.2 \left(\frac{\nu}{3\text{GHz}} \right)^{-0.7} \left(\frac{\theta}{8''} \right)^{10/3} \mu\text{Jy}$$

Using the sensitivity performance values for SKA1-mid drawn from Table 7, SKA1-mid would produce images with ~ 23 nJy of noise after a 1000-hr integration. In order that the confusion noise be significantly less than the thermal noise limit, SKA1-mid requires an angular resolution better than 1.7 arcseconds at 1.4 GHz, corresponding to a baseline length of at least 30 km. Allowing for potential uncertainties, a nominal value of 50 km for the extent of SKA1-mid is reasonable. Other approaches have yielded larger values, and in this document the maximum baseline for SKA-mid is nominally 200 km, indicating a need for review to settle on a final value.

Following the survey scenario outlined in [18], a continuum survey would reach a thermal limit of ~ 2 μJy per beam, assuming 10000 hrs is allocated to cover 30000 deg^2 of sky. Thus SKA1-survey would not be confusion limited in carrying out this survey.

These considerations are for radio continuum observations. In general, spectral line observations (e.g., HI) should not be confusion limited in the same way as continuum observations because spectral line observations reflect the 3-D distribution of the sources. Similarly, by virtue of the time dependence, a survey that incorporates time domain information can also probe well below the continuum confusion limit.

4.3 Science Data Processing Capabilities

The imaging capabilities of the telescope are due to the careful design and construction of all the hardware systems but equally so of the algorithms, software, and computers that process the visibility data emerging from the correlator into science data products such as calibrated visibility data, images, spectral cubes, time-series, etc. Much of the science depends critically on efficient and accurate calibration and imaging. The science goals typically require much higher sensitivity and dynamic range than achieved previously. The push to higher sensitivity implies both more data to be processed and more sophisticated processing algorithms. A new generation of processing algorithms has arisen from the work on the precursors (LOFAR, ASKAP) and pathfinders (e.g. JVLA). Along with the new algorithms has come an intensified interest in distributed and parallel processing.

The deep understanding of a telescope that leads to optimal data processing comes relatively late in the commissioning. Hence for the precursors and pathfinders, we can expect that significant progress in processing will continue to be made for a number of years to come, overlapping with SKA1 preconstruction and construction. Thus at the commissioning of SKA1 telescopes, we can expect that only low-performance science capabilities will be available. Low-performance means low dynamic range and relatively short (12 – 24) hour integrations. Over time, the more advanced processing algorithms from the precursors and pathfinders will become available and understanding of the SKA1 telescopes will improve. As this happens, the scientific capabilities will grow.

Recent modelling work [24] shows that in 2019 it should be possible to procure a computing system at reasonable cost that will be able to process SKA1 data, provided some careful choices about array parameters are made. For full-field imaging, the dominant processing costs go as the cube of the

baseline/diameter ratio. The steepness of this scaling means that large changes in computing requirements can be made by relatively small changes in scientific capabilities.

5 Global Assumptions

In addition to the considerations in the previous section, the following working assumptions have provided guidance in developing this baseline design :

- By default, common approaches to design will be used. These include common standards, common components, common interfaces, etc. with the aim of maximising re-use and minimising redundant design effort.
- Maximal use will be made of the precursor telescope sub-systems, infrastructure and components, based on cost-benefit analyses.
- Reasonable efforts will be made to enable the precursors to operate during construction of SKA1, at least part time.
- All three receptor arrays and their respective support services will operate concurrently and continuously, except for planned maintenance shutdowns or exigencies.
- The Dish Arrays can use only one feed at a time (PAF or SPF).
- All of the SKA1 telescopes can operate independently as multiple sub-arrays (i.e., collecting area split and allocated to separate, concurrently observing programmes).
- The two main receptors in Australia (SKA1-low and SKA1-survey) will occupy spatially separated cores, serviced by roads, power, data transport, and time transfer sub-systems optimised for those particular telescopes. The distance between the cores will be based on a cost-benefit analysis, recognising the potential for mutual radio frequency interference if they are too close.
- Extensibility to SKA2 will be taken into account for SKA1-low and SKA1-mid.
- Forward estimates of technology, which changes rapidly over time, are needed for some of the estimates in this document. A technology freeze date of 2016 is assumed for equipment that must be available for continuous construction and testing of the telescopes. A freeze date of 2019 is assumed for commercially available computer equipment for the initial science data processing, or for signal processing that does not need to be available until after construction. Later dates may be assumed for the higher-end HPC equipment, which may not be needed until the most sophisticated processing is undertaken.

6 SKA1-low

The primary science case for SKA1-low is detection of the ‘21-cm HI-line’ (emission and/or absorption) resulting from density fluctuations at redshifts from between 5 and 6 to between 25 and 35 in the early Universe (“Cosmic Dawn” and “Epoch of Reionisation” periods) [25] corresponding to frequencies from 40 to 237 MHz. These will be referred to in this document as EoR observations.

A secondary science case is HI-line absorption against continuum sources over the redshift range from ~ 0 to ~ 20 . This entire redshift range cannot be covered by one technology. Aperture arrays (AAs) will be used for the lower frequencies, while dishes will be used for the higher frequencies. The precise cross-over is to be determined by an optimised combination of scientific priority, cost

and feasibility. The expected sensitivity of $1000 \text{ m}^2/\text{K}$ meets SKA1 expectations for sensitivity in the frequency range from 110 to 350 MHz.

In contrast to EoR observations, absorption observations against compact background sources require high point-source sensitivity. This means that for that specific purpose, the shape and sidelobe structure of the synthesised beam is less important. For additional types of observations, such as for pulsars and continuum sources, point source sensitivity is also more important. Although not definitive, an emphasis on brightness temperature sensitivity at the low end of the band and point source sensitivity at the high end seems justified as a starting point.

For SKA2 coverage of this range may be more important if sensitivity can be improved so that the HI-line can be observed in emission in this redshift range. This application could then, again, be brightness temperature sensitivity limited.

6.1 Key Design Requirements and Parameters

A low-frequency aperture array (AA) is the only practical technical solution for building a telescope in the meter-range of wavelengths implied by the above science. The basic AA design consists of an array of antenna elements, grouped into stations. The signals from the antenna elements in each station are used to form one or more beams. The key design parameters for AAs are highly coupled, principally because the collecting area is composed of quasi-resonant antennas. Although they have been “broad-banded” as much as possible, this fundamentally constrains the frequency range and the filling factor in arrays.

The receptor parameters that most influence the science are:

1. *Frequency Range:* As recommended in [25] and for the purposes of this document, the frequency ranges of greatest interest are between 54^1 and 215 MHz, corresponding to $z = \sim 25$ and 5.5, respectively. Since AAs cannot be built with flat frequency response, a frequency of 108 MHz has been identified in [25] as optimum for the peak sensitivity. Frequency coverage above 215 MHz is required for tracing galaxy evolution through observations of the HI-line in absorption against background continuum sources, the secondary science case.
2. *Sensitivity:* Because the EoR sensitivity requirements are expressed as a brightness temperature, the array configuration and the frequency range are coupled. At 108 MHz, rms noise of $\sim 1 \text{ mK}$ on scales of $\sim 5 \text{ arcmin}$ is required to detect the signal, which is expected to be $\sim \pm 10 \text{ mK}$ peak deviation from a spectral baseline on scales of $\sim 100 \text{ kHz}$. Since AA sensitivity falls off with zenith angle as $\cos(Z)$ for small zenith angles at the lowest frequencies where the array are in the ‘dense regime’, this value has been taken as the sensitivity at zenith.

Note that sensitivity as a function of frequency is determined by total noise, the gain of each element in the pointing direction and the total number of elements within a radius from the centre determined by the required array resolution. The first two are strong functions of frequency since noise scales as $f^{-2.55}$ (see section 6.8) and antenna element gain scales as f^2 above the critical frequency of the station array.

¹ Note that the legislation in Australia, the location of this instrument, provides legal protection only as low as 70 MHz. This means that usage of frequencies below this limit is at some risk of interference from legitimate users in the protected region.

3. *Polarisation capability:* Dual polarization capability is required, mainly to remove continuum ‘foreground emission’. Extremely accurate characterisation of instrumental polarization, which is a function of position in the field-of-view and of pointing direction, will be needed to correct for the effects of strong, polarized continuum emission, which could otherwise generate results that mimic the signature of HI-line emission/absorption.
4. *Instantaneous Field-of-View:* EoR observations will be very sensitive to spatial fluctuations on angular scales from ~5-10 arcmin to several degrees. This translates into a smoothness requirement of <1 mK in fields where typical emission is ~10 K (ie, 10⁴:1). Synthesising a field-of-view by stitching multiple beams entails a high risk of not achieving this requirement. To minimise this risk, the angular size of a station beam at 108 MHz is specified as >5 degrees at zenith.
5. *Array Configuration:* The parameters of the array configuration have been selected to approximately meet the above requirements. Once the station size is determined, the number of stations is determined by the sensitivity and the gain of the individual antenna elements. Variations of the signal on scales of several arcminutes permits a very compact array, which makes the brightness temperature limit easier to achieve. However, there is a limit, imposed by a completely filled array with antenna elements whose minimum size is determined by the minimum frequency range. Additional frequency range can only be had by building more than one array.

The detection of the EoR signal will be strongly influenced by the ability to subtract well calibrated “foregrounds”. One of the most important foreground signals is the assembly of unresolved continuum sources in the low resolution beam used to detect the EoR signal. A lower sensitivity, high resolution array is needed to make accurate maps of these sources, including polarisation, over a fraction of the sky sufficient to include all of the side-lobes of the station beam (possibly a large fraction).

6. *Sky Coverage:* The AA stations will have steerable beams, possibly more than one. There are two major limiting factors influencing both the station beam shapes and the sensitivity away from the zenith where beam-shapes are best behaved and the sensitivity is maximum. The first is the fall-off of antenna element sensitivity with Z. The second factor is the cos(Z) foreshortening factor, which applies when the array is in the dense regime. Moreover even with careful array design, sidelobes tend to increase at large zenith angles, and even grating lobes will appear at frequencies where the stations are sparsely sampled. For an observation as sensitive to systematic effects as the EoR observation, it is assumed here that no observations at zenith angles greater than 40 degrees will be seriously utilised.

6.2 Aspects of the Array Configuration

Based on the above, the following properties for the core (not including the spiral arms) can be derived:

- A circularly symmetric array of randomly distributed stations whose density falls off approximately as a Gaussian distribution.
- A very compact array. It is suggested in [14] that 75% of the collecting area lie within a 1000 m radius. While this may not be quite possible, the goal is to be as compact as possible.
- Station beamwidth >5 degrees in approximately the centre of the EoR frequency range.

- Array resolution of ~ 5 arcmin in approximately the centre of the EoR frequency range. This indicates a maximum core radius of ~ 3000 m.
- Sufficient collecting area to reach the ~ 1 mK brightness temperature sensitivity limit (rms).

Approximately 10-20% of the collecting area distributed so to obtain ~ 100 km baselines[25]. As for SKA1-mid, this has been implemented as three spiral arms.

- Three spiral arms beginning at a radius of 2500 m, with a power-law decrease in spacing between stations on the spiral, out to a ~ 50 km radius from the array centre, thus yielding maximum baseline lengths of ~ 100 km.

6.2.1 Expansion of the Array to SKA2

Figure 6 shows the SKA1-low configuration on the Boolardy site. Section 3.1 discusses two routes the expansion could take, implying one or both of the following: a second array operating at the upper end and/or an expansion of collecting area and baseline lengths at the lower end of the SKA1-low band. Additional possibilities are likely to arise in the future.

If it is assumed that the boundaries of the Boolardy site are not a constraint for SKA2, then there are few topological barriers to expansion of the array configuration.

If a second array operating at a higher frequency range were installed there is available space for a third core on the site, and for additional arms.

If the SKA1 core is greatly expanded in size, it may interfere with SKA1-survey at that time. This may be a reason to consider a location for SKA1-low that is farther away from the SKA1-survey core.

6.3 Antenna Elements

The properties of the antenna elements influence the design of the array. Three types of elements were considered:

1. Droopy dipoles with λ_0 equivalent to 65 MHz (“long”).
2. Droopy dipoles with λ_0 equivalent to 100 MHz (“short”).
3. Log-periodic dipole antennas λ_0 equivalent to 125 MHz.²

The first two are patterned after LOFAR droopy dipoles [15] which are mature technology, and the third variety has been specifically studied recently for the SKA [16], but not yet used on a large scale. Additional element types have been studied[47], but they do not at this point appear to be as well suited as droopy dipoles or log-periodic antennas for SKA1-low.

There are two main motivations for the selection of log-periodics. The prime motivation is the frequency range (a high/low frequency ratio of 6:1 or perhaps even a bit more). With one array this element enables coverage from ~ 50 MHz to 300+ MHz.

The second motivation is the capability to design for a particular gain, within a range of ~ 6.5 to >10 dBi. There is essentially a trade between more gain, which provides greater A/T for a given number of elements and sky coverage of the array. Or for a given A/T requirement, fewer elements are needed if each one has higher gain (but sky coverage is less).

² In the case of droopy dipoles λ_0 is the resonant wavelength of the dipole. In the case of log-periodic antennas, λ_0 is the resonant wavelength of the longest radiating element.

Further description of these element designs is given below and in the references. Useful formulae for the analysis of the designs are given in Appendix B.

6.4 SKA1-low with Log-Periodic Dipoles

Log-periodic antennas belong to a family of self-similar designs whose most important feature is wide bandwidth ratio (ratio of upper to lower frequency limits). The antennas considered here in this baseline design are log-periodic dipole antennas [16], which consist of half-wavelength dipoles of different dimensions spaced along a boom and fed by a transmission line. The operating frequency ratio, which can be as much as 6:1, is determined mainly by the ratio of the lengths of the longest to shortest dipoles. This feature will enable SKA1-low frequency coverage from 50 – 300 MHz, albeit with a very sparse array at the high end. Like all quasi-resonant structures, effective area falls off as λ^2 . Log-periodic antennas can be designed to have higher directivity than simple dipoles. For SKA1-low, the directivity can range from 7 to >10 dBi. A slight advantage of higher directivity is resistance to interference from low elevation angles.

The extended frequency range, compared with dipoles, will enable SKA1-low and SKA1-mid to connect in frequency, a very important feature of this design.

Log-periodic arrays for SKA1-low are in some respects more “experimental” than droopy dipoles, which have been used at scale in LOFAR, and they will likely be somewhat higher cost to construct. Detailed characteristics when used in arrays must be determined experimentally, especially smooth frequency and beam responses, predictable beams and sufficiently low noise at the high frequency end.

6.5 Element and Station Properties

For the log-periodic arrays the station beamsize (5 degrees) has been set at 100 MHz, close to the centre of the EoR frequency range. The station size and the number of elements per station can be determined (see performance tables).

It has been found experimentally and by simulation [47] that log-periodic antennas do not work well if the element filling factor is greater than 0.7. It is assumed here that if this minimum separation is used, that their performance in the sparse frequency range or in the transition region will be free of resonances or other behaviour that might affect response smoothness in either the frequency or angular dimensions.

6.6 Configuration

Figure 3 shows the distribution of stations with radius, based on a Gaussian distribution with radius. There are 911 stations (866 in the core; 45 in the spiral arms). Note that the distribution reaches 650 stations at a radius of 1000 m, as desired. This leads to a significant over-density in the core.

The total number of antenna elements needed to reach the required sensitivity is 250000 (using an element directivity of 8 dBi).

Figure 4 shows the station configuration at various scales. As for previously proposed configurations, it contains a core of quasi-randomly placed stations in a compact core, surrounded by spiral arms.

The array configuration is meant only to show the general distribution, not the detailed positions of individual stations. Clearly, changes to fit the topology of the Australian site are possible without changing the distribution or its performance.

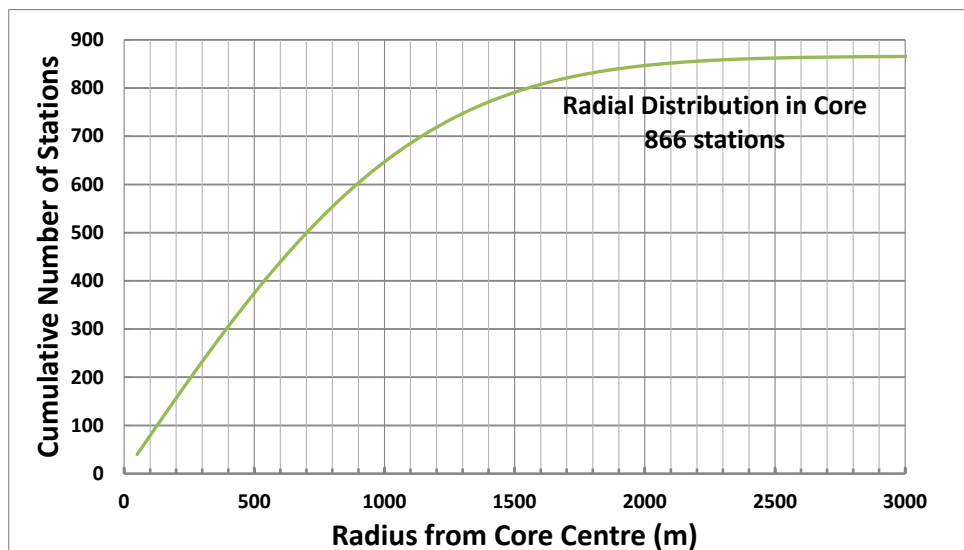


Figure 3 Cumulative collecting area as a function of core radius in the SKA1-low array.

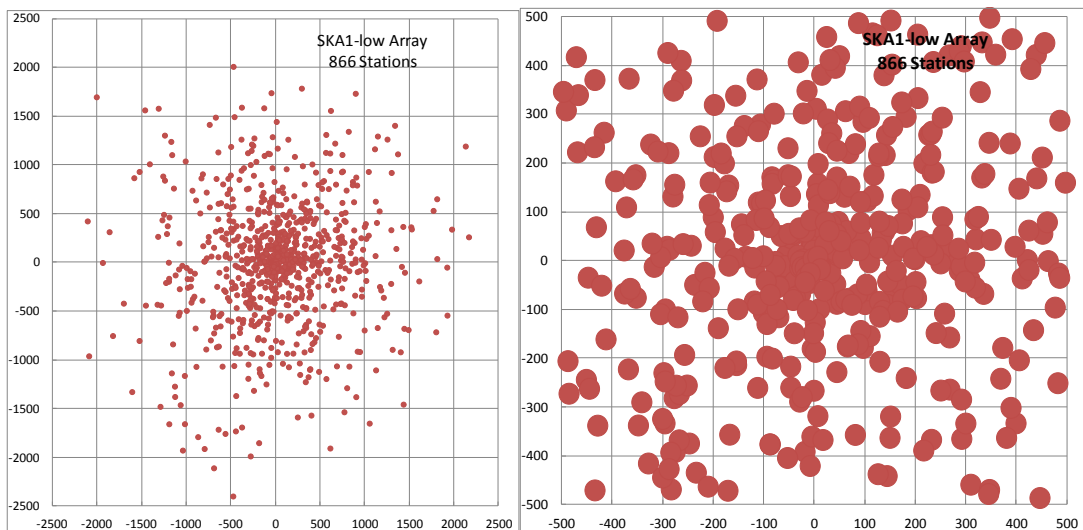


Figure 4 The SKA1-low configuration in the core (35-m diameter stations).

6.7 Performance

Table 2 and Table 3 show the main configuration and performance parameters for the SKA1-low core array, using log-periodic dipole elements. The station size is ~ 35 m.

Table 2 SKA1-low – Log-Periodic Dipoles

| <i>Aperture Array</i> | | |
|--------------------------------|-------------------------------|------------------------------------|
| Lower Frequency | 50 MHz | Dual polarization (2 orthogonal) |
| Upper Frequency | 300 MHz | Single element covering full range |
| Number of antennas per station | 289 | Log-Periodic-Dipole antennas |
| Total physical aperture | $8.0 \times 10^5 \text{ m}^2$ | |
| Area per antenna | 2.25 m^2 | |

| | | |
|--|----------------------|--|
| Element filling factor in station | 0.7 | Areal filling factor |
| Dense/Sparse Transition | 111 MHz | A_e per element is equal to packing density |
| Array Configuration | | |
| Station Diameter | 35 m | |
| Number of stations | 911 stations | 866 in core; 45 in spiral arms |
| Core (radius <600 m) | ~50% (~433 st'ns) | Fractional total number of core stations |
| Core (radius <1000 m) | ~75% (650 st'ns) | " |
| Spiral Arms | ~4% (45 stations) | 15 stations per spiral arm |
| Av'g St'n filling factor (radius <220 m) | 0.91 | Stations must be close-packed or overlapped to radius of 650 m. |
| Station Beam Forming | | |
| Number of beams | 1 | "Average" number of beams per pol'n required to 300 MHz |
| Instantaneous bandwidth per beam | 250 MHz | Assumes full bandwidth is available (50-300 MHz) |
| Digital Outputs | | |
| Sample streams | 2 | Max - sub-bands |
| bits per sample | 8 | Sent from Beamformers |
| Signal Transport System | | |
| Data rate per station | 10 Gb/s * | Optical fibre to signal processor |
| Radius < 3000 m | 8.7 Tb/s | 866 stations |
| 3 km < Radius < 50 km | 450 Gb/s | 45 stations |
| Signal Processing System | | |
| Fine Frequency channels** | 2.5×10^5 | Channel Bandwidth = 1 kHz |
| Complex Correlations | 4.1×10^{11} | $911^2/2)$ baselines x (1) bms x 4 pol'n prod's x 2.5×10^5 chans |
| Complex Correlations: Spiral Arms | 0.4×10^{11} | $(911^2-866^2)/2$ baselines |
| Core (radius<3 km) Dump Time | ~10.6 s | Station diameter = 34 m; max baseline = 6 km |
| Minimum Dump Time | ~0.6 s | Station diameter = 34 m; max baseline = 100 km |
| Science Computing System | | |
| Input data rate (1 kHz channels) | 842×10^9 | Byte s ⁻¹ av'ge from correlator (4-Byte x 2 for complex) (3.8 corr's/10.6 s + 0.3 corr's/0.6 s) x 10^{11} x 8 (8-Byte complex) |
| Input data rate (100 kHz channels) | 8.4×10^9 | Assumes some preprocessing at 1 kHz, then averaging |

* 250 MHz x 2 (Nyquist) x 8 (bits) x 2 (streams) x 1.25 (coding) = 10 Gbit s⁻¹, assuming that channelization and beamforming are carried out at the stations.

*** Assuming that the entire frequency range is channelized at 1 kHz resolution. For EoR observations this can be channel-summed to 100 kHz resolution, possibly after initial pre-processing for interference.

Brightness temperature sensitivity (Figure 5) reaches the 1 mK level for this array, except for frequencies below 110 MHz. At 50 MHz sensitivity is 7 times worse. Improving the low-frequency response is possible, but is likely either to be expensive or to further sacrifice sensitivity at the high end.

Frequency range is shown as 370 MHz. The log-periodic antennas may function at higher frequencies. Additional simulation and/or experimental work will be needed to establish the upper frequency limit.

Sky coverage is reduced, compared to that available for droopy dipoles. This is the price to be paid for more effective area per element and greater frequency coverage. Higher directivity improves sensitivity directly as compared (for a single) object available tracking time per day, which in some sense improves sensitivity only as the square root (lengthens observing time per day).

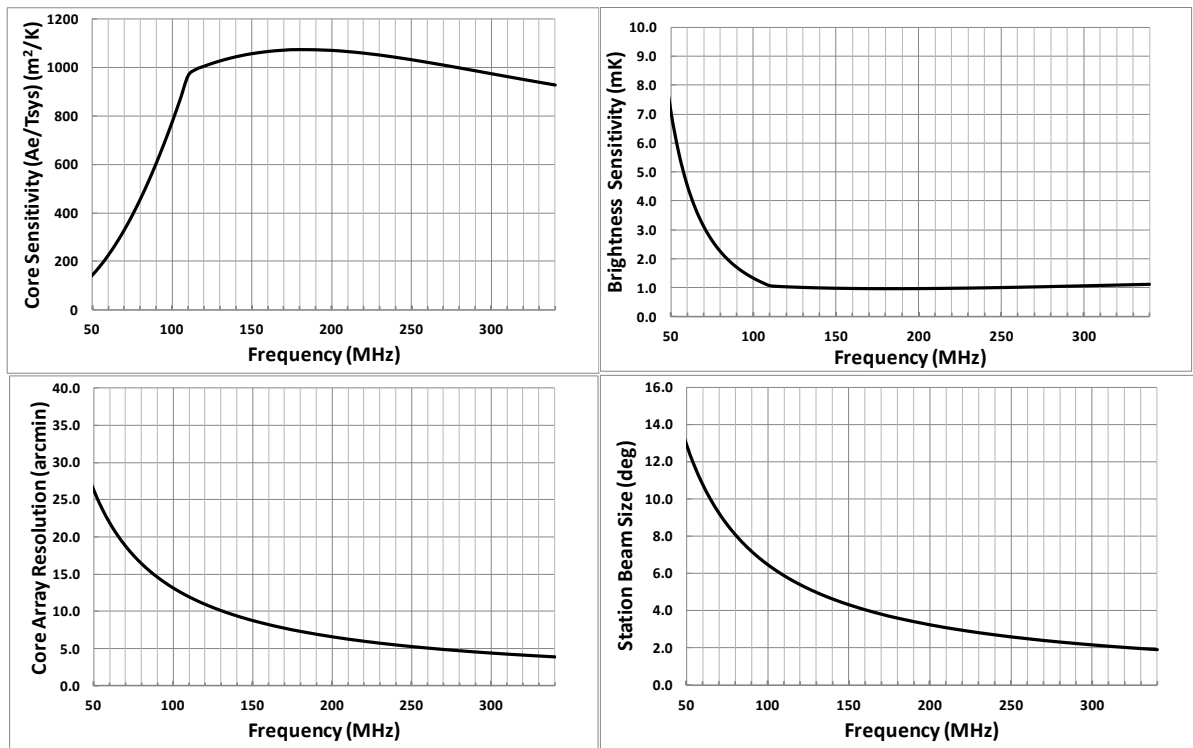


Figure 5 Sensitivity (A_e/T_{sys} and brightness temperature), resolution, and field-of-view of the core array as a function of frequency for the arrays consisting of log-periodic elements.

However, the main driver for sky coverage is range in declinations of sources to be observed. For EOR observations the number of regions chosen for extended observations may be only a few, picked among other things pass close to the zenith. This aspect requires further study. A potential “fix” would be to design the elements to be tilted to lower elevation angles, something that might be carried out only rarely (or even once) for extended observation campaigns at high zenith angles.

Table 2 and Table 3 contain more detailed design assumptions and performance information.

Table 3 Key System Performance Factors for Log-Periodic Dipoles

| | | |
|---|------------------------|---|
| Antenna Radiation Efficiency* | 85-99% | 85% at 50 MHz; 99% at 300 MHz |
| Projection loss | $\text{Cos}(Z)$ | Z is zenith angle |
| T_{rvr} | $0.1T_{sky} + 40$ K | Receiver Noise |
| T_{sys} at 50 MHz** | 5600 K | 5800 K nominal sky noise |
| 110 MHz | 830 | 775 K |
| 160 MHz | 370 | 300 K |
| 220 MHz | 200 | 132 K |
| Station Sys. Equiv. Flux Density (SEFD) at 50 MHz | 19 Jy | Bore sight at zenith |
| 110 MHz | 2.9 | " |
| 160 MHz | 2.6 | " |
| 220 MHz | 2.6 | " |
| Station Beam Area (single beam FoV) @ 50 MHz** | 133 | Bore sight at zenith (deg^2), no taper |
| 110 MHz | 27 | " |
| 160 MHz | 13 | " |
| 220 MHz | 6.9 | " |

| | | | |
|---|-----------------------|--|--|
| A _e /T _{sys} @ 50 MHz, bore sight, all antennas | 144 m ² /K | A _e per antenna element = 3.2 m ² (dense) | |
| 110 MHz | 970 | A _e per antenna = 3.2 m ² (dense) | |
| 160 MHz | 1070 | 1.6 m ² | |
| 220 MHz | 1060 | 0.85 m ² | |
| S _{Bmin} ***@ 50 MHz | 25.1 μJy | 100 kHz bandwidth, 1000 hr integration, 2 pol'n, no taper, no weight | |
| 110 MHz | 3.1 | | |
| 160 MHz | 3.4 | | |
| 220 MHz | 3.4 | | |
| T _{Bmin} ***@ 50 MHz | 7.2 K | 100 kHz bandwidth, 1000 hr integration, 2 pol'n, no taper, no weight | |
| 110 MHz | 1.1 | " | |
| 160 MHz | 1.0 | " | |
| 220 MHz | 1.0 | " | |

* As used in the sense of $A_e = (\lambda^2/4\pi)\eta D$, where A_e is the element effective area, η is the radiation efficiency, and D is the directivity. This formula applies only to frequencies above the dense-sparse transition. For droopy dipoles $\eta = 0.9$ and $D = 6.6$ dBi, independent of frequency in the sparse region, equivalent to $A_e = \lambda^2/3.0$.

** $T_{sys} = T_{rcvr} + T_{sky}$, where $T_{sky} = 60\lambda^{2.55}$.

** $FoV_{beam} = (\pi/4)(1.3\lambda/d_{station})^2$.

*** $T_{bmin} = (\lambda^2/2k_B)(S_{min}/\Omega_{array})$, where k_B is Boltzmann constant, Ω_{array} is the beam area of the array beam. $S_{min} = SEFD_{array}/(\eta_s(2\Delta v \tau)^{1/2})$, where η_s is the system efficiency, Δv is the channel bandwidth, and τ is the total integration time. $SEFD_{array} = 2k_B T_{sys}/A_e$. Note that for a single polarisation $S_{min} = 2k_B T_{sys}/(\eta_s A_e (\Delta v \tau)^{1/2}) = SEFD_{array}/(\eta_s (\Delta v \tau)^{1/2})$, which is $2^{1/2}$ larger for S_{min} .

6.8 Centres of Array Configurations

As noted above, the over-density is partly an artefact of selecting this particular function for distributing the antennas and is not fundamental. Nevertheless, a very compact array is the most cost-efficient way of reaching the brightness temperature sensitivity limit at these frequencies. In a Gaussian distribution overlap occurs out to radii of 220 m.

6.9 Fit to the MRO/Boolardy Site

The boundaries of Boolardy station will contain both the SKA1-survey telescope (incorporating ASKAP) and SKA1-low, the least expensive means of accommodating SKA1 since the station is already leased by CSIRO. ASKAP will be at the core of SKA1-survey, thus fixing its location, and establishing a zone of avoidance for the core of SKA1-low. Mutual interference between the two telescopes is a potential problem, especially since the low-frequency elements have quasi-omnidirectional responses. Separation of ~10 km would provide ~92 dB of free-space loss between them at 100 MHz³, which seems a reasonable estimate of required protection. Stations outside the core are less likely to be a problem because they are less likely to receive an undelayed common interference signal. (Note also, however, that “delay protection” is really effective only with wide-band interference).

Figure 6 shows a preliminary SKA1-low configuration, designed to fit within the boundaries of Boolardy station. One of the outer stations on the East arm has been omitted. Also in Figure 6 is a possible configuration of SKA1-survey, centred on the ASKAP array. The centre of the SKA1-low

³ Using the standard relation, Free-space Loss (dB) = 32.45+20log(d)+20log(f), where d is distance in km and f is frequency in MHz.

array is about 11 km from ASKAP antenna 1. Figure 6 illustrates that both arrays may fit within the Boolardy station, even if both have ~100-km maximum baselines. The angles of the SKA1-low spiral arms have been adjusted to approximately fit within the boundaries of the Boolardy station (blue lines).

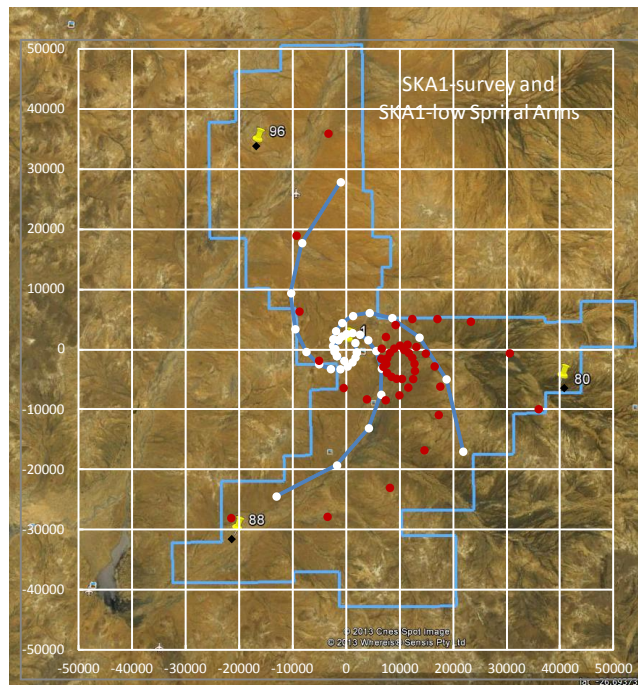


Figure 6 SKA1-low configuration of stations (white dots) on a Google Earth image. The red dots are a potential configuration for SKA1-survey, incorporating ASKAP.

6.10 Front-end Amplifiers and Receiver Noise

Front-end receiving amplifiers for the sky-noise dominated regime (see Section xxx) are designed to essentially “sniff” the signal (ie, most of the signal is reflected). The model for amplifier noise used in this document is a contribution of 10% of sky noise plus a constant 40K. This is sufficient for frequencies below ~250 MHz.

At frequencies above 250 MHz, sky-noise is less dominant; front-end noise is significant, and a “noise-match” design is required. This indicates a specialised amplifier design that satisfies both low and high frequency requirements.

For log-periodic antennas, special attention will be needed to make the frequency response smooth (i.e. free of resonances or rapid changes as activity switches between dipoles).

6.11 Digital Data Back Haul

The purpose of this part of the system is to transport digital data from the AA-low stations to the input of the SKA1-low correlator located in the central signal processing centre. If possible, the processing centre will be located at the same site as the current ASKAP central processing building. If indicated by cost analysis, it may be located closer to the SKA1-low core. As for the other

telescopes, it will be a point-to-point deterministic optical network in which the data flows unidirectionally from the array station nodes to the central processor.

The physical layer network on the output of the nodes within the array will be based upon single mode fibre optic cable. The connective architecture of these links is likely to be a star configuration, although requirements derived from the operations plan and safety critical functionality may drive the design to additional link redundancy.

As noted in Section 6.6 , the SKA1-low core will contain much of the collecting area in close-packed formation. Thus a “global” cost optimisation of the number of enclosures for beamformers, the delivery network of power, delivery network of signals from the array elements, and digital data backhaul from the enclosures to the central signal processing centre is clearly indicated.

6.12 SKA1-low Central Signal Processor

Figure 7 is a context diagram for the central signal processor for SKA1-low on the Australian site. The signal processor, itself, handles the following main functions: delay correction, channelization in frequency and correlation. In a design, these functions may be combined or carried out in stages (e.g. coarse and fine channelization). These are outlined in subsequent sub-sections, although not in “design detail”. The data from the array stations will be delivered optically to interface cards at the input of the signal processor system. In some renditions of a design, the optical signal may be split and delivered to more than one place.

In addition there may be other functions provided. For example, an external transient trigger to permit the delay buffers to be stored when a transient is suspected to have occurred; a stream of a small fraction of incoming data streams could be provided in raw form to a facility for experiments to be carried out that cannot be precisely defined in advance.

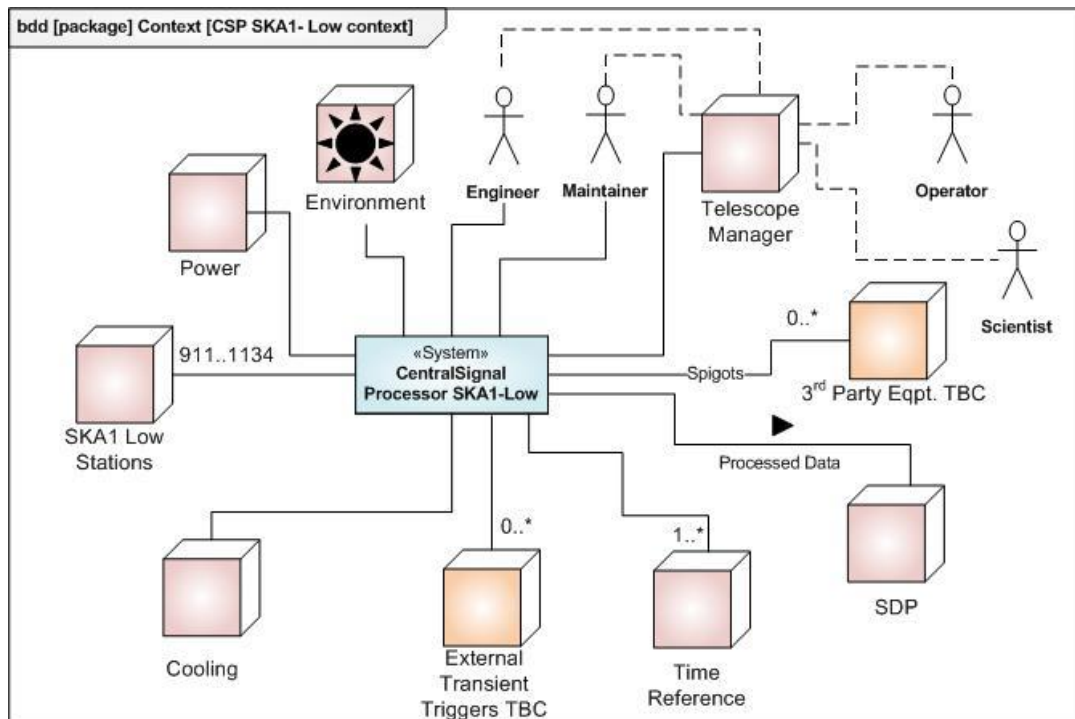


Figure 7 SKA1-low Context Diagram - Central Signal Processing

This section details the signal processor and computing equipment present at the Central Processing Facility for the SKA1-low telescope. Figure 7 provides a complete context diagram. Some aspects detailed in the SKA1-survey and SKA1-low context diagrams may be common due to the likely co-location of equipment and common infrastructure but this is not currently assumed.

Transient triggers and 3rd party equipment are optionally detailed but may not be present in the final design. Third party equipment potentially includes (but may not limited to) transient processors.

It should be noted that flexibility in the configuration of AA-low arrays, in terms of the number of contributing elements, is identified earlier in this document. It is assumed that 1134 stations is the upper limit and that any reconfiguration will reduce the number of stations. The prospect of having more than one beam for the larger stations potentially has an architectural impact on the correlator.

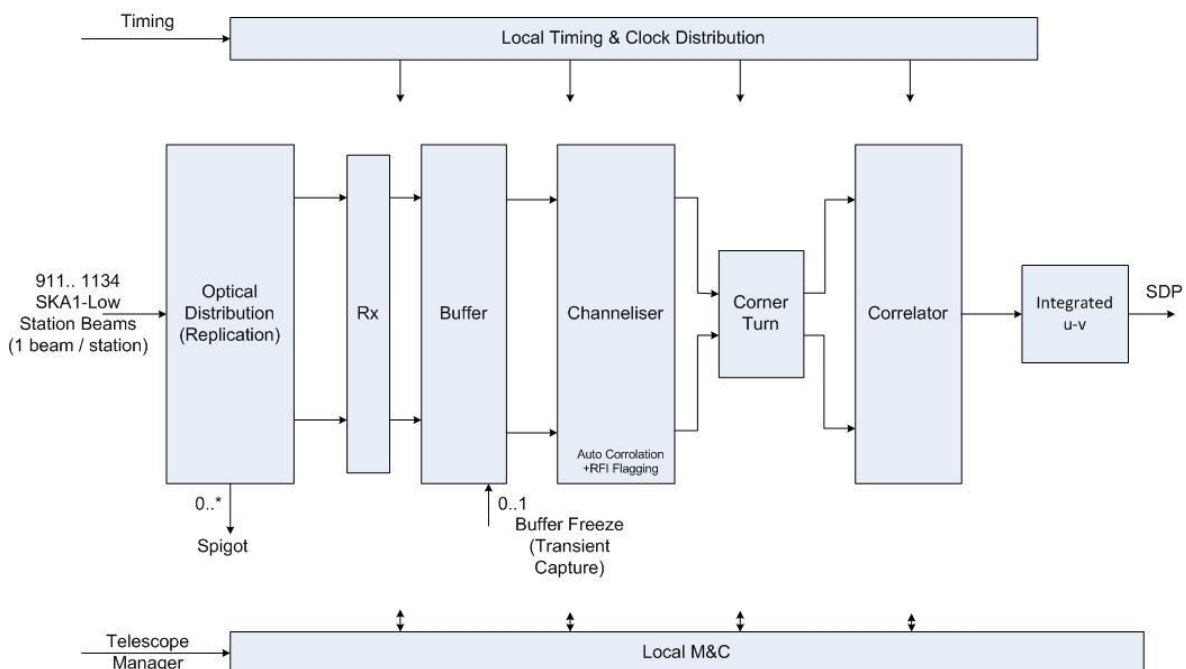


Figure 8 SKA1-Low Correlator Functional Architecture

Full Stokes correlation (I,Q,U,V) is provided by the SKA1-low correlator in the form of a set of integrated product-pairs of like signals from the array stations (u-v data-points or visibilities) for each frequency channel. Table 4 shows key data flow and loading parameters for the SKA-low correlator. Note that delay correction and some channelization is required before correlation can be performed on the data. Final channelization can also be carried after correlation in some designs. Figure 8 shows an FX implementation of the functional architecture which is commonly regarded as the most efficient. This readily maps to differing technology including ASIC, FPGA and Software implementations.

The processing load for a large correlator is dominated by the product, N^2B , where N is the number of antennas inputs being correlated and B is the total bandwidth.

The output data rate from the correlator is a critical factor in the loading of downstream science data processing and in transmitting data to the science processing centre. This rate depends upon the integration time (dump time), which in turn is proportional to the radius of the processed field-

of-view and the length of the particular baseline in wavelengths. There is typically some tolerance of coherence loss (smearing) at the edge of the field. For the purposes of design it is taken as 2% in this document, but it can be adjusted at observation time. Since the baseline length is variable, there are opportunities to integrate longer for many of the baselines in the array, thus reducing this rate. The correlator will be capable of generating more data than can be handled downstream. The maximum rate depends on the science program, particularly whether full-field imaging is required at the longest baselines at the lowest frequencies.

Table 4 Correlator Parameters for SKA1-low

| Correlator SKA1-Low Log Periodic Option | | |
|---|----------------------|--|
| Fine Frequency channels*** | 2.5×10^5 | Channel Bandwidth = 1kHz |
| Actual channelisation | 262,144 | As power of 2 for FFT: 2^{18} |
| Channeliser stop band rejection | >60dB | > Telescope spectral dynamic range |
| Complex Correlations | 4.1×10^{11} | $911^2/2$ baselines x (1) bms x 4 pol'n prod's x 2.5×10^5 chans |
| Complex Correlations: Spiral Arms | 0.4×10^{11} | $(911^2-866^2)/2$ baselines |
| Corr. Load Factor for 250 MHz bandwidth | 1660 T MACS | $911^2/2$ baselines, 1 beam |
| Core (radius<3 km) Dump Time**** | ~10.6 s | Station diameter = 34 m; max baseline = 6 km |
| Minimum Dump Time | ~0.6 s | Station diameter = 34 m; max baseline = 100 km |

6.13 SKA1-low Science Data Processing

SKA1-low is a challenge for data processing for a number of reasons. First, the receptors (stations composed of dipoles) are not as simply behaved as parabolic dishes and so more effects must be modelled in the imaging process. The dipoles see nearly all the sky, with strong polarization effects, and the stations continuously changing shape as seen from the sky. Second, at the low frequencies needed for the EoR observations, the ionosphere becomes non-isoplanatic on baselines of more than 5-10 km. Third, the sky is bright at all frequencies, consisting of large numbers of discrete sources off the Galactic plane, and with strong structure added on the Galactic plane. Fourth, the EoR signal is intrinsically very weak.

The various SKA pathfinders that are targeting EoR detection are addressing these problems. Recent test observations with LOFAR [27] show sensitivity close to the thermal noise for a moderate-duration observation. However, observations planned for EoR must go a factor of ten deeper. To do so will require overcoming time-variable station beams and the ionosphere. Algorithms to do just this are in development [26] but the computation load becomes even more daunting because of the necessity to recalculate the effects of the time-variability every 10-30 seconds.

7 Reflector Antennas

Reflector antennas are used for both SKA-survey and SKA-mid. Ideally the same antenna will be used for both single-pixel and phased-array feeds. Slightly different antennas may be required for the two feed applications or in the very non-ideal case, completely different ones. This aspect is discussed in Section 8 (SKA1-mid). In most other respects, this section applies to both cases.

The selected antennas are 15-m projected diameter, offset Gregorian optics, and designed for very high A_e/T_{sys} per unit of currency. Table 5 contains a summary of the most important requirements. The following are important qualitative characteristics required for SKA1 antennas:

- High aperture efficiency.

- Excellent pointing.
- Excellent stability of key parameters (beam shape, pointing, etc.).
- Smoothness of response in spatial and spectral dimensions, as limited by fundamental physics (e.g. edge diffraction). Scattering objects tend to generate low-level resonances, which will have relatively fine frequency structure and/or chromatic sidelobes.
- Space at the focus for five independent receivers.
- Very low sidelobes beyond the first one.
- Excellent polarisation performance.
- Circular beam.
- Excellent performance down to ~450 MHz, good performance to 350 MHz.
- Excellent performance to 15 GHz, good performance to 20 GHz.

Table 5 Subset of Dish Performance Requirements

| | | |
|---|--------------------|---------------------------------------|
| Equivalent physical aperture diameter | 15 m | |
| Low Frequency | 350 MHz | |
| High Frequency | 20 GHz | |
| Optics | Clear aperture | |
| Efficiency | >77 % | |
| Total spillover noise | 3 K | L-band |
| Other losses | <2 K | L-band |
| 1 st sidelobe | -21 dB | |
| Far-out sidelobe level | <-50 dB | |
| Polarization purity | -30 dB | Within HPBW |
| Beam symmetry | TBD | |
| Receivers | 5 | Cryo-cooled, spanning frequency range |
| Elevation limit | <15 deg | |
| Azimuth range | ±270 deg | |
| Pointing repeatability | 10, 17, 180 arcsec | P, S, D respectively arcsec, rms |
| Receiver noise temperature & Feed Losses | <15 K | Assumed for performance estimates |
| Classes of Environmental Operating Conditions | Precision | Wind <7 m/s; night |
| | Standard | Wind <7 m/s; day |
| | Degraded | Wind <20 m/s |
| Operation | continuous | Except for extreme weather. |

7.1 Receiver Cryo-cooling and Noise

Cryo-cooling of receivers for SKA1-mid is essential to reach the system temperatures required for performance indicated here. All current major radio telescopes utilise cryo-cooled receivers, but in the case of SKA1, the numbers of receivers required is unprecedented. Hence a much greater emphasis on operational cost, including maintenance, is needed. An initial cryogenics study was carried out in 2012 to examine options and to develop a cost model for the SKA [20]. The main conclusion of this study is for a given requirement for A_e/T_{sys} performance, that cooling of receivers to physical temperatures between 20 and 100 K is cost effective by a large factor. The optimum temperature depends on the contributions of operations costs (electricity and maintenance), dish capital cost, and the fraction of total system cost attributable to the dishes. Various forms of Stirling and more traditional Gifford-McMahon coolers were evaluated. As would be expected, the higher the system cost per dish, the more cost-effective cryo-cooled receivers become. Or for a given A_e/T_{sys} , fewer dishes are needed when the receivers are cooled.

Innovative new techniques, such as low vacuum insulation, combined with practical approaches to design have been described [20] but not been developed at the scale needed for the SKA.

For dishes that have been carefully optimised to provide low spillover noise (~ 4 K), the other controllable sources of noise, principally receiver noise (LNA, OMT, waveguide), must be kept low to realise the overall capability of the antenna.

8 SKA1-mid

The primary science cases for determining the required performance of SKA1-mid are:

1. Use of the 21-cm HI-line to study the evolution of galaxies, both local ($z \sim 0$) and high redshift, both in emission/absorption for local galaxies and in mainly in absorption against continuum sources for high redshift galaxies. The maximum redshift will depend on the lowest useful frequency of the dish array and on the sensitivity of the array at the high-redshift end.
2. A survey of the entire visible sky for pulsars to a pseudo-luminosity depth of 0.1 mJy kpc^2 at 1400 MHz out to a distance of 10 kpc. Regions defined mainly by dispersion-measure will determine the optimum frequency ranges for each one: Galactic plane, Galactic centre, off-Galactic plane (higher Galactic latitudes).
3. Follow-up observations of detected pulsars at high resolution (<20 mas resolution).
4. Carrying out a decade long timing campaign to time most detected pulsars and others.

8.1 Key Design Parameters

The following summarises the key open design parameters and the constraints for SKA1-mid. Further details are provided in subsequent sections.

1. *Array Configuration:* The array configuration is constrained entirely by the need to incorporate the MeerKAT antennas, for which the array configuration is pre-defined. The only way to expand this array is to share the same core location, and to in-fill with SKA1 antennas (i.e. a dual core array would produce an unusable synthesised beam). As an “existence test”, it is shown below that a good facsimile of the previously worked-out array configuration can be accommodated under this constraint. Moreover, a reasonable plan to expand the array to several thousand antennas, as expected for SKA2, can be carried out utilising the SKA1 (and possibly the MeerKAT) antennas.
2. *Frequency Range:* SKA1-mid should ideally link up in frequency range with SKA1-low, and be capable of being extended to the highest frequency sustainable on the South African site for SKA2. For SKA1 emphasis is on the bands below 1420 MHz (the HI line at rest) and on bands best suited to pulsar detection and timing. Further information is contained in Section 7.3.1.
3. *Sensitivity:* Sensitivity is essentially defined by the affordability of the system per dish. The previously defined target for SKA1 was 250 15-m dishes, now including the incorporation of 64 MeerKAT dishes. The array considered in this document consists of 190 + 64 dishes. Given this assumption, sensitivity (both A/T and survey speed forms) is determined by sources of noise and receiver bandwidth, subject to data transport and processing capability (both signal and science data).

4. *Polarisation capability:* This is essential to properly calibrate the telescope. It is also fundamental to pulsar timing, at least at the field centre. For imaging observations (continuum and spectral line), instrumental polarization must be accurately characterized across the processed field-of-view, which may be larger than the science field-of-view.
5. *Sky Coverage:* Given the latitude of the site, sky coverage depends upon the minimum elevation of the antennas and to some extent on “shadowing” of one antenna by another in the array. Sky coverage is a “soft” requirement, in the sense that coverage of lower elevations is desirable but not easily quantifiable. Moreover, the large air column at low elevations quickly erodes sensitivity at high frequencies and to a lesser extent the ionosphere produces a similar effect at low frequencies. Potentially, VLBI observations at near Earth-diameter baselines would be the main beneficiaries of coverage to the horizon.
6. *Extension to SKA2:* Extension of the core array configuration to SKA2 is discussed below. In addition, plans for SKA2 will have to include extension of the collecting area in the arms out to ~180 km in the “connected array” and also to very long baselines. This kind of extension has little impact on the design of SKA1, and will not be considered further.

A key requirement is to retain upgrade flexibility in designing the dishes so that receivers can be individually replaced. It is unlikely that the SKA1 dishes will be equipped with a full suite of receivers. In SKA2 it is assumed that additional receivers will be needed. The receiver “slots” have been populated with this in mind, although there is also a distinct possibility that receiver bands will be completely re-arranged for SKA2.

8.2 Array Configuration

Prior to the site selection process, the SKA1 configuration was common to both SKA1-mid and SKA1-low. This distribution has been retained as the baseline for SKA1-mid. It is strongly centrally condensed to support pulsar searching observations and has reasonably good *u-v* coverage for imaging. The collecting area is allocated approximately as a scale-free distribution of baselines (ie, not favouring any particular angular scale), which requires a power-law decreasing density of collecting area with radius.

Two components of the configuration (Figure 9) are defined: the core, consisting of a central condensation of antennas, quasi-randomly distributed in a broadly symmetric array; the spiral arms of which there are three for SKA1. The spiral arms are a subset of the five spiral arms planned for SKA2.

The following are additional features of the baseline design SKA1-mid array configuration:

1. The SKA1-mid array will be centred in the same location as the MeerKAT array and utilise the MeerKAT dishes.
2. There will be 133 SKA1 dishes in the core. In addition there will be 64 MeerKAT dishes out to a radius of 4 km.
3. The configuration of collecting area within the SKA1 core and inner regions will be a subset of locations designed for SKA2, but they will not be in the SKA2 core (see below).
4. Each spiral arm will extend from 2500 m to 100 km from the centre, and contain 19 antennas (57 total in spiral arms).

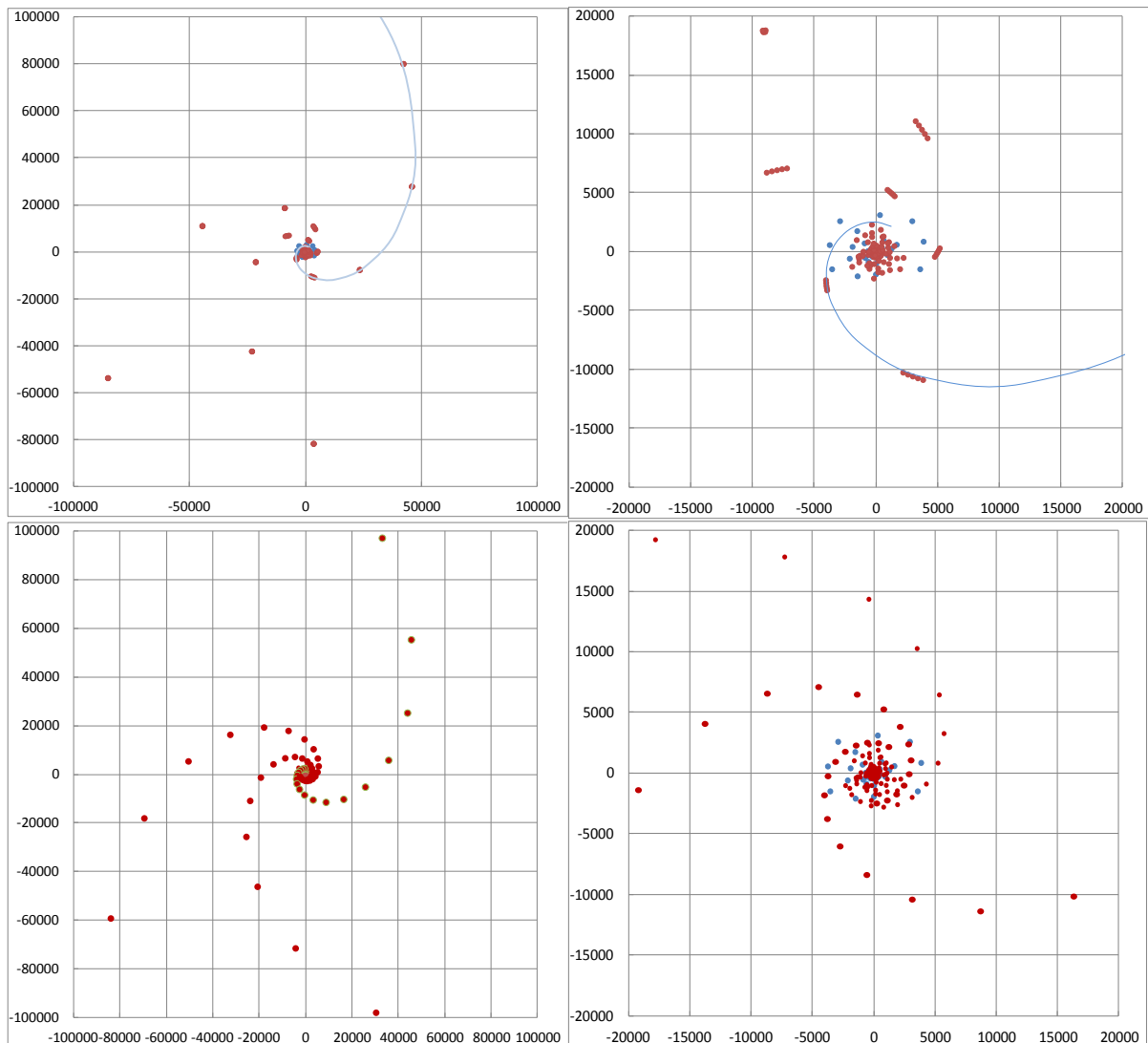


Figure 9 SKA1-mid array configurations for dishes at 100 km (left) and 20 km scales (right). SKA dishes are shown in red; MeerKAT dishes in blue. Top panels: The generic SKA1 configuration with clumped spiral arms. The red dots beyond a radius of 2.5 km are clusters of 5 antennas. The blue line is a spiral “generator” line. Bottom panels: An SKA1 configuration in which the clumps in the spiral arms have been replaced by evenly spaced (in the logarithmic sense) antennas.

Figure 10 shows the sensitivity of the telescope at different baseline scales, where the density of baselines in different length intervals is a proxy for sensitivity at different scales. This plot applies only to “snapshot” sensitivity, since Earth rotation will generally create elliptical u - v tracks that tend to fill in gaps. The “envelope” of baseline density shows the power-law fall-off with radius, as expected for a “scale-free” configuration. When normalised by wavelength, this figure can be used to provide a rough performance indication for observations of sources with differing angular scales. The dips in sensitivity at 8000, 40000, and 70000 m are likely the result of clusters of collecting area; these would be filled in if the clustered antennas were spread out along the spiral arms. There is also a deficit of baselines at short spacings, which may affect sensitivity to extended emission.

Figure 11 shows the u - v coverage plots for the SKA1-mid array: an 8-hr observation centred on the meridian, field centre passing through the zenith. The dimensions of the left box are ± 160 km E-W

and ± 200 km N-S. The right box, showing u - v density in the core region is ± 6.5 km E-W and ± 6 km N-S. In both cases, a 20% fractional bandwidth is used.

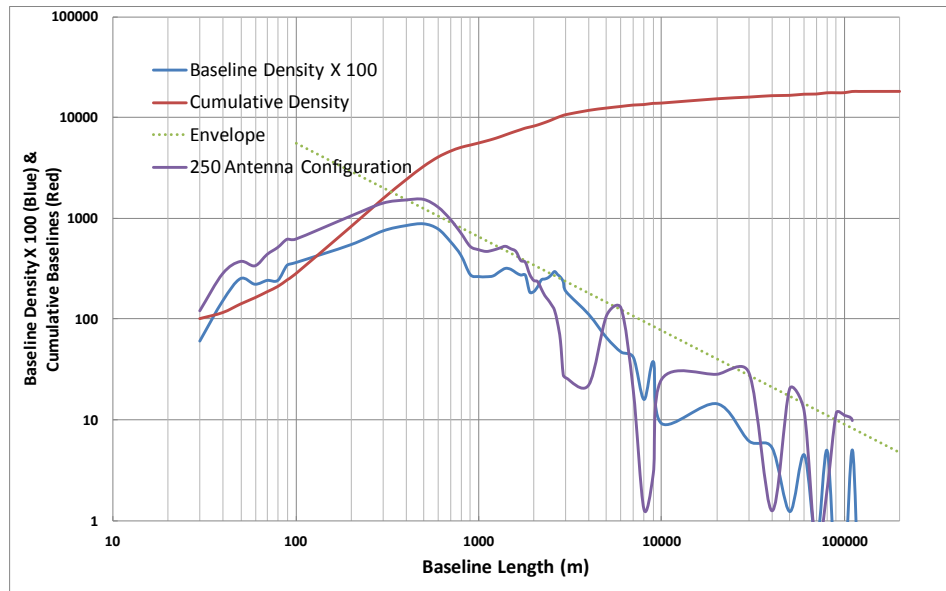


Figure 10 Distribution of baselines for SKA1-mid. The purple line is from the configuration containing 250 and clumped spiral arms. The blue line is for a configuration containing 190 antennas and logarithmically distributed antennas on the spiral arms.

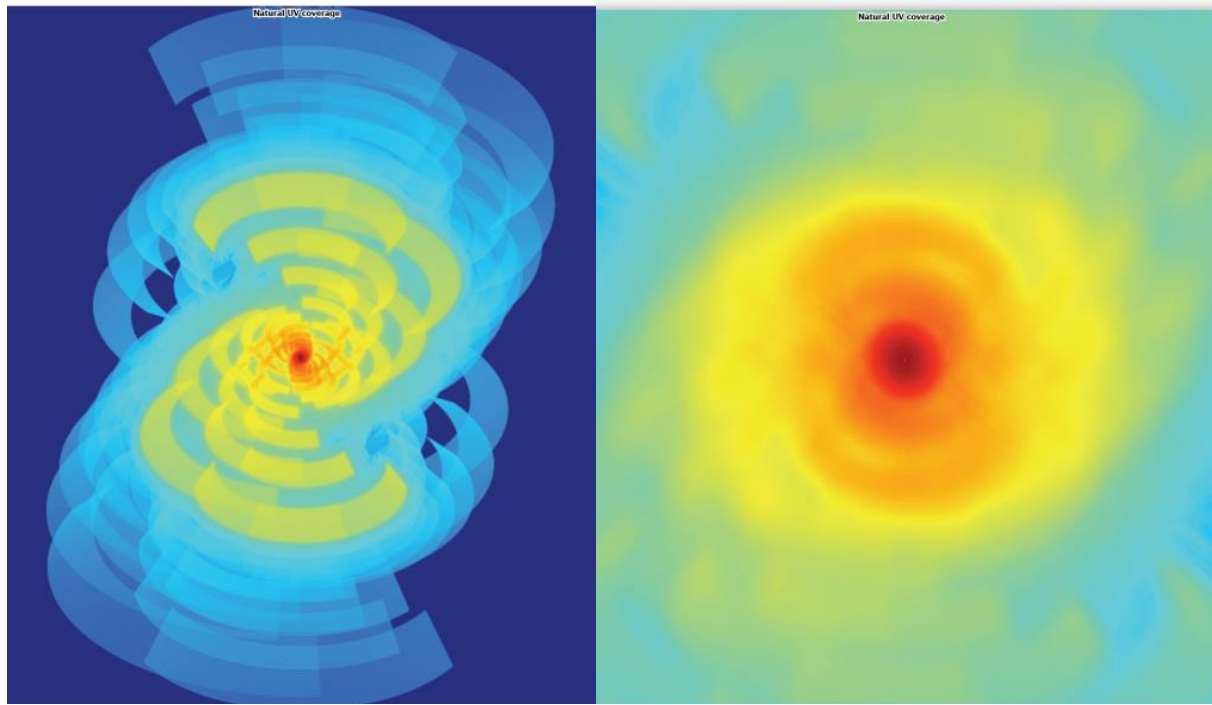


Figure 11 u - v coverage for SKA1-mid. In general these antenna positions are representative, and not optimised. In particular, the u - v coverage would improve if the maximum baseline were 100 km instead of 200 km. The very strong emphasis on core density enables a sensitive pulsar survey to be done, but results in patchy u - v coverage, especially for short, narrow-band (spectral line) observations at medium and long baselines. On the other hand, as is demonstrated in Figure 10, the u - v coverage out to about 6 km is very dense.

8.2.1 Site Topology

The generic configuration, shown in Figure 9, does not match the topology around the SKA1-mid site, and may also have to be adjusted for exposure to local sources of RFI. Figure 12 (right) shows the SKA1 generic configuration at relatively large scales. This illustrates that there is enough space between dishes in the core, even if no “black dot” dishes were deleted from the configuration. In practice, MeerKAT dishes would be substituted for an approximately equal number of dishes in the generic SKA1 array.

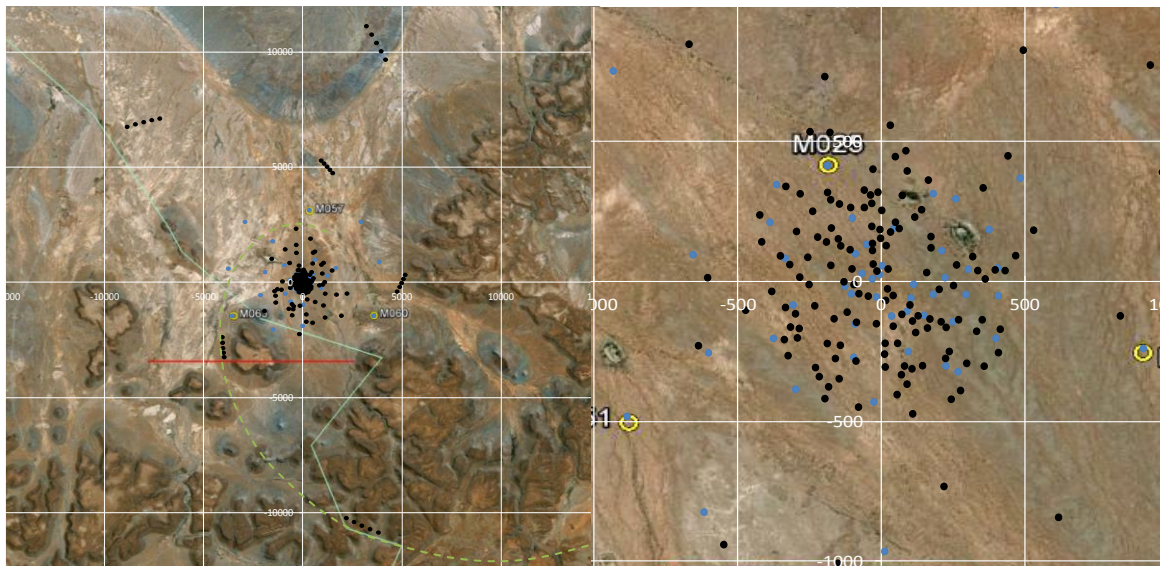


Figure 12 The generic SKA1-mid configuration superimposed on the site topology. No attempt here has been made to adapt to the landscape or other mask components. The black dots are SKA dishes; blue are MeerKAT dishes. The black dots are drawn from a 250-dish configuration and represent an over-density in the core.

In the spiral arms, the array configuration will have to be first optimised by rotation, and then individual clusters relocated to fit the topography. If the shifts in position are not large, then the array performance will be unaffected. Actually randomising the positions of clumps could improve the $u-v$ coverage.

8.2.2 Progression to SKA2

Figure 13 shows the generic SKA2 configuration superimposed on the SKA1 and MeerKAT antennas, centred on the MeerKAT position. This illustrates a means by which the system could expand from SKA1/MeerKAT to SKA2. The offset direction is chosen to the Northwest because the topology in that direction provides less obstruction.

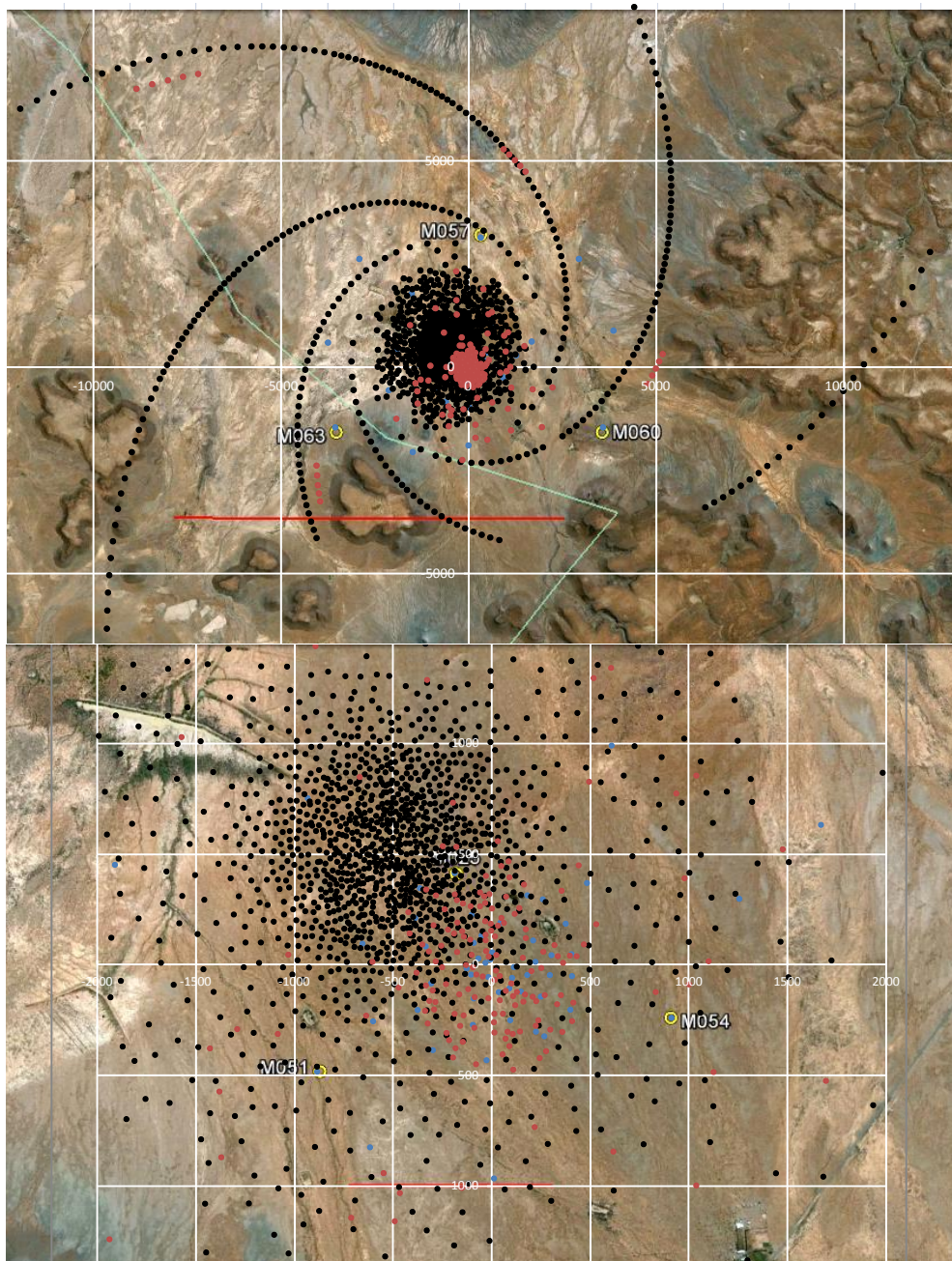


Figure 13 The generic SKA2 configuration with the SKA1 configuration embedded in a position in which the antenna densities of the two configurations are matched. Red dots are SKA1; blue are MeerKAT; black are SKA2 antennas.

These diagrams are illustrative only; they are not optimised in detail. As noted in the next section, investigation will be needed of the practicalities of extending the services to the new antennas in the SKA2 core while SKA1 is in operation.

8.3 Receiver Bands

For SKA1 it is assumed that between 3 and 5 feeds are available and can be fitted for each antenna. To cover key SKA1 science, only the two lower-frequency feeds need be populated, although that would leave out pulsar searches at the Galactic centre, which would require a much higher

frequency. Ultimately, it is important to cover the largest frequency range possible, and to be able to provide low-frequency coverage to connect with the high-frequency end of SKA1-low. The lowest frequency easily feasible for offset Gregorian dishes at the secondary focus is 300 – 350 MHz, where the efficiency is dropping quickly and feed sizes are large. This will provide continuous frequency coverage from SKA1-low to SKA1-mid. Dishes can be designed to handle frequencies up to 20 GHz without incurring a major cost penalty. The dishes must be designed to support both SKA1 and SKA2 science. SKA2 will ultimately require frequency coverage up to a limit fundamentally imposed by tropospheric effects on the chosen sites. This is a somewhat soft limit, but it is reasonable to expect that the dishes will be expected to operate efficiently at 20 GHz in the best observing conditions (night, low wind). The most advanced candidate dishes can achieve aperture efficiencies of ~78% and spillover noise temperatures of <4 K [22] over much of the required frequency range. For this reason the receivers will have to be cryo-cooled to achieve commensurately low receiver noise.

Figure 14 shows a set of frequency bands and feeds for the SKA antennas. In selecting these feeds the following considerations have guided the process:

Science considerations:

- Continuous frequency coverage from ~350 MHz to ~> 14 GHz is important for spectral line observations in the cm-wave bands. In the final SKA1 system this may only be achieved with gaps, but provision should be made so that these gaps can be cleanly filled, either through upgrades to SKA1 or through SKA2.
- The coverage from 1420 to 350 MHz corresponds to a redshift range for HI-line observations of 0 – 3.1. In principle, higher sensitivity at the larger redshifts would be ideal, but sky-noise, ionospheric effects, and lower dish performance conspire to push sensitivity in the opposite direction. It is not necessary to cover these in one receiver band, since the amount of integration time per observation point will typically be much larger for the low frequencies.
- The ideal frequency range for pulsar searches varies with the dispersion measures (DM) in the region being searched, the amount of interstellar scattering and to some extent with the type of pulsar (millisecond or normal): Scattering in the Galactic centre region requires frequencies above 10 GHz, but the size of the region is very small. The Galactic plane, where most millisecond pulsars are likely to be found, requires frequencies centred at 800 MHz (Smits et al paper). Lower frequencies, around 400 MHz, are indicated for the higher Galactic latitude regions, where the electron column densities (hence DMs) are lowest. The instantaneous bandwidth that can be utilised depends on the frequency and the range of dispersion measures (DM). Provisionally, a 400 MHz bandwidth is assumed for the Galactic plane, centred on 800 MHz and a 100 MHz bandwidth centred at 450 MHz for the Galactic latitudes higher than $|b| = 5$ degrees. Much larger bandwidths at frequencies greater than 10 GHz will be needed for sufficient sensitivity.

The optimum frequencies will be modified in practice by the sensitivity, survey speed, sky coverage, and availability of telescopes at the relevant frequencies. Within limits, the

receiver bands selected for SKA1 should enhance the optima as much as possible. Some overlap of frequency bands may be indicated for pulsars.

- The best frequency range for pulsar timing is between 0.8 and 2 GHz, except of course in special circumstances like the Galactic centre.
- The best possible continuum performance is required at frequencies between ~1 GHz and ~5 GHz, where the atmosphere-ionosphere combination is most favourable. An optimum combination, which may change with time, of instantaneous bandwidth and system sensitivity is required. The scientific impact of SKA2 will depend upon the ability to make ultra-deep images (rms noise of <10 nJy) in continuum so that identifications and comparisons with deep images in optical/infrared can be made.
- Apart from the HI-line, a key spectral line series are the OH-lines that span the frequencies from 1612 to 1720 MHz, with the most frequently observed lines near 1665 and 1667 MHz (rest frame).

Instrumental considerations:

- The best feed/dish system sensitivity can be realised using horn designs if the bandwidth ratio is no more than 1.8. Note that good polarisation purity across the entire beam area plays a large role here. However, if wider bandwidth feeds become available in the future, then these feeds can be replaced with others.
- Since at lower frequencies sky noise is a greater factor, receiver noise can be higher and efficiency can be lower without a significant effect on overall performance. At the lowest frequency it is important to provide a relatively compact feed (although it will still be larger than any other feed). At the frequencies below ~400 MHz, the optics design will limit the efficiency and spillover noise, even with a large feed. For example, with a small sacrifice in efficiency, a quad-ridge feed design is both fairly compact and has the potential for wide bandwidth. A 3:1 feed design has been selected here. Other feed designs, such as an Eleven feed [49] may also be suitable.
- At the highest frequencies the atmosphere contributes a small amount of additional noise. A 3:1 receiver has been selected here, which does not represent a large reduction in performance but offers a lot of frequency range (and bandwidth) in one package. For example, the Australia Telescope has recently been equipped with feeds that cover 4-12 GHz.
- Feed system flexibility: Once the dish designs are fixed, the main avenue for improvement of the system is by replacing feeds and receivers with better models. A critical design requirement for SKA1 dishes is the capability to allow this to be done with as little interference with other parts of the system, especially other feed bands.

- Wide-band Single Pixel Feeds (WBSPF) with a relatively modest 3:1 bandwidth ratio have already been assumed in the feed line-up; indeed they exist and are operational at the ATCA in the 4-12 GHz band. Particularly at the low frequencies it will be useful to have more overlap with the L-band feed (Band 2), if this can be done without sacrificing performance. This is a reasonable possibility since there is no direct proportionality between bandwidth ratio and performance in these WBSPF designs. At the highest frequency it would be even more beneficial to extent the frequency range at the upper end. It would also provide the possibility of more overlap of bands at the intermediate frequency.
- Figure 14 also shows the MeerKAT frequency bands. Since the SKA1-mid array will contain both MeerKAT and SKA1 antennas, the frequency ranges must overlap. There is also the possibility that changes or additions to the MeerKAT receivers can be made to increase their frequency range. Only the L-band receiver is in the final stages of design, and there may be opportunities to make changes to the UHF and X-band receivers (see Figure 14).

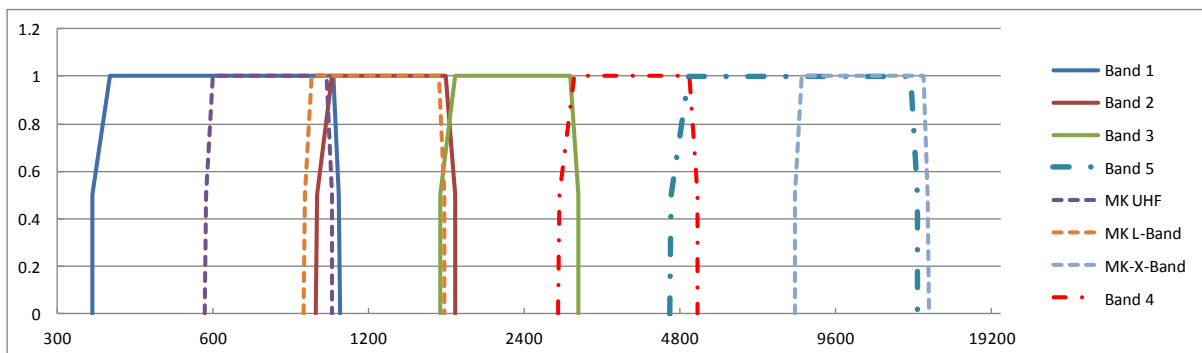


Figure 14 Receiver bands for SKA1-mid (solid and dash-dot), shown with the planned receiver bands for MeerKAT (dashed). SKA1 bands are numbered 1-5. The band-edge frequencies are provided in Table 6.

8.4 SKA1-mid Overall Performance

The following sub-sections provide a performance view of the SKA1-mid telescope. It is assumed that MeerKAT will be operating as a separate telescope until the construction of SKA1-mid begins. The MeerKAT antennas may be operated separately after construction if they are the only antennas with X-band receivers.

Section 8.4.2 describes the performance of the combined array. Combining two arrays is a very complex activity, and numerous assumptions must be made to make progress in describing the “shape” of the system, and in estimating performance and cost.

8.4.1 The SKA1 Antenna Array

Based on the configuration described in Section 8.2 and the receiver bands described in Section 8.3, Table 6 describes the other properties of the array of SKA1 antennas only. Table 7 describes its performance.

Table 6 SKA1-Mid Array

| | | |
|---|-------------------------|--|
| Aperture | | 190 x 15-m (equiv. dia.) offset Gregorian reflectors |
| Total physical aperture | 33576 m ² | |
| Antenna Aperture Efficiency* | | |
| 300 MHz | ~60 % | Gradual degradation to 400 – 300 MHz |
| 400 MHz | ~65 % | |
| 600 – 8000 MHz | ~78 % | |
| 8 – 15 GHz | 70% | |
| 15-20 GHz | ~65 % | Gradual degradation to 15 – 20 GHz |
| Minimum Elevation Angle | 15 deg | All Azimuths |
| Array Configuration | | |
| radius <~400 m | ~40% (76 ant.) | Filling factor = 2.7% |
| ~400 m < radius < ~1000 m | ~14% (26 ant.) | 0.17% |
| ~1000 m < radius < 2500 m | ~16% (31 ant.) | 0.033% |
| ~2500 m < radius < 4000 m | ~11% (21 ant.) | 0.012% |
| ~4000 m < radius < 100000 m | ~19% (36 ant.) | 3.2×10^{-5} % |
| Antenna RF System | | Only one Feed available at a time |
| Band 1 (GHz) | 0.350 – 1.050 | Dual polarization (2 orthogonal), cryo-cooled LNA |
| Band 2 | 0.95 – 1.76 | " |
| Band 3 | 1.65 – 3.05 | " |
| Band 4 | 2.80 – 5.18 | " |
| Band 5 | 4.6 – 13.8 | Dual polarization (2 orthogonal), cryo-cooled LNA & feed |
| Maximum Available Bandwidth | | |
| Band 1 | 700 MHz | Each polarization |
| Band 2 | 808 MHz | " |
| Band 3 | 1403 MHz | " |
| Band 4 | 2380 MHz | " |
| Band 5 | 9200 MHz | " |
| Sampled IF Sub-bands** | | |
| Band 1 | 1 x 1 GHz | IF Chans x Bandwidth (each polarization) |
| Band 2 | 1 x 1 GHz | " |
| Band 3 | 1 x 2.5 GHz | " |
| Band 4 | 1 x 2.5 GHz | " |
| Band 5 | 2 x 2.5 GHz | " |
| Digital Outputs | | |
| Number of Sample streams per dish | | Sampled bands (both polarisations) |
| Band 1 | 2 x 8 bits | |
| Band 2 | 2 x 8 bits | |
| Band 3 | 2 x 6 bits | |
| Band 4 | 2 x 4 bits | |
| Band 5 | 4 x 3 bits | |
| Signal Transport System | | Optical fibre to signal processor |
| Digitised data rate per antenna*** | | |
| Band 1 | 48 Gbit s ⁻¹ | |
| Band 2 | 48 | |
| Band 3 | 90 | |
| Band 4 | 60 | |
| Band 5 | 90 | |
| Signal Processing System | | |
| Correlator | | |
| Max. No. input data streams | 760 | 190 ants x (4 streams @ X-band; 2 streams other bands) |
| Frequency channels (over widest sampled (BW)) | 256000 | Selected for $\sim 1 \text{ km-s}^{-1}$ resolution except Band 1 |
| Available frequency Resolution | | |

| | | |
|---|------------------------------------|--|
| Band 1 | $3.3 \text{ km}\cdot\text{s}^{-1}$ | 3.9 kHz |
| Band 2 | 1.2 | 3.9 |
| Band 3 | 1.8 | 9.7 |
| Band 4 | 1.1 | 9.7 |
| Band 5 | 0.64 | 9.7 |
| Complex Correlations**** | 1.8×10^{10} | ($190^2/2$) baselines x 4 pol'n prod's x 256,000 chans |
| Corr. Load Factor for 2.5 GHz bandwidth | 1436 Tera-MACs | 5.0 GHz in 2 x 2.5 GHz bands at X-band |
| Minimum Dump Time***** | 1.6 s | For 10 km Baselines (HPBW – processed FoV) |
| | 0.08 | For 200 km Baselines (HPBW – processed FoV) |
| Array Beam Former | | |
| Full beamformer | 190 antennas | |
| Optimum No. Antennas: Pulsar Searching | 108 antennas | Maximising $(N_{\text{dish}} A_{\text{dish}} / D_{\text{array}})^2$ as a function of array radius yield maximum survey speed per array beam. |
| Associated Optimum Array Diameter | 950 m | 108 antennas within this radius. |
| Beam Area at 1 GHz | 1.56 arcmin^2 | $\pi/4(1.3 \lambda_{1\text{GHz}} / D_{\text{array}})^2$ |
| Number of beams for 1 deg ² at 1 GHz | 2301 | |
| Maximum number of beams at 1 GHz | 4011 | Number of beams to fill the dish beam to ½ power point. |
| Total Bandwidth | 300 MHz | Based on pulsar search requirements |
| Frequency Channels | 1267 | Chan.-Bandwidth x array-crossing-time = 1 |
| Science Computing System | | |
| Input data rate (GByte-s ⁻¹) for | | Byte s ⁻¹ av'ge from correlator (4-Byte x 2 for complex) |
| 10 km max baseline | 90 | |
| 200 km max baseline | 1800 | |

* Expected aperture efficiency using well designed, realisable feeds.

** Either of two digitised bandwidths available: 1 GHz and 2.5 GHz.

*** Total Bandwidth (GHz) x 2 (Nyquist) x 4 or 8 (bits) x 1.25 (8B/10B encoding) x 1.2 (oversample) x 2 (pol'n streams); output of Digital Down Converter at antenna.

**** For max. number of frequency channels.

***** The following approximation produces a 2% drop in visibility amplitude at the edge of the primary beam: $\Delta t = 1200 (D_{\text{station}} / B_{\text{max}})$.

Table 7 Key System Performance Factors for SKA1-mid Array

| Antenna/Feed/Receiver Performance | | |
|-----------------------------------|--------|------------------------|
| Antenna/Feed Efficiency* | | |
| Band 1 | 0.65 | Average over frequency |
| Band 2 | 0.78 | |
| Band 3 | 0.78 | |
| Band 4 | 0.78 | |
| Band 5 | 0.74 | |
| Average T_{sys} | | |
| Band 1 | 28 K | Average over RF bands |
| Band 2 | 20 | |
| Band 3 | 20 | |
| Band 4 | 22 | |
| Band 5 | 25 | |
| Continuum Sensitivity | | |
| SEFD (each antenna, Stokes I) | | |
| Band 1 | 673 Jy | |
| Band 2 | 400 | |
| Band 3 | 400 | |
| Band 4 | 441 | |
| Band 5 | 528 | |
| SEFD (190 antennas, Stokes I)** | | |
| Band 1 | 4.4 Jy | |
| Band 2 | 2.1 | |
| Band 3 | 2.1 | |

| | | |
|---|-----------------------------|--|
| Band 4 | 2.3 | |
| Band 5 | 2.8 | |
| Minimum detectable flux (rms) (ΔS_{\min}) *** | | |
| Band 1 | $105 \mu\text{Jy s}^{-1/2}$ | |
| Band 2 | 58 | |
| Band 3 | 44 | |
| Band 4 | 27 | |
| Band 5 | 31 | |
| Sensitivity as A_e/T_{sys} (all antennas) | | |
| Band 1 | $779 \text{ m}^2/\text{K}$ | |
| Band 2 | 1309 | |
| Band 3 | 1309 | |
| Band 4 | 1190 | |
| Band 5 | 994 | |
| Field-of-View @ centre freq. (deg^2)**** | | $\Omega_{\text{beam}} = (\pi/4) (66\lambda/D)^2 \text{ deg}^2$ |
| Band 1 | 2.8 | |
| Band 2 | 0.75 | |
| Band 3 | 0.25 | |
| Band 4 | 0.086 | |
| Band 5 | 0.016 | |
| Equivalent "pill-box" Field-of-view (deg^2) | | $\Omega_{\text{eqw}} = 1.17(\lambda/D)^2 \text{ ster.}$ |
| Band 1 | 3.1 | |
| Band 2 | 0.84 | |
| Band 3 | 0.28 | |
| Band 4 | 0.097 | |
| Band 5 | 0.18 | |
| SSFoM (all Antennas) | | |
| Band 1 | 17 | $\times 10^5 \text{ m}^4 \text{ K}^{-2} \text{ deg}^2$ |
| Band 2 | 13 | " |
| Band 3 | 4.3 | |
| Band 4 | 1.2 | |
| Band 5 | 0.2 | |
| SSFoM x BW (all Antennas) | | |
| Band 1 | 1.2 | $\times 10^9 \text{ m}^4 \text{ K}^{-2} \text{ deg}^2 \text{ MHz}$ |
| Band 2 | 1.0 | |
| Band 3 | 0.080 | |
| Band 4 | 0.60 | |
| Band 5 | 0.29 | |
| Imaging Dynamic Range (Band 2)***** | 2.6×10^6 (64 dB) | Based on 1000-hr single-field integration. |
| Spectral Dynamic Range | TBD dB | |

* Expected aperture efficiency using well designed, realisable feeds.

** System Equivalent Flux Density: SEFD = $2 k_B T_{sys} / A_e$ Jy, where k_B is Boltzmann's constant (1380 Jy-m² / K), A_e is antenna effective area of the array.

*** Minimum detectable flux (1 σ): $\Delta S = \text{SEFD} / \eta_s (2 \Delta v)^{1/2}$ Jy s^{-1/2} for Stokes I, where Δv is the bandwidth. η_s is assumed to be 0.9.

**** This is the FoV used for the science performance evaluation. Assumes illumination tapers to zero at the edge of the dish and follows $E(x) = 1 - 2r^{2/3}$, where r is the distance from the dish centre. This results in a first sidelobe level of -23 dB.

***** Ratio taken between the flux of a typical L-band continuum source in field of 100 mJy and 1 σ noise level after a 1000-hr integration on a single field.

8.4.2 The Combined SKA1 and MeerKAT Dish Array

This section describes the performance available from the array consisting of the 64 MeerKAT dishes and the 190 SKA1-mid dishes.

The following principles underlie the more detailed assumptions made in this section:

- The merged array described in Section 8.2 is feasible, and additional SKA1 dishes and service corridors can be installed without destroying similar MeerKAT infrastructure.
- The overall cost will be minimised if the MeerKAT system can be utilised in as large a “chunk” as possible.
- Connections/interfaces to MeerKAT should be as non-intrusive and as simple as possible.
- The capability to operate MeerKAT as a separate instrument should be preserved for as long as possible.
- Digital signal processing equipment (correlator, beamformer, and other processors) and computing equipment have a sufficiently short life-span that low-priority will be given to incorporating them into the new system. However, this equipment may be vital during a transition phase if it can be used as a tool to test segments of the new system.

The following additional assumptions are made with the above principles in mind:

- The key parts of the MeerKAT system will be incorporated into the joint array, the dishes, receivers, synchronisation and time distribution, and data transport system. In addition, the associated telescope infrastructure including the correlator building is assumed to be re-usable or expandable. (Note in general all infrastructure will be re-used, but much of it is not directly attached to performance.) This approach is designed to re-use as much as possible, while at the same time keep the MeerKAT system intact for as long as possible.
- System interfaces to the re-used equipment occur in three principal places:
 - The dishes and associated control and support systems. It is assumed that the SKA1 control system will interface to a system that controls all of the MeerKAT dishes. It is further assumed that the MeerKAT antennas can be separately controlled as a sub-array of the overall system, but will otherwise be integrated into an overall control system that can be managed as one. Support systems such as power management will also be centrally interfaced to the new system.
 - Synchronisation reference signals delivered to the dishes. If possible, this interface will be central, but some sort of conversion may be needed at each antenna to ensure adequate synchronisation.
 - Data delivery to the correlator building. It is assumed that data can be de-formatted/reconstructed and delivered to the correlator system, most likely the delay system, in a compatible manner and that time stamps can be recovered, sample-errors/bad-data recorded, etc.
- The parts of the MeerKAT system “outside” of these boundaries will be discarded or retired in an orderly transition.
- Performance or cost sacrifices in the design of SKA1 dishes to accommodate the MeerKAT dishes will not be made or will be minimised.
- To avoid disturbing equipment that is presumed to be “shaken down”, the general approach will be to make as few changes to MeerKAT equipment as possible, with preference given to interface convertors or adaptors.

- MeerKAT will be complete and equipped with the presently planned receivers (UHF, L-band and X-band).
- SKA1 dishes will be equipped with receivers that have almost 100% overlap in frequency with the MeerKAT receivers. There are slight disparities at the band edges of two of the bands (see section 8.3).
- The number of sub-arrays can be as large as the number of antennas.
- Only one receiver can operate on any antenna at one time. However, some receiver bands may be divided into sub-bands, only one of which may overlap a MeerKAT band. In that case the other band can be correlated as one or more sub-arrays of SKA1 antennas.
- At least SKA1 bands 1 and 2 will be available. Depending on funds, not all of the other SKA1 receivers will be initially available. This document provides performance data as if they are all available and fully serviced by down-stream sub-systems. It is assumed that the correlator, non-imaging processor and similar equipment will be sized to fit the maximum requirements shown here, or will be specifically designed to be expandable to such.

Table 8 and Table 9 have been assembled using the above assumptions and calculations outlined in the footnotes.

Table 8 Combined SKA1-mid Array

| | | |
|------------------------------------|----------------------|--|
| Aperture | | 190 x 15-m (equiv. dia.) offset Gregorian reflectors Plus 64 x 13.5-m (equiv. dia.) offset Gregorian reflectors |
| Total physical aperture | 42737 m ² | |
| Minimum Elevation Angle | 15 deg | All Azimuths |
| Array Configuration | | |
| radius <~400 m | ~42% (106 ant.) | Filling factor = 3.5% |
| ~400 m < radius < ~1000 m | ~17% (42 ant.) | 0.26% |
| ~1000 m < radius < 2500 m | ~16% (41 ant.) | 0.042% |
| ~2500 m < radius < 4000 m | ~11% (29 ant.) | 0.016% |
| ~4000 m < radius < 100000 m | ~14% (36 ant.) | 2.0 x 10 ⁻⁵ % |
| Baselines | | |
| SKA1-mid dishes | 17955 | |
| MeerKAT dishes | 2016 | |
| Mixed dish | 12160 | |
| Total | 32131 | |
| Antenna RF System | | |
| Overlapping Common Frequencies* | | |
| Band 1 (UHF-band) | 0.58 – 1.015 GHz | Dual polarization (2 orthogonal), cryo-cooled LNA |
| Band 2 (L-band) | 0.9 – 1.67 | " |
| Band 5 (X-band) | 8.0 – 13.8 | Dual polarization (2 orthogonal), cryo-cooled LNA & feed |
| Maximum Available Common Frequency | | |
| Band 1 (UHF-band) | 435 MHz | Each polarization |
| Band 2 (L-band) | 720 | " |
| Band 5 (X-band) | 5800 | " |
| Sampled IF Sub-bands** | | Only overlapping frequencies can be correlated. |
| SKA1-mid Band 1 | 1 x 1000 MHz | Each polarization |
| Band 2 | 1 x 1000 | " |
| Band 5 | 1 x 2500 | " |
| MeerKAT UHF-band | 1 x 435 MHz | Each polarization |
| L-band | 1 x 770 | " |
| X-band | 1 x 2000 | " |

| | | |
|---|-------------------------|---|
| Digital Outputs | | |
| No. of Common Sample streams per dish | | Sampled bands (both polarisations) |
| Band 1 (UHF-band) | 2 x 8 bits or 10 bits | 8/4 bits for SKA1 dishes; 10 bits for MeerKAT dishes |
| Band 2 (L-band) | 2 x 8 bits or 10 bits | " |
| Band 5 (X-band) | 2 x 4 bits or 10 bits | " |
| Signal Transport System *** | | Optical fibre to signal processor |
| See Table 6 for SKA1 antennas | | |
| MeerKAT antennas: from footnote. | | |
| Signal Processing System **** | | |
| Correlator | | |
| Max. Data streams requiring correlation | 888 | (190 ants x 4) + (64 ants x 2) streams |
| Frequency channels | 256000 | All bands: $\sim 1 \text{ km-s}^{-1}$ resolution except Band 1 ($\sim 3 \text{ km-s}^{-1}$) |
| Available frequency Resolution | | |
| Band 1 (UHF-band) | 3.3 km-s^{-1} | 3.9 kHz |
| Band 2 (L-band) | 1.2 | 3.9 |
| Band 5 (X-band) | 0.64 | 9.8 |
| Complex Correlations***** | 3.3×10^{10} | $(254^2/2)$ baselines x 4 pol'n prod's x 256,000 chans |
| Max. Corr. Load Factor | 2003 Tera-MACs | 2.5 GHz on all baselines + 2.5 GHz on SKA1-mid baselines |
| Minimum Dump Time***** | 1.6 s | 10 km Baselines (SKA1-mid dish HPBW – processed FoV) |
| | 0.08 | 200 km Baselines |
| Array Beam Former | | |
| Full beamformer | 254 antennas | |
| Optimum No. Antennas for Pulsar Search | 125 antennas | Maximise $(N_{\text{dish}} A_{\text{dish}} / D_{\text{array}})^2$ with array radius |
| Associated Optimum Array Diameter | 900 m | 125 antennas within this radius. |
| Beam Area at 1 GHz | 1.7 arcmin ² | $\pi/4(1.3 \lambda_{1\text{GHz}} / D_{\text{array}})^2$ |
| Number of beams for 1 deg ² at 1 GHz | 2100 | |
| Maximum number of beams at 1 GHz | 3600 | Number of beams (15-m dish) |
| Total Bandwidth | 300 MHz | Based on pulsar search requirements |
| Frequency Channels | 1200 | Chan.-Bandwidth x array-crossing-time = 1 |
| Science Computing System | | |
| Input data rate (GByte-s ⁻¹) for | | Byte s ⁻¹ av'ge from correlator (4-Byte x 2 for complex) |
| 10 km max baseline | 162 | |
| 200 km max baseline | 3250 | |

* MeerKAT L-Band Available 2016; UHF-Band Available 2017; X-Band Available 2018.

** Either of two digitised bandwidths available: 1 GHz and 2.5 GHz.

*** Bandwidth x 2 (Nyquist) x 10 (bits) x 1.25 (8B/10B encoding) x 1.13 (oversample) x 2 (pol'n streams); output of Digital Down Converter at antenna.

**** Correlation and array beamforming are available concurrently.

***** For max. number of frequency channels.

***** The following approximation produces a 2% drop in visibility amplitude at the edge of the primary beam: $\Delta t = 1200 (D_{\text{station}} / B_{\text{max}})$.

Table 9 Key System Performance Factors for Combined SKA1-mid Array

| | | |
|-----------------------------------|------|------------------------|
| Antenna/Feed/Receiver Performance | | |
| Antenna/Feed Efficiency* | | |
| SKA1-mid dish Band 1 | 0.65 | Average over frequency |
| Band 2 | 0.78 | |
| Band 5 | 0.74 | |
| MeerKAT dish UHF-band | 0.7 | |
| L-band | 0.65 | |
| X-band | 0.65 | |
| Average T_{sys} | | |
| SKA1-mid dish Band 1 | 28 K | Average over RF bands |
| Band 2 | 20 | |
| Band 5 | 25 | |
| MeerKAT dish UHF-band | 29 | |
| L-band | 20 | |

| | | |
|--|----------------------------|--|
| X-band | 25 | |
| <i>Continuum Sensitivity</i> | | |
| SEFD (each antenna, Stokes I) | | |
| SKA1-mid dish Band 1 | 673 Jy | |
| Band 2 | 400 | |
| Band 5 | 528 | |
| MeerKAT dish UHF-band | 831 | |
| L-band | 551 | |
| X-band | 742 | |
| SEFD (254 antennas, Stokes I)** | | |
| Band 1 + UHF-band | 2.78 Jy | |
| Band 2 + L-band | 1.69 | |
| Band 5 + X-band | 2.24 | |
| Minimum detectable flux (rms) (ΔS_{\min})*** | | |
| Band 1 + UHF-band | 87 $\mu\text{Jy s}^{-1/2}$ | |
| Band 2 + L-band | 47 | |
| Band 5 + X-band | 27 | |
| <i>Sensitivity as A_e/T_{sys} (all antennas)</i> | | |
| Band 1 + UHF-band | 992 m^2/K | |
| Band 2 + L-band | 1600 | |
| Band 5 + X-band | 1200 | |
| <i>Field-of-View @ centre freq.</i> **** | | |
| Band 1 + UHF-band | 2.15 deg ² | $\Omega_{\text{beam}} = (\pi/4) (66\lambda/D)^2 \text{ deg}^2$ |
| Band 2 + L-band | 0.83 | |
| Band 5 + X-band | 0.11 | |
| <i>Equivalent "pill-box" Field-of-view</i> | | |
| Band 1 + UHF-band | 2.42 | $\Omega_{\text{eqw}} = 1.17(\lambda/D)^2 \text{ ster.}$ |
| Band 2 + L-band | 0.93 | |
| Band 5 + X-band | 0.012 | |
| <i>SSFoM (all Antennas)</i> | | |
| Band 1 + UHF-band | 21 | $\times 10^5 \text{ m}^4 \text{ K}^{-2} \text{ deg}^2$ |
| Band 2 + L-band | 22 | " |
| Band 5 + X-band | 0.16 | " |
| <i>SSFoM x BW (all Antennas)</i> | | |
| Band 1 + UHF-band | 0.92 | $\times 10^9 \text{ m}^4 \text{ K}^{-2} \text{ deg}^2 \text{ MHz}$ |
| Band 2 + L-band | 1.6 | " |
| Band 5 + X-band | 0.033 | " |
| Imaging Dynamic Range (L-band)***** | 3.0×10^6 (65 dB) | Based on 1000-hr single-field integration. |
| Spectral Dynamic Range | TBD dB | |

* SKA1 antennas only. Expected aperture efficiency using well designed, realisable feeds.

** SEFD_{array}=1/(n/SEFD_{MK} + m/SEFD_{SKA}), where SEFDs are the n MeerKAT and m SKA antennas, respectively. SEFD = $2k_B T_{\text{sys}} / A_e$ for an individual antenna.

*** $S_{\min} = \text{SEFD}_{\text{array}} / (\eta_s (2\Delta v \tau)^{1/2})$, where η_s is the system efficiency, Δv is the channel bandwidth, and τ is the total integration time. Note that for a single polarisation $S_{\min} = 2k_B T_{\text{sys}} / (\eta_s A_e (\Delta v \tau)^{1/2}) = \text{SEFD}_{\text{array}} / (\eta_s (\Delta v \tau)^{1/2})$, which is $2^{1/2}$ larger for S_{\min} . S_{\min} is given for $\tau = 1$ s. η_s is taken as 0.9.

**** This is the FoV used for the science performance evaluation. Assumes illumination tapers to zero at the edge of the dish and follows $E(x) = 1 - 2r^{2/3}$, where r is the distance from the dish centre. This results in a first sidelobe level of -23 dB.

***** Ratio taken between the flux of a typical L-band continuum source in field of 100 mJy and 1σ noise level after a 1000-hr integration on a single field.

8.5 Digital Data Back-Haul

The digital data backhaul system for the SKA1-mid array will transmit data from the output of the digitising stage at the receiver to the input of the signal processing system. The transmission will use optical fibre to carry digitised data. It will be a point-to-point deterministic network in which the data flows in a uni-directional fashion from the antennas to the central processor for SKA1-mid. The precise locations of points of data ingress and egress to the system have yet to be defined.

8.6 SKA1-mid Central Signal Processor

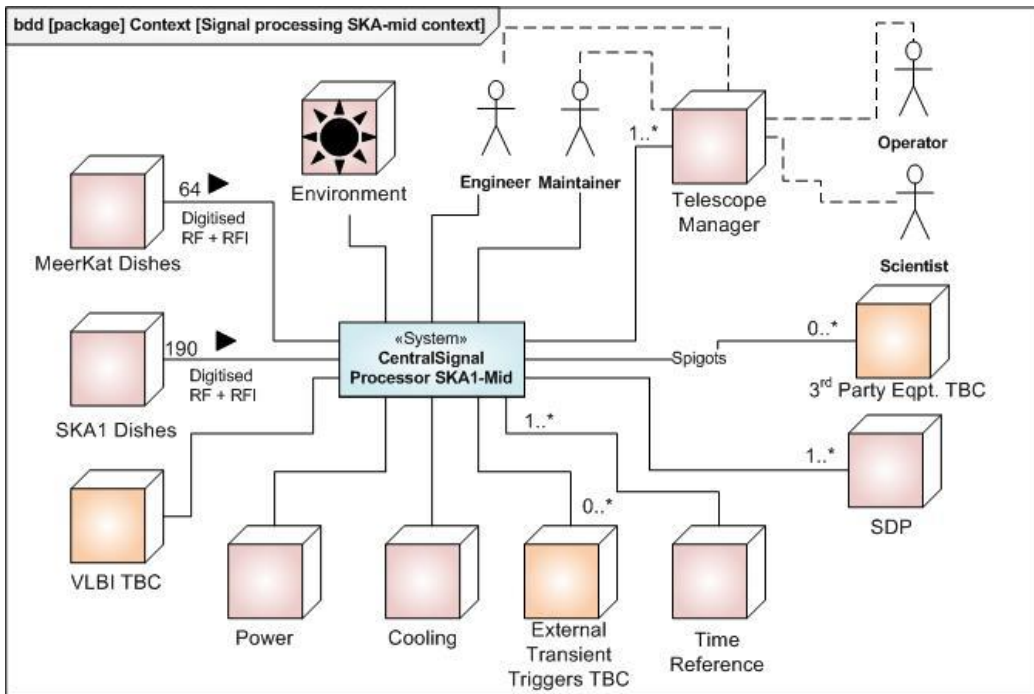


Figure 15 SKA1-mid Context Diagram – Central Signal Processing

Digitisers and subsequent digital stages will have to be appropriately shielded. The ideal shielding approach permits power and RF only as electrical input connections. All other signals are on optical fibre. At the other end of the digital data backhaul system, termination could be at the input to both the F-part of the SKA1-mid correlator and the array beamformer or to a shared channeliser at the input of the processing system.

In the generalised scheme, the combined array will reuse the existing MeerKAT data transmission system if possible.

The architectural aspects of the SKA-mid correlator (Figure 15) are similar to those of the SKA1-low correlator. As such, detail is not repeated in this section. However, the number of correlations for SKA1-low is significantly greater, with up to 1134 stations compared with up to 254 dishes for SKA-mid.

8.6.1 SKA1-mid Correlator

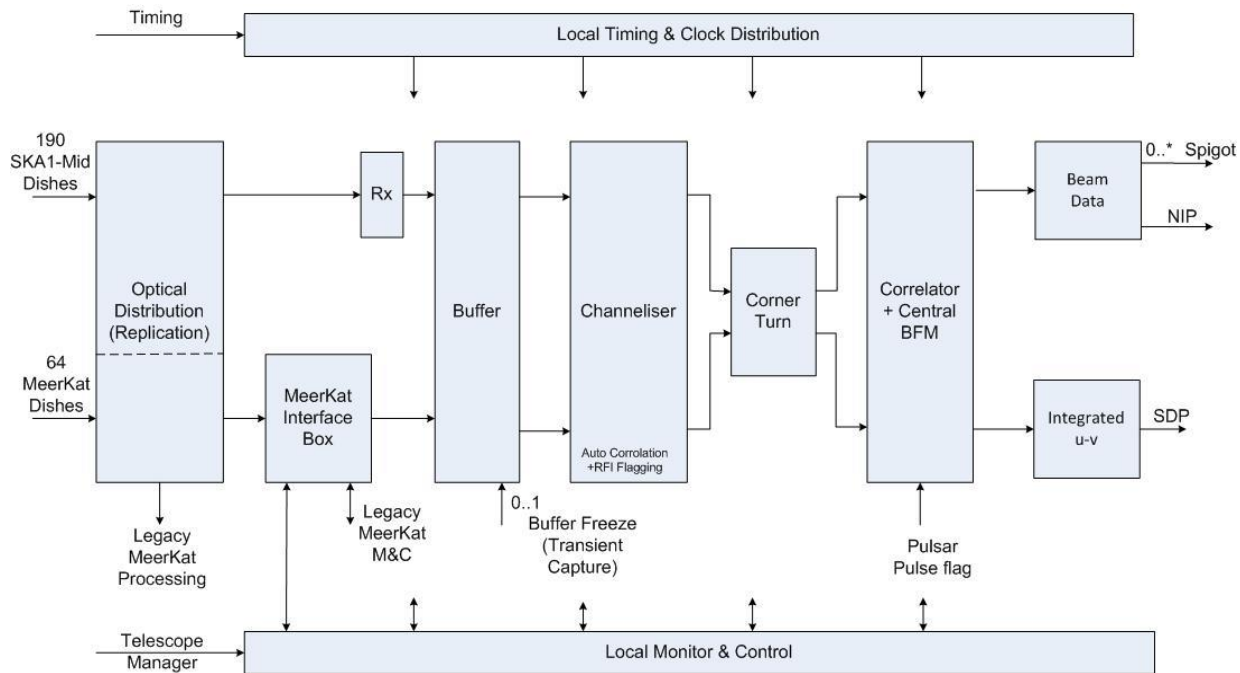


Figure 16 SKA1-Mid Correlator Functional Architecture

Figure 16 illustrates the functional architecture of the SKA1-Mid Correlator including channelization and correlation. If an optimised design indicates as such, these two functions may be shared with central beam-forming. Beam-forming may also be incorporated into a system that shares signal distribution or other aspects

To provide maximal reuse of the of MeerKAT capability, an interface box is provided to translate between legacy interfaces and SKA1. The data from the MeerKAT dishes is replicated across SKA1 and the legacy MeerKAT processing equipment if present. Similarly, the SKA1 Mid dish data could be made available as a set of spigots TBC.

To increase signal-to-noise when observing pulsars, particular for pulsar astrometry, the correlator will provide pulsar gating capability. The correlation data will be integrated into fifty separate temporal phase bins across the pulsar pulse. The full set of resultant data is to be forwarded to the SDP for the creation of Visibilities for a user specified subset of these.

Table 10 summarizes the parameters associated with the functionality of the SKA1-Mid correlator. Equipment estimates are contained in Appendix B.

Table 10 Correlator Parameters SKA1-mid

| Correlator SKA1-mid Array (15-m antennas only) | | |
|--|------------------------------------|---|
| Max. No. input data streams | 760 | 190 ants x (4 streams @ X-band; 2 streams other bands) |
| Frequency channels (over widest sampled (BW)) | 256000 | Selected for $\sim 1 \text{ km}\cdot\text{s}^{-1}$ resolution except Band 1 |
| Actual channelisation | 262,144 | As power of 2 for FFT: 2^{18} |
| Available frequency Resolution | | |
| Band 1 | $3.3 \text{ km}\cdot\text{s}^{-1}$ | 3.9 kHz |
| Band 2 | 1.2 | 3.9 |

| | | |
|---|------------------------------------|---|
| Band 3 | 1.8 | 9.7 |
| Band 4 | 1.1 | 9.7 |
| Band 5 | 0.64 | 9.7 |
| Complex Correlations* | 1.8×10^{10} | ($254^2/2$) baselines x 4 pol'n prod's x 256,000 chans |
| Corr. Load Factor for 2.5 GHz bandwidth | 1436 Tera-MACs | 5.0 GHz in 2 x 2.5 GHz bands at X-band |
| Minimum Dump Time** | 1.6 s | For 10 km Baselines (HPBW – processed FoV) |
| | 0.08 | For 200 km Baselines (HPBW – processed FoV) |
| Output data rate (GByte·s ⁻¹) for | | Byte s ⁻¹ av'ge from correlator (4-Byte x 2 for complex) |
| 10 km max baseline | 90 | |
| 200 km max baseline | 1800 | |
| Correlator Combined SKA1-mid Array | | |
| Max. Data streams requiring correlation | 888 | (190 ants x 4) + (64 ants x 2) streams |
| Frequency channels | 256000 | All bands: $\sim 1 \text{ km}\cdot\text{s}^{-1}$ resolution except Band 1 ($\sim 3 \text{ km}\cdot\text{s}^{-1}$) |
| Actual channelisation | 262,144 | As power of 2 for FFT: 2^{18} |
| Available frequency Resolution | | |
| Band 1 (UHF-band) | $3.3 \text{ km}\cdot\text{s}^{-1}$ | 3.9 kHz |
| Band 2 (L-band) | 1.2 | 3.9 |
| Band 5 (X-band) | 0.64 | 9.8 |
| Complex Correlations*** | 3.3×10^{10} | ($254^2/2$) baselines x 4 pol'n prod's x 256,000 chans |
| Max. Corr. Load Factor | 2003 Tera-MACs | 2.5 GHz on all baselines + 2.5 GHz on SKA1-mid baselines |
| Minimum Dump Time* | 1.6 s | 10 km Baselines (SKA1-mid dish HPBW – processed FoV) |
| | 0.08 | 200 km Baselines |
| Output data rate (GByte·s ⁻¹) for | | Byte s ⁻¹ av'ge from correlator (4-Byte x 2 for complex) |
| 10 km max baseline | 162 | |
| 200 km max baseline | 3250 | |

* For max. number of frequency channels.

** The following approximation produces a 2% drop in visibility amplitude at the edge of the primary beam: $\Delta t = 1200 (D_{\text{station}}/B_{\text{max}})$.

*** Visibilities are available during the beamforming at the same frequency resolution as the beam former setup. This is used for phasing up the beam, but is also available for other processing if required.

8.6.2 SKA1-mid Central Beam-former

Central Beam-forming across the SKA-mid array of antennas produces beams with the full sensitivity of the array by essentially adding together inputs from each antenna. The architecture is detailed in the diagram in the SKA1-mid Correlator section. The outputs will support Non Imaging Processing including Pulsar Survey and Timing.

The beams generated by the Central Beam-former will typically be narrow, compared with the antenna beams (width proportional to $(\lambda/D)^2$, where D is the dimension of the array; thus many of them will be needed to cover a significant area of sky. The beam is steered to follow the pointing direction by delay insertion before addition. Coherency must be maintained over the frequency band. This is done either by inserting finely divided time delays, or by channelizing the signal, and using phase insertion to approximate delays in the narrow-band channels.

As with the SKA1-mid correlator, the architecture readily maps to ASIC, FPGA and GPU or Multi Integrated Core implementations.

The beamformer must be designed to support beams from any number of sub-arrays.

Table 11 Central Beamformer Parameters SKA1-mid

| <i>Central Beamformer SKA 1 Mid Array</i> | | |
|---|--------------------------|--|
| Full beamformer | 190 antennas | |
| Optimum No. Antennas: Pulsar Searching | 108 antennas | Maximising $(N_{\text{dish}} A_{\text{dish}} / D_{\text{array}})^2$ as a function of array radius yield maximum survey speed per array beam. |
| Associated Optimum Array Diameter | 950 m | 108 antennas within this radius. |
| Beam Area at 1 GHz | 1.56 arcmin ² | $\pi/4(1.3 \lambda_{1\text{GHz}} / D_{\text{array}})^2$ |
| Number of beams for 1 deg ² at 1 GHz | 2301 | |
| Maximum number of beams at 1 GHz | 4011 | Number of beams to fill the dish beam to ½ power point. |
| Total Bandwidth | 300 MHz | Based on pulsar search requirements |
| Frequency Channels | 1267 | Chan.-Bandwidth x array-crossing-time = 1 |
| <i>Central Beamformer Combined SKA1-mid Array</i> | | |
| Full beamformer | 254 antennas | |
| Optimum No. Antennas for Pulsar Search | 125 antennas | Maximise $(N_{\text{dish}} A_{\text{dish}} / D_{\text{array}})^2$ with array radius |
| Associated Optimum Array Diameter | 900 m | 125 antennas within this radius. |
| Beam Area at 1 GHz | 1.7 arcmin ² | $\pi/4(1.3 \lambda_{1\text{GHz}} / D_{\text{array}})^2$ |
| Number of beams for 1 deg ² at 1 GHz | 2100 | |
| Maximum number of beams at 1 GHz | 3600 | Number of beams (15-m dish) |
| Total Bandwidth | 300 MHz | Based on pulsar search requirements |
| Frequency Channels | 1200 | Chan.-Bandwidth x array-crossing-time = 1 |

Table 11 provides beamformer parameters for both the array of SKA1-mid (15-m) antennas and for the full array of mixed antennas. Equipment estimates are contained in Appendix B.

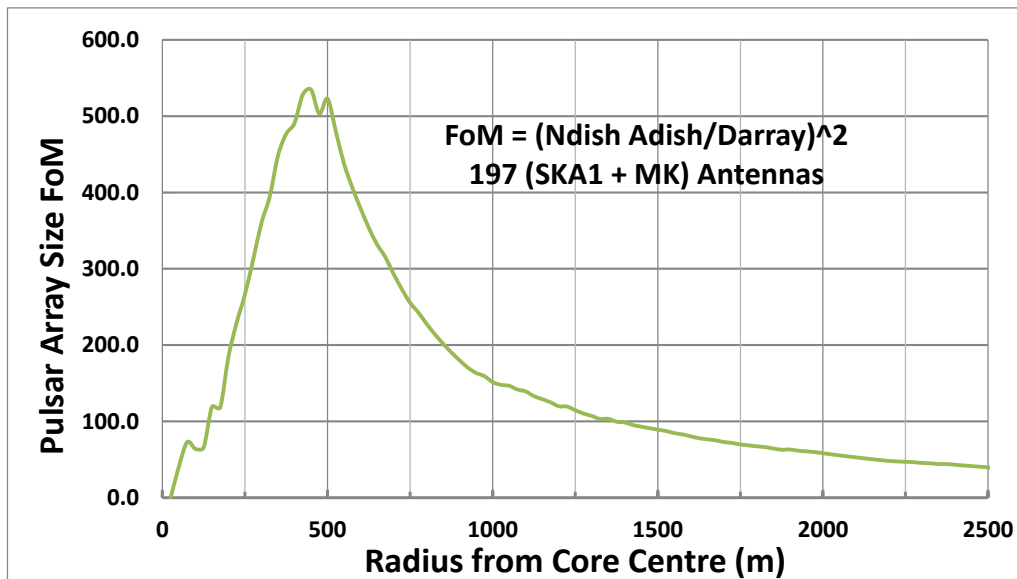


Figure 17 Figure-of-Merit used to select the optimum array diameter (~450 m) for pulsar searches.

The optimum array configuration for pulsar searching, the main user of the beamformer, is a maximally compact array. However, such an array would be very poor for imaging. Thus the array configuration is a compromise. Given a configuration of antennas with identical T_{sys} , the maximum beam sensitivity over the widest field (a form of survey speed FoM) can be found by maximizing the

following figure-of-merit for D_{array} : $FoM_{array_size} = \left(\frac{N_{dish} A_e}{D_{array}} \right)^2$. Figure 17 shows that this maximum for the SKA1-mid array is an inner sub-array of radius ~ 450 m.

8.6.3 SKA1-Mid Non-Imaging Processor

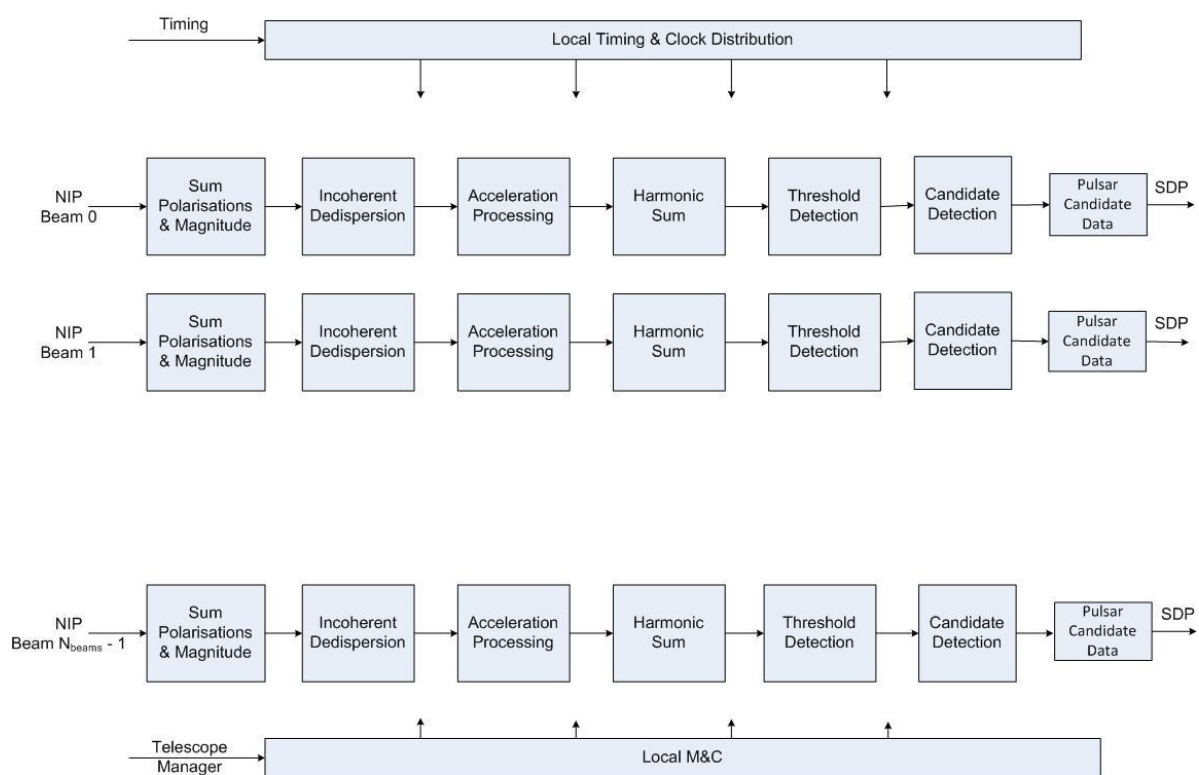


Figure 18 SKA1-Mid Non-Imaging Processor Functional Architecture

8.6.3.1 Pulsar Survey

A major science goal for SKA1-mid is to carry out a search of the Galaxy for pulsars down to a well-defined level of completeness, in which completeness is defined in a multi-parameter way (pulse period, dispersion measure, acceleration (if present), etc.).

A representative observing plan is needed in order to estimate the scope of the design needed for the pulsar search. The representative plan approximately follows that outlined in [17]. As a starting point it is assumed that the required full sky survey (nominally $36,000$ deg 2) will nominally be completed within two years on the sky. Each pointing would be observed for approximately 600 s, with 50 μ s sampling. The resulting functional architecture for SKA1 pulsar survey is presented in the Figure 18. Incoherent de-dispersing is assumed, as coherent de-dispersion processing does not currently appear to be cost-effective. The most processing intensive part is the Acceleration

processing providing binary search. This scales linearly with the number of beams and number of trial dispersion measures (along with the number of acceleration trials and 2-D FFTs [17] across the individual observation time). Thus the net processing load scales inversely with frequency (i.e. lower for higher observation frequencies).

Based on pulsar brightness, scattering and sky temperature, a centre frequency of 800 MHz maximises search sensitivity [17]. A bandwidth is 300 MHz is assumed here, although it could be somewhat larger if indicated by a more thorough cost-benefit analysis.

Temporal smearing varies as a function of DM/f^2 , where DM is the dispersion measure, the integral of electron density (column density) along the line-of-sight to the pulsar. As would be expected, DM is a strong function of Galactic coordinates, with the highest electron densities in the Galactic plane and towards the Galactic centre. Figure 19 shows average DM as a function of Galactic latitude, extracted from the NE2001 electron density model, 91[51].

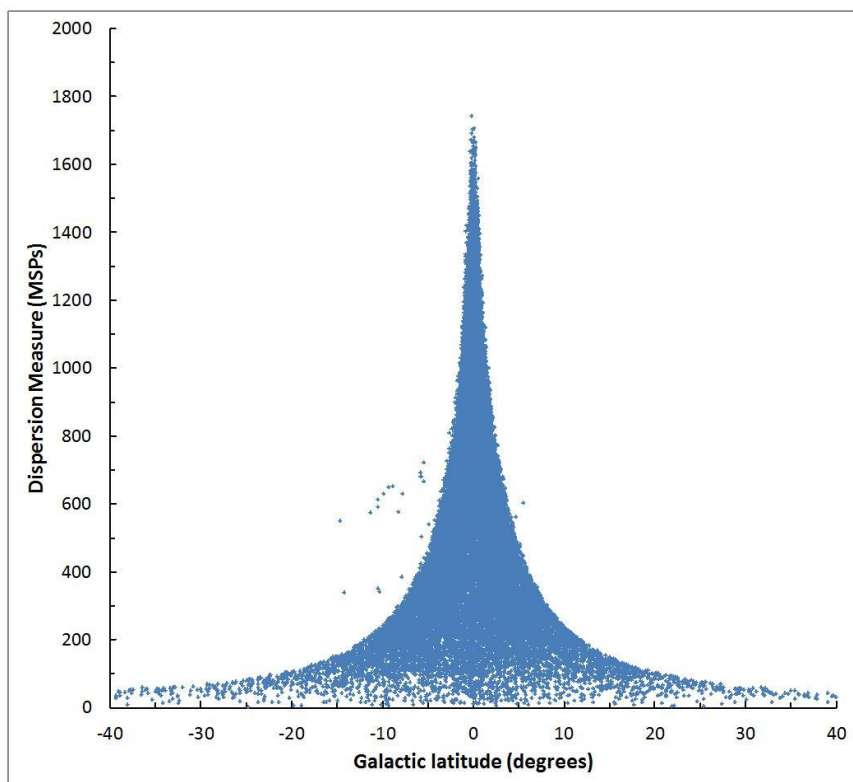


Figure 19 Average DM vs Galactic latitude

Processing load is directly related to the number of trials for the Dispersion Measure. Upper limits for processing load can thus be extracted from this model. As described below, processing load can be balanced across the entire survey by calculating only the trial dispersion measures needed for a particular search region. Table 12 shows suggested ranges of Galactic latitude that could be used to define different search regions. These need not be rigidly adhered to, however, since some high electron-density (high DM) regions do occur at high Galactic latitudes.

Table 12 Pulsar Search Regions

| Galactic Latitude $ b $ (deg) | Maximum Dispersion Measure (cm^{-3} pc) of region | Search Area* (deg 2) | Observation Frequency (MHz) | Achievable DM at 50us resolution DM_{\max}^{**} | Number of DMs*** | Frequency Resolution kHz |
|-------------------------------|---|--------------------------|-----------------------------|--|------------------|--------------------------|
| < 1 | 3000 | 720 | 1400 | 827 | 15350 | 20 |
| 1 – 5 | 1000 | 2875 | 1400 | 827 | 15350 | 20 |
| 5 – 15 | 500 | 7082 | 800 | 154 | 16113 | 20 |
| 15 – 30 | 100 | 9950 | 800 | 100 | 10448 | 31 |
| >30 | 60 | 39847 | 800 | 60 | 6269 | 51 |

* Above a horizon limit of 15 deg.

** $\text{DM}_{\max} = \text{tsamp} (\mu\text{s}) * f_c^3 (\text{GHz}) / (8300 * \text{fres GHz})$; fres = 20 kHz

*** $\text{NDM} = 4150 * \text{DM} * ((1/f_l)^2 - (1/f_h)^2) / \text{tsamp}$. Tsamp = 50us

Achieving high Dispersion Measures often requires a trade off against time resolution as it is not usually possible to achieve both simultaneously due to the effects of scattering. As a result, measurements along the galactic plane and galactic centre are possibly better suited to higher frequency observations. It is also likely that the number of DMs is one area that can be reduced in cost benefit trade-offs.

Table 13 summarises the survey parameters for SKA1-mid. Equipment estimates are contained in Appendix B.

Table 13 Pulsar Survey Parameters SKA1-mid Array

| | | |
|------------------------------|------------------------------------|------------------------------------|
| Core | | |
| diameter | 950m | |
| No. dishes | 95 + 46 | SKA1 + MeerKat |
| Survey time | | |
| On sky | 2 years | |
| Observation time | 600 seconds | |
| Observations per survey | 105120 | |
| All visible sky area | $\sim 36,000 \text{ deg}^2$ | |
| t_{samp} | 50us | |
| Survey | | |
| Centre frequencies | 800 & 1400 MHz | 0 to 5 degrees latitude at 1400MHz |
| Processed bandwidth | 300MHz | |
| Minimum frequency resolution | 20kHz | |
| Number of Channels | 15,000 | |
| Beam size @ 950MHz | $4.1 \times 10^{-4} \text{ deg}^2$ | 1.5 arc minutes |
| Beam size @ 1550MHz | $1.5 \times 10^{-4} \text{ deg}^2$ | 0.5 arc minutes |
| No beams per observation | 835 | 0 to 5 degrees latitude |
| No beams per observation | 2222 | Greater than 5 degrees latitude |

8.6.3.2 Pulsar Timing

Precision pulsar timing requires the maximum collecting area in the region of 0.8 to 3GHz [DRM]. As this straddles two SKA1-Combined frequency bands, timing is implemented in both namely Band 2 and Band 3. However, the MeerKat dishes do not provide coverage in band 3. Consequently, the timing in this band is constrained to 190 Dishes. Table 14 contains the pulsar timing parameters for SKA1-mid.

It is assumed preliminary measurements are made prior to timing to ascertain parameters such as the optimal Dispersion measure appropriate to the timing resolution.

Table 14 Pulsar Timing Parameters SKA1

| Timing Array | | |
|--|-----------------------------|---|
| Array Diameter | 200km | |
| No.SKA1 dishes | 190 | |
| No. MeerKat dishes | 64 | Limited in the bandwidth applicable to pulsar timing |
| Pulsar Timing | 48 hours every month TBC | Over a six month period |
| Individual time to stable MSP profile | 5 minutes* | |
| Individual binary with neutron star or black hole time to stable profile | 7 minutes* | |
| Required S/N | >1000 | Strong field tests of General Relativity 1ms pulsar 10% duty cycle 100ns time resolution |
| Min integration time band 2 | 3 minutes* | Time to achieve S/N for 254 dishes** |
| Min integration time band 3 | 12 minutes* | Time to achieve S/N for 190 dishes** |
| Frequency range | | |
| Band 2 | 0.95 to 1.67 GHz | MeerKaT and SKA1 - mid |
| Processed bandwidth Band 2 | 808 MHz | |
| Band 3 | 1.65 to 3 GHz | |
| Processed bandwidth Band 3 | 1403 MHz | |
| | 10 years | |
| Timing resolution | 100ns | |
| Number of simultaneous beams | 10 | |
| Coherent Dedisperion | | |
| DMmax | 3000 | |

*doesn't take into account pulse jitter noise

8.7 SKA1- mid Science Data Processing

SKA1-mid is a relatively straightforward telescope for data processing. It is single field with well-behaved diffraction-limited primary beam. A lot of the knowledge from JVLA and WSRT will be directly relevant. To reach the sensitivity limit for long observations usually requires imaging of sources over the entire primary beam and beyond. This is because unsubtracted sidelobes from these sources will dominate over the receiver noise. For the long baselines required for unconfused continuum imaging, both multi-frequency synthesis and correction of the w term (off-field-centre delay) will be necessary, bringing a substantial increase in processing load. In addition, for the highest dynamic range, very accurate pointing and possibly self-calibration of pointing errors will be necessary [23].

For high dynamic range HI absorption and high sensitivity HI emission observations, it will be necessary to remove the continuum as accurately as possible. Currently this involves imaging the continuum sources in the field accurately and then removing the effect of these sources from the full resolution spectral line visibility. The forward modelling of the visibility function from the continuum sources must be done accurately and will include at the minimum multi-frequency synthesis, w-term, and a model of the antenna primary beam.

Although the algorithms for SKA1-mid may be close to those currently in use, the implementations will not be. The current paradigm for High Performance Computing (HPC) is a large number of

compute nodes, each of which has up to 12 cores. Efficient parallelization on the node is marginally possible with considerable work. LOFAR, ASKAP, and EVLA all have considerable experience with this model. In the next five years, the node will probably be one of two choices – a Graphical Processing Unit (GPU) of many thousands of nodes or an Intel Many Integrated Core (MIC) system in which 50 – 100 x86-lite cores are integrated on a very fast interconnect. Programming for either of these two models cannot be ignored and will be time-consuming. Thus a substantial amount of algorithm tuning and development will be required.

9 SKA1-survey

The science motivation for SKA1-survey will be to provide large-scale surveys patterned after the ASKAP surveys: Evolutionary Map of the Universe [45] and Widefield ASKAP L-band Legacy All-sky Blind surveyY [46]. The motivation is to capitalise on the Phased Array Feed (PAF) technology as applied to these surveys, but to deliver much higher sensitivity results than ASKAP alone can reasonably manage. Details of the predicted detections can be found in [45] and [46].

Greater sensitivity in the HI-line emission will enable higher redshift objects to be observed as part of the surveys. In addition SKA1-survey may be best placed to carry out HI-line surveys of near-by galaxies.

Greater sensitivity in continuum emission will require sufficient resolution to avoid confusion.

9.1 Key Design Parameters

The following summarises the key open design parameters and the constraints for SKA1-survey. Further details are provided in subsequent sections.

1. *Array Configuration:* The location of the array configuration is constrained entirely by the need to incorporate the ASKAP antennas, for which the array configuration is pre-defined. As with SKA1-mid, SKA1-survey dishes are added to the core to increase sensitivity at core baselines. Additional antennas are added in spiral arms, which overlap the core so as to provide a smooth transition. There is no single optimum configuration. The main adjustable parameters are the weight of the core, the smoothness in the progression of baselines in an approximately scale-free fashion, and the absence of significant gaps in the u-v plane for both short and long observations. The longest baseline depends on continuum confusion at the lowest frequencies. A preliminary estimate indicates that a maximum baseline of 50 km is “safe” (see Section 8.2). It is important that the distribution of collecting area out to the 50-km limit is “even” on a logarithmic scale.
2. *Frequency Range:* The basic motivation for the SKA1-survey frequency range is HI-line at modest redshift and continuum emission surveys over the whole observable sky. It is assumed that the dishes can easily accommodate three PAFs for different frequency ranges, but only one would be populated for SKA1. A discussion of the receiver bands is contained in Section 9.4.
3. *Sensitivity:* Sensitivity is essentially defined by the system affordability per dish and per PAF beam. Sensitivity (both A/T and survey speed forms) is also determined by sources of noise and receiver bandwidth, subject to data transport and processing capability.

4. *Polarisation capability:* This is essential to properly calibrate the telescope. For imaging observations (continuum and spectral line), instrumental polarization must be accurately characterized across the multiple beams that are used to assemble the image over the final field-of-view.
5. *Sky Coverage:* As with SKA1-mid, sky coverage depends upon the minimum elevation of the antennas and to some extent on “shadowing” of one antenna by another in the array. Since the considerations are identical, see Section 8 for discussion.
6. *Upgrade Path:* It is not anticipated that SKA1-survey will be expanded to SKA2. SKA1-survey could be enhanced by the addition of more PAF arrays to cover a greater frequency range. In principle, these could be added in such a way as to share the beamformers. Additional processing features could also be added, such as transient detection equipment.

9.2 Antennas

In this baseline, the SKA1-survey antennas are assumed to be the same design as those for SKA1-mid, but equipped only with PAF feeds. In principle the only requirement for PAFs is the capture all of the energy reflected by the optical system. Processing can correct phase and amplitude errors, provided that the wave front is adequately sampled. Appropriate weights ensure that spillover noise and efficiency are optimised.

Another consideration is the rotation of the PAF with respect to the sky and feeds legs (if present). Both ASKAP and APERTIF avoid this by using a ‘sky-mount’, on which the entire dish is rotated to offset rotation in parallactic angle. This system will work only with a symmetric dish design. An alternative is to rotate the focal package. Future tests with ASKAP will shed light on this.

Some features of the SKA1 dishes may have to be altered to accommodate PAFs efficiently. It is conceivable that slightly different optical surfaces from the SKA1-mid dishes can be used for SKA1-survey, while sharing the mechanical structure and the local dish infrastructure (mount, foundation, control, etc.). Significant investigative effort is still needed to determine whether PAFs can be combined efficiently with offset Gregorian dishes. For the purposes of this document, this assumption has been made, but may have to be reviewed in the light of further results.

9.3 Array Configuration

With the deep ASKAP EMU[45] and WALLABY [46] surveys as guides and other constraints noted below, the main characteristics of the array configuration are:

- A core of collecting area that will provide good brightness temperature sensitivity for detection of the HI-line.
- Sufficient resolution to avoid confusion in continuum, along with a smooth distribution of sensitivity with baselines out to the equivalent of the confusion limit (plus a reasonable margin) (see Section 8.2). The orientation of the arms will be adjusted to fit inside the boundaries of the Boolardy station in such a way that coverage of the $u-v$ plane is satisfactory. Space is available for arms out to ~ 50 km.
- The antenna configuration for SKA1-survey has not been optimised with regard to the distribution of sensitivity. Work must be done to design a configuration to ensure a

significant improvement in capability over ASKAP for deep HI and continuum surveys, and to ensure that such surveys are not significantly affected by confusion.

- The core of the SKA1-survey telescope will be in the same location as the current ASKAP array. This will permit the incorporation of the ASKAP antennas into SKA1-survey in a single-core configuration.
- A constraint that both the SKA1-low and SKA1-survey arrays fit into the boundaries of the Boolardy station in Western Australia. This will be the most cost-effective solution since the station has been leased by CSIRO.
- The core-spiral arm structure has been adopted for SKA1-survey. It is important that the spiral arms are sufficiently “wrapped” that good instantaneous u-v coverage is provided for short (“snapshot”) observations, and to reduce the number of gaps in u-v coverage, a measure of quality used for the SKA.
- Detailed positioning of the individual antennas or stations and their services will have to take into account inspection of affected areas for indigenous artifacts.
- As described in Section 6, the core of SKA1-low should be sufficiently far away from the ASKAP core to provide interference protection. This does not affect the SKA1-survey array in general, although the positions of some antennas may be moved to improve resilience to interference.
- To the extent possible, the two arrays should share servicing corridors for power and communications, as well as existing roads.

Figure 20 shows the inner part of the SKA1-survey configuration showing both ASKAP and SKA1 antennas.

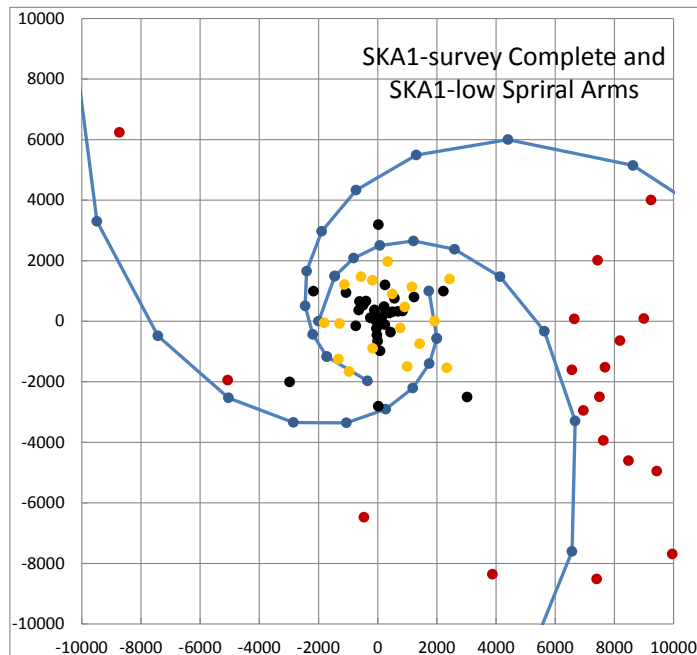


Figure 20 The inner 400 km^2 of SKA1-survey. The black dots are ASKAP antennas; the yellow ones are SKA1 core antennas; the blue ones are SKA1 antennas on spiral arms. The arms are connected by lines. Although

the lines are included for clarity, they could become service corridors. The red dots are nearby SKA1-low stations.

Figure 21 shows the position of the SKA1-survey array on the Boolardy station scale, along with the SKA1-low array in juxtaposition. Note that these positions are meant to be representative, not final. Numerous adjustments may be needed, provided the overall distribution is preserved.

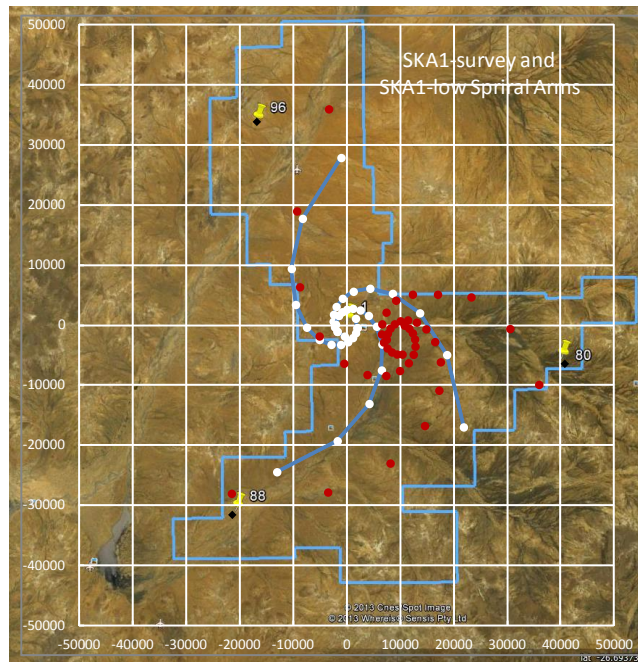


Figure 21 The array configuration for SKA1-survey. The spiral arm SKA1 antennas are shown as white dots. The SKA1 antenna core and ASKAP antennas are not shown. The red dots represent the SKA1-low stations, which are on the same site.

Figure 22 shows the run of collecting area with radius. It is a reasonably smooth distribution, although the slight dip centred around 1700 m might be improved.

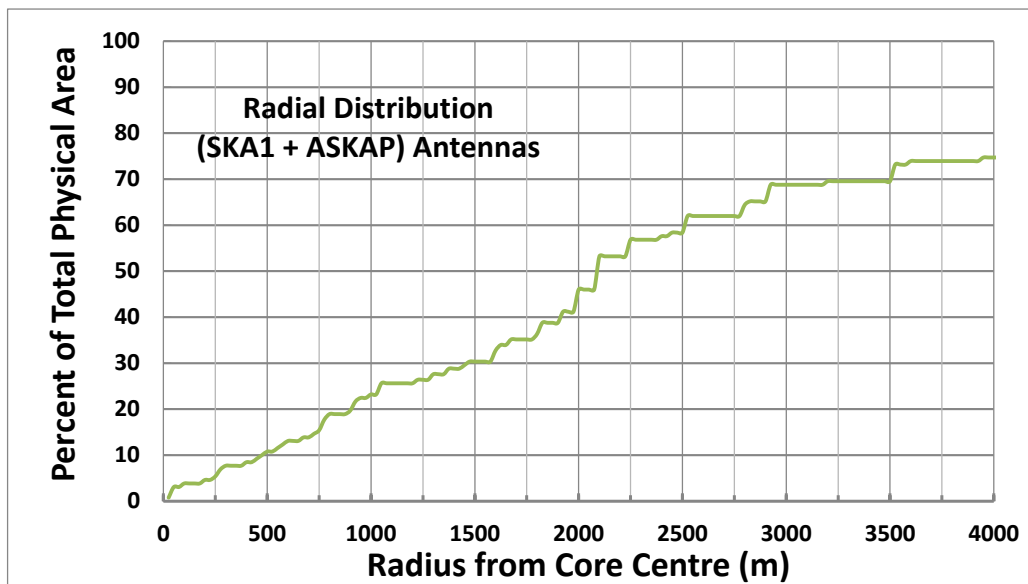


Figure 22 The distribution of fractional physical collecting area from the centre of the SKA1-survey array out to a radius of 4 km.

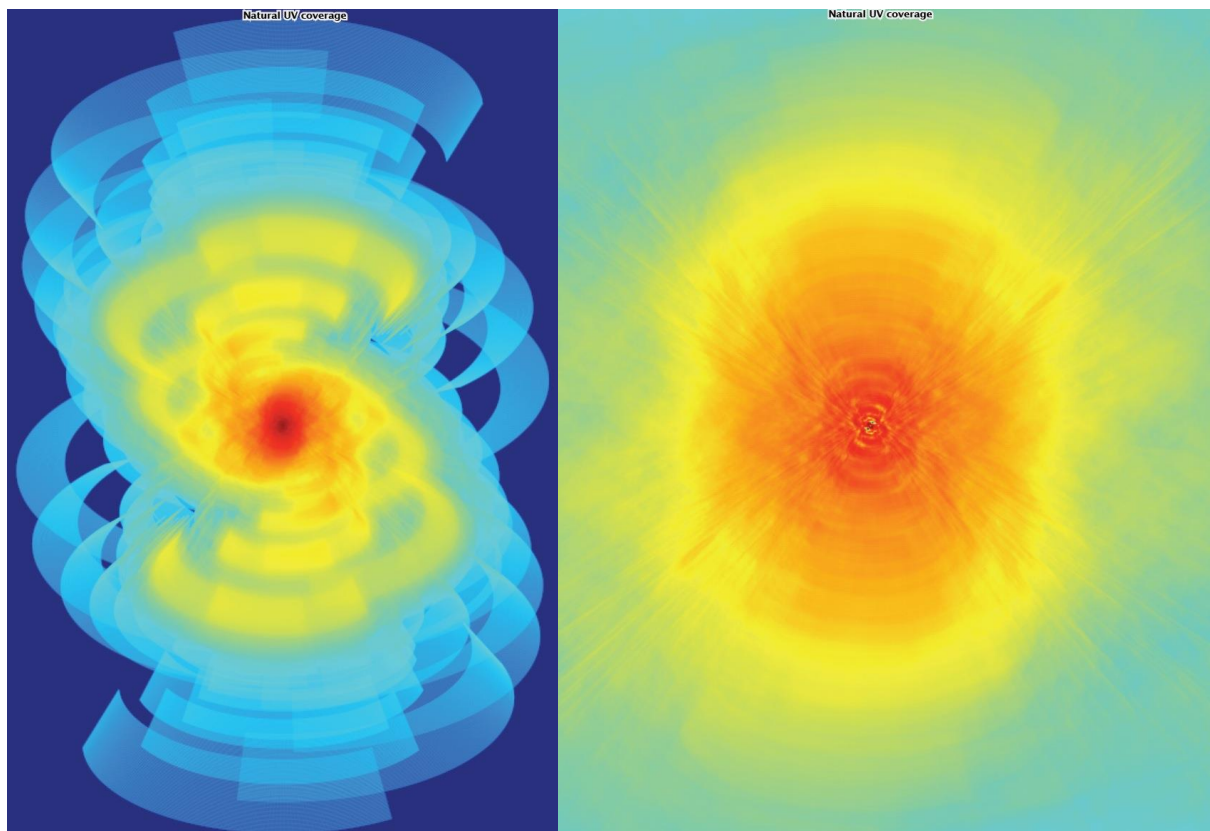


Figure 23 *u-v* coverage corresponding to the antenna layout in Figure 20 and Figure 21. In general these antenna positions are representative, and not optimised. Brightness temperature sensitivity is determined mainly by the coverage in the core, which is quite dense.

Figure 23 shows the *u-v* coverage plots for the SKA1-survey array: an 8-hr observation centred on the meridian, field centre passing through the zenith. The dimensions of the left box are ± 40 km E-

W and ± 50 km N-S. The right box, showing $u-v$ density in the core region is ± 5 km E-W and ± 6.5 km N-S. In both cases, a 20% fractional bandwidth is used.

9.4 PAF Receiver Bands

The optimum frequency range for SKA PAFs is discussed in [19], in which HI Surveys, continuum surveys (including polarization/magnetism), and pulsar searches/timing are considered. As noted above, the emphasis in the SKA1 Design Reference Mission is on HI-surveys (high-redshift HI-line absorption against strong continuum sources and low redshift (nearby galaxy) HI-line emission. OH-lines are not considered. For HI-line surveys 570 – 1425 MHz, and for continuum and polarized emission, 800 – 2000 MHz are favoured, respectively. In both cases they have used a upper/lower frequency ratio of 2.5 for these bands.

The planned ASKAP Mark II PAFs will cover a frequency range from 700 – 1800 MHz, which is a 2.57:1 frequency ratio, and is taken as a technically feasible ratio.

Using a ratio of 2.57:1, a reasonable compromise for SKA1-survey PAF Band 2 is 650 – 1670 MHz, and these have been chosen in this document as working numbers. The low end is not quite as low as the ideal for HI-line surveys, but the high end is quite good for continuum emission. The rest-frequency 1670-MHz OH-lines are also captured.

For SKA-survey a third generation of PAFs (Mark III) will be available, which will have significant improvements in performance, and will cover PAF Band 2.

The SKA dishes are designed to accommodate several receivers that can be moved into the focal position as needed. Two additional bands have been allocated on a provisional basis, one below PAF Band 2 and the other above it in frequency. Again, a frequency ratio of 2.57:1 has been assumed.

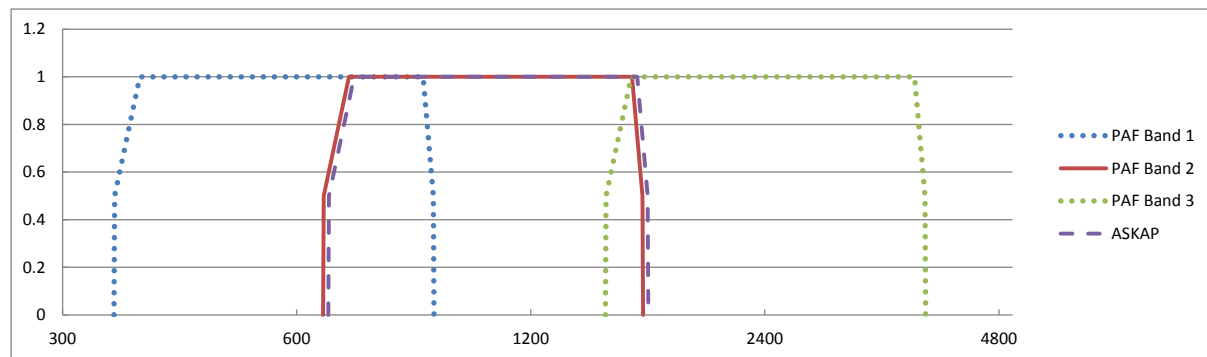


Figure 24 Receiver bands for SKA1-survey. The ASKAP band is shown as a dashed line, slightly offset for clarity, but is designed to overlap PAF Band 2 completely. The dotted lines are potential future bands.

9.5 SKA1-survey Overall Performance

The ASKAP array will be operated independently of the SKA for as long as possible, before being incorporated into an expanded SKA1-survey.

9.5.1 The SKA1-survey Array

This section describes the performance available from the array consisting of the 36 ASKAP dishes and the 60 SKA1-survey dishes.

The following principles underlie the more detailed assumptions made in this section:

- Because the frequency bands are common the combined array will be operated mainly as a single array, although splitting the array into sub-arrays will be part of the design. Unlike SKA1-mid, where there are different frequency bands available for MeerKAT and SKA1 dishes, there is complete frequency overlap for SKA1-survey dishes and ASKAP dishes. Apart from sub-arrays, it is unlikely that SKA1-survey dishes will ever be operated as a separate array.
- The merged array described in Section 9.5 is feasible, and additional SKA1 dishes and service corridors can be installed without destroying similar ASKAP infrastructure.
- The overall cost will be minimised if the ASKAP system can be utilised in a large intact “chunk”. This will permit the independent operation of ASKAP for as long as possible.
- Digital signal processing equipment and computing equipment have a sufficiently short life-span that low-priority will be given to incorporating them into the new system. However, this equipment may be vital during a transition phase if it can be used as a tool to test segments of the new system.

The following additional assumptions are made with the above principles in mind:

- The ASKAP dishes, receivers, and the data transport system will be incorporated into the joint array.
- The capabilities of the sky-mount of the ASKAP antennas will either be reproduced on the SKA1 antennas or the sky-mount will be disabled during joint observations. There will not be an observing mode in which one set of PAFs rotate on the sky with respect to the other set.
- The Mark III PAFs can be designed to be identical for both the ASKAP dishes and the SKA1-survey dishes. If not quite identical, they can be designed so that, with the appropriate beamforming techniques, the beam positions on the sky and the frequency ranges are identical as seen at the outputs of their respective beamformers. It is assumed that the Mark III PAFs can produce 500 MHz of instantaneous bandwidth.
- The following two possibilities result in slightly different approaches to interfacing with PAFs and ASKAP equipment to the combined telescope system:
 1. The ASKAP Mark III PAFs are likely to utilise RF-over-Fibre to transport the RF in analogue form from each element of the PAF array to a processing centre, where digitisation takes place. In the case of ASKAP, the processing centre is the central correlator building. However, the maximum reach of RF-over-Fibre is about 10 km. Thus if this model is adopted for more distant SKA1 antennas, then enclosures supplied with power will be needed at strategic points in the array configuration. Digital data would then be transported from these enclosures to the central building. Optionally, beamforming will also take place in these enclosures to reduce the amount of data transmitted.

- 2. If the Mark III PAFs are equipped with internal digitisers (or upgraded to such), then digital data will be transmitted all the way to the central correlator building. Optionally, beamforming will take place in or near the antennas to reduce the amount of data transmitted.
 - In addition, the associated telescope infrastructure including the correlator building is assumed to be re-usable or expandable. (Note in general all infrastructure will be re-used, but much of it is not directly attached to performance.) This approach is designed to re-use as much as possible, while at the same time keep the ASKAP system intact for as long as possible.
 - System interfaces to the re-used equipment occur in three principal places:
 - The dishes and associated control and support systems. It is assumed that the SKA1 control system will interface to a system that controls all of the ASKAP dishes. It is further assumed that the ASKAP antennas can be separately controlled as a sub-array of the overall system, but will otherwise be integrated into an overall control system that can be managed as one. Support systems such as power management will also be centrally interfaced to the new system.
 - Synchronisation reference signals delivered to the dishes. If possible, this interface will be central, but some sort of conversion may be needed at each digitisation point (enclosure or antenna) to ensure adequate synchronisation. In the unlikely event that Local Oscillators are used in the receivers, synchronisation signals will also be needed at the antennas.
 - Data delivery to the correlator building. Ideally, the interface to ASKAP data would be at the output of the digitisers in the correlator building. Otherwise the interface should be at the electrical output of the RF-over-Fibre system.
- If a change is made on ASKAP to digitise at the antennas or intermediate enclosures, it is assumed that data can be de-formatted/reconstructed and delivered to the correlator system, most likely the delay system, in a compatible manner and that time stamps can be recovered, sample-errors/bad-data recorded, etc.
- The parts of the ASKAP system “outside” of these boundaries will be discarded or retired in an orderly transition.
 - To avoid disturbing equipment that is presumed to be “shaken down”, the general approach will be to make as few changes to ASKAP equipment as possible, with preference given to interface convertors or adaptors.
 - The number of sub-arrays can be as large as the number of antennas.

Table 15 and Table 16 have been assembled using the above assumptions and calculations outlined in the footnotes.

Table 15 SKA1-Survey Array

| Aperture | | 60 x 15-m (equiv. dia.) offset Gregorian reflectors plus 36 x 12-m dia. symmetric reflectors |
|-------------------------|----------------------|---|
| Total physical aperture | 14674 m ² | |

| | | |
|--|----------------|--|
| <i>Antenna Aperture Efficiency*</i> | | |
| 300 MHz | ~60 % | Gradual degradation to 400 – 300 MHz |
| 400 MHz | ~65 % | |
| 600 – 8000 MHz | ~78 % | |
| 8 – 15 GHz | 70% | |
| 15-20 GHz | ~65 % | Gradual degradation to 15 – 20 GHz |
| Minimum Elevation Angle | 15 deg | All Azimuths |
| <i>Array Configuration</i> | | |
| radius <~400 m | ~12% (11 ant.) | Filling factor = 0.25% |
| ~400 m < radius < ~1000 m | ~20% (18 ant.) | 0.082% |
| ~1000 m < radius < 2500 m | ~32% 31 ant.) | 0.031% |
| ~2500 m < radius < 4000 m | ~16% (15 ant.) | 0.008% |
| ~4000 m < radius < 25000 m | ~22% (21 ant.) | 1.2×10^{-5} % |
| <i>Baselines</i> | | |
| ASKAP dishes | 630 | |
| SKA1-survey dishes | 1770 | |
| Mixed dish | 2160 | |
| Total | 4560 | |
| <i>Antenna RF System</i> | | Only one Feed available at a time, common across |
| PAF Band 1 | 350 – 900 MHz | Dual polarization (2 orthogonal) |
| PAF Band 2 | 650 – 1670 | " |
| PAF Band 3 | 1500 – 4000 | " |
| <i>Maximum Available Bandwidth</i> | | |
| PAF Band 1 | 500 MHz | Each polarisation |
| PAF Band 2 | 500 | " |
| PAF Band 3 | 500 | " |
| <i>Sampled IF Sub-bands**</i> | | |
| PAF Band 1 | 1 x 500 MHz | Each polarisation |
| PAF Band 2 | 1 x 500 | " |
| PAF Band 3 | 1 x 500 | " |
| <i>Phased Array Feed (PAF)</i> | | |
| PAF Diameter | | |
| PAF Band 1 | 1.82 m | $\sim 5.5 \lambda_{\min}$; 6.8 HPBW |
| PAF Band 2 | 1.0 | " |
| PAF Band 3 | 0.41 | " |
| PAF Number of Elements | | |
| PAF Band 1 | 94 | Each polarisation |
| PAF Band 2 | 94 | " |
| PAF Band 3 | 94 | " |
| PAF Number of Beams | | |
| PAF Band 1 | 36 | Assuming a beam deviation factor of 1.25 HPBW/ λ |
| PAF Band 2 | 36 | " |
| PAF Band 3 | 36 | " |
| Average Efficiency | | |
| PAF Band 1 | Unknown | |
| PAF Band 2 | 0.80 | |
| PAF Band 3 | Unknown | |
| <i>Digital Outputs</i> | | |
| No. of sample streams per PAF element | | Sampled bands (both pol'ns) |
| PAF Band 1 | 2 x 8 bits | |
| PAF Band 2 | 2 x 8 | |
| PAF Band 3 | 2 x 8 | |
| <i>Signal Transport System</i> | | |
| RF-over-Fibre (analog) to Digitizer Location | 188 fibres | One switchable RF-over-Fibre subsystem per antenna. |

| | | |
|--|---------------------------|---|
| Digitised Data Rate before PAF Beamformer | | To be transported if remote enclosures do not contain beamformers. |
| PAF Band 1 | 2256 Gbit s ⁻¹ | |
| PAF Band 2 | 2256 | |
| PAF Band 3 | 2256 | |
| Digitised Data Rate after PAF Beamformer | | To be transported if remote enclosures contain beamformers. |
| PAF Band 1 | 864 Gbit s ⁻¹ | |
| PAF Band 2 | 864 | |
| PAF Band 3 | 864 | |
| Signal Processing System | | |
| Correlator | | |
| Max. No. input data streams | 6912 | 96 ants x 2 pol'n x 1 IF x 36 beams |
| Freq. chans (over widest sampled (BW)) | 256000 | Selected for $\sim 1 \text{ km-s}^{-1}$ resolution in PAF Band 2 |
| Available frequency Resolution | | |
| PAF Band 1 | 1.67 km-s ⁻¹ | 1.95 kHz |
| PAF Band 2 | 0.90 | " |
| PAF Band 3 | 0.39 | " |
| Complex Correlations**** | 17×10^{10} | (96 ² /2) blns x 4 pol'n prod's x 256,000 chans x 36 bms |
| Corr. Load Factor for 2.5 GHz bandwidth | 1313 Tera-MACs | 5.0 GHz in 2 x 2.5 GHz bands at X-band |
| Minimum Dump Time***** | 1.4 s | For 10 km Baselines |
| | 0.3 | For 50 km Baselines |
| Science Computing System | | |
| Input data rate (GByte-s ⁻¹) for | | Byte s ⁻¹ av'ge from correlator (4-Byte x 2 for complex) |
| 10 km max baseline | 934 | |
| 50 km max baseline | 4670 | |

* SKA1 antennas only. Expected aperture efficiency using well designed, realisable feeds. For ASKAP antennas see [xxx].

Footnotes invalid

** Either of two digitised bandwidths available: 1 GHz and 2.5 GHz.

*** Total Bandwidth (GHz) x 2 (Nyquist) x 4 or 8 (bits) x 1.25 (8B/10B encoding) x 1.2 (oversample) x 2 (pol'n streams); output of Digital Down Converter at antenna.

**** For max. number of frequency channels.

***** The following approximation produces a 2% drop in visibility amplitude at the edge of the primary beam: $\Delta t = 1200 (D_{\text{station}}/B_{\text{max}})$.

Table 16 Key System Performance Factors for SKA1-survey Array

| | | |
|-----------------------------------|--------|--|
| Antenna/Feed/Receiver Performance | | |
| Antenna/Feed Efficiency | | |
| SKA1-survey Antennas* | | |
| PAF Band1 | 0.80 | Area-weighted Average over beams and frequency |
| PAF Band2 | 0.80 | " |
| PAF Band3 | 0.80 | " |
| ASKAP Antennas | | |
| PAF Band2 | 0.80 | Area-weighted Average over beams and frequency |
| Average T _{sys} | | |
| SKA1-survey Antennas | | |
| PAF Band1 | 50 K | Average over RF bands |
| PAF Band2 | 30 | |
| PAF Band3 | 40 | |
| ASKAP Antennas | | |
| PAF Band2 | 30 | |
| Continuum Sensitivity | | |
| SKA1-survey Antennas | | |
| SEFD (each antenna, Stokes I) | | |
| PAF Band1 | 976 Jy | |
| PAF Band2 | 586 | |
| PAF Band3 | 781 | |
| ASKAP Antennas | | |
| PAF Band2 | 915 | |

| | | |
|--|-----------------------------|---|
| SEFD (96 antennas, Stokes I)** | | |
| PAF Band1 | 12 Jy | |
| PAF Band2 | 7.0 | |
| PAF Band3 | 9.4 | |
| Min. detectable flux (rms) (ΔS_{\min})*** | | |
| PAF Band1 | $584 \mu\text{Jy s}^{-1/2}$ | |
| PAF Band2 | 351 | |
| PAF Band3 | 467 | |
| <i>Sensitivity as A_e/T_{sys} (all antennas)</i> | | |
| PAF Band1 | $235 \text{ m}^2/\text{K}$ | |
| PAF Band2 | 391 | |
| PAF Band3 | 212 | |
| Single Beam Area @ centre freq. (deg^2)**** | | $\Omega_{\text{beam}} = (\pi/4)(66\lambda/D)^2 \text{ deg}^2$ |
| PAF Band1 | 3.5 | 15-m dishes |
| PAF Band2 | 1.0 | " |
| PAF Band3 | 0.18 | " |
| ASKAP Antennas | | |
| PAF Band1 | 5.5 | 12-m dishes |
| PAF Band2 | 1.6 | " |
| PAF Band3 | 0.28 | " |
| Equivalent "pill-box" Single Beam Area (deg^2) | | $\Omega_{\text{eqw}} = 1.17(\lambda/D)^2 \text{ ster.}$ |
| PAF Band1 | 3.9 | 15-m dishes |
| PAF Band2 | 1.4 | " |
| PAF Band3 | 0.2 | " |
| ASKAP Antennas | | |
| PAF Band1 | 6.2 | 12-m dishes |
| PAF Band2 | 1.8 | " |
| PAF Band3 | 0.32 | " |
| PAF FoV all Beams (deg^2) | | FoV for the combined array, limited by 15-m dishes |
| PAF Band1 | 61 | Based on 36 times beam area at highest freq. |
| PAF Band2 | 18 | " |
| PAF Band3 | 3.1 | " |
| ASKAP Antennas | | FoV for ASKAP array alone |
| PAF Band1 | 95 | Based on 36 times beam area at highest freq. |
| PAF Band2 | 28 | " |
| PAF Band3 | 4.8 | " |
| SSFoM all Antennas | | |
| PAF Band1 | 34 | $\times 10^5 \text{ m}^4 \text{ K}^2 \text{ deg}^2$ |
| PAF Band2 | 27 | " |
| PAF Band3 | 2.7 | " |
| SSFoM x BW (all Antennas) | | |
| PAF Band1 | 16800 | $\times 10^5 \text{ m}^4 \text{ K}^2 \text{ deg}^2 \text{ MHz}$ |
| PAF Band2 | 13500 | |
| PAF Band3 | 1326 | |
| Imaging Dynamic Range (PAF Band2)***** | | Based on 1000-hr single-field integration. |
| PAF Band1 | 3.6×10^5 | 55 dB |
| PAF Band2 | 6.0×10^5 | 56 |
| PAF Band3 | 4.5×10^5 | 54 |
| Spectral Dynamic Range | TBD dB | |

* Expected aperture efficiency using PAFs feeds.

** $\text{SEFD}_{\text{array}} = 1/(n/\text{SEFD}_{\text{ASKAP}} + m/\text{SEFD}_{\text{SKA}})$, where SEFDs are the n ASKAP and m SKA antennas, respectively. $\text{SEFD} = 2k_B T_{\text{sys}}/A_e$ for an individual antenna.

*** $S_{\min} = \text{SEFD}_{\text{array}}/(\eta_s(2\Delta v \tau)^{1/2})$, where η_s is the system efficiency, Δv is the channel bandwidth, and τ is the total integration time. Note that for a single polarisation $S_{\min} = 2k_B T_{\text{sys}}/(\eta_s A_e (\Delta v \tau)^{1/2}) = \text{SEFD}_{\text{array}}/(\eta_s (\Delta v \tau)^{1/2})$, which is $2^{1/2}$ larger for S_{\min} . S_{\min} is given for $\tau = 1$ s. η_s is assumed to be 0.9.

**** This is the FoV used for the science performance evaluation. Assumes illumination tapers to zero at the edge of the dish and follows $E(x) = 1 - 2r^{2/3}$, where r is the distance from the dish centre. This results in a first sidelobe level of -23 dB.

***** Ratio taken between the flux of a typical L-band continuum source in field of 100 mJy and 1σ noise level after a 1000-hr integration on a single field.

9.6 Digital Data Back-Haul

The RF over fibre system currently adopted for ASKAP has a 7 km reach. It may be possible to extend this reach, however it is likely that a digitising stage will be required in the field for the longest baselines of the SKA1-survey array. This may be at the antennas themselves or at shared nodes in the network (ie shielded enclosures that service several nearby antennas) and may include a beamformer. The transmission will use optical fibre to carry digitised data. It will be a point to point deterministic network in which the data flows in a uni-directional fashion from the digitising stage/beamformer nodes to the central processor.

The integrated ASKAP array will reuse the existing data transmission system and will not be part of the SKA1-survey digital data backhaul design.

9.7 SKA1-survey Central Signal Processor

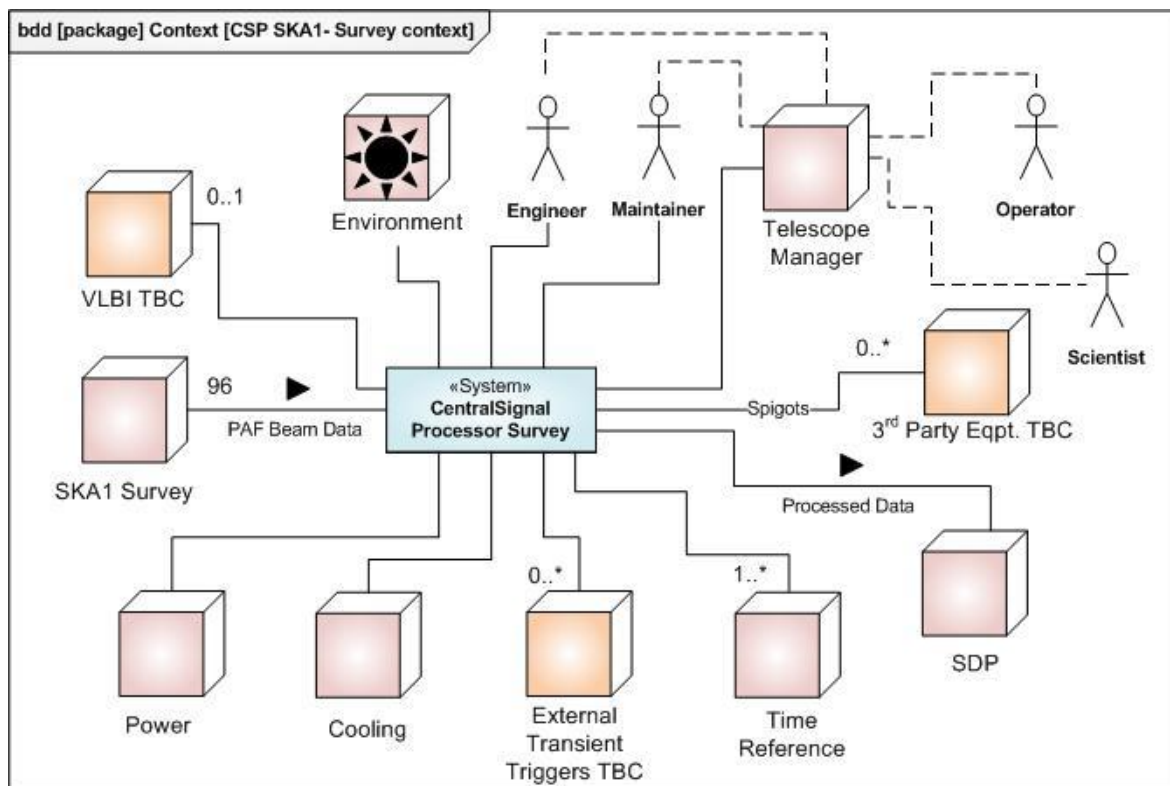


Figure 25 SKA1-survey Context Diagram – Central Signal Processing

This section details the signal processor and computing equipment present at the Central Processing Facility in Australia for the SKA1-survey telescope. Figure 25 shows the complete context diagram. Some aspects detailed in the SKA1-survey and SKA1-low context diagrams may be common due to the likely co-location of equipment and common infrastructure but this is not currently assumed.

VLBI, external transient triggers and 3rd party equipment are detailed. These are included for completeness and are illustrated with multiplicities that include zero. Third party equipment

potentially includes (but is not limited to) transient processors. It is anticipated that potential access to a limited subset of data will be made available providing the provision of spigots.

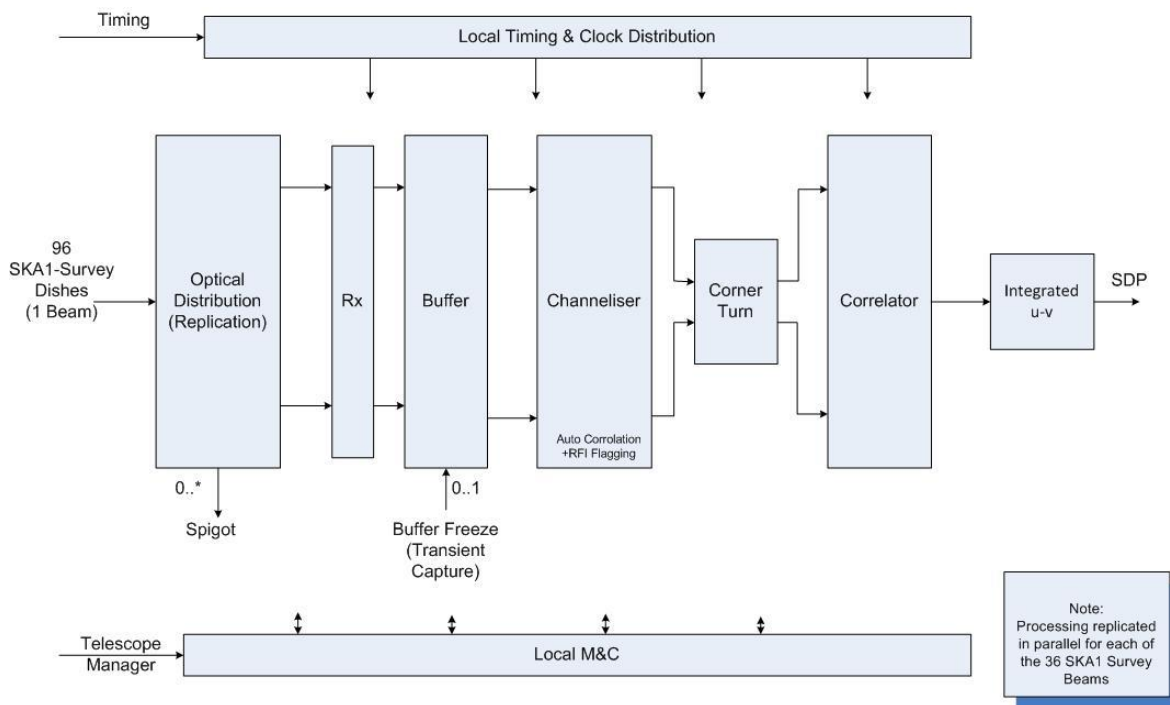


Figure 26 SKA1-survey Functional Architecture

The SKA1-survey correlator differs from the others presented, as it has to provide correlation for multiple beams. The processing load for a large N correlator of this type scales as the $N_{\text{beams}} \cdot N^2 \cdot B$, where N is the number of antennas inputs being correlated and B is the total bandwidth and N_{beams} the number of beams. This difference may warrant a different physical implementation from a single beam correlator.

The functional architecture for a single beam slice of the correlator is provided in Figure 26. Other beams are processed in exactly the same manner but in parallel.

It is assumed that the Survey beam-former may be providing either array or beam data to external transient detection equipment.

The buffer at the front end of the correlator may provide the ability to freeze and down load the data flagged by external transient detection equipment.

Table 17 summarizes the parameters associated with SKA1-survey correlation. Equipment estimates are contained in Appendix B.

Table 17 SKA1-Survey Correlator Parameters

| Correlator SKA Survey | | |
|--|-------------------------------------|---|
| Max. No. input data streams | 6912 | 96 ants x 2 pol'n x 1 IF x 36 beams |
| Freq. chans (over widest sampled (BW)) | 256000 | Selected for $\sim 1 \text{ km}\cdot\text{s}^{-1}$ resolution in PAF Band 2 |
| Actual channelisation | 262,144 | As power of 2 for FFT: 2^{18} |
| Available frequency Resolution | | |
| PAF Band 1 | $1.67 \text{ km}\cdot\text{s}^{-1}$ | 1.95 kHz |
| PAF Band 2 | 0.90 | " |
| PAF Band 3 | 0.39 | " |

| | | |
|---|---------------------|---|
| Complex Correlations**** | 17×10^{10} | (96 ² /2) blns x 4 pol'n prod's x 256,000 chans x 36 bms |
| Corr. Load Factor for 2.5 GHz bandwidth | 1313 Tera-MACs | 5.0 GHz in 2 x 2.5 GHz bands at X-band |
| Minimum Dump Time***** | 1.4 s | For 10 km Baselines |

9.8 SKA1-survey Science Data Processing

Processing for SKA-Survey is essentially simultaneous (as opposed to sequential) mosaicking. The AW projection ([23] and [24]) can thus be used to construct images efficiently. To reach high dynamic range, at least the following will be required: careful calibration of the PAF LNAs, multi-frequency synthesis to estimate and correct spectral effects, and accurate modelling of radio sources, etc.

SKA-survey and SKA1-low are similar in that the beam pattern is formed by a phased array with many active elements. If, as in ASKAP, the phased array is held fixed with respect to the sky, the remaining source of instability is the intrinsic gain variations of the phased array elements. Unlike the ionosphere for SKA1-low, these gains can in principle be measured directly using, for example, radiators on the dish surface. At the best, such measurement would fully stabilize the gains. More likely is that fast variations are removed, leaving slower, minute-timescale, variations to be tracked from astronomical sources. If these amount to just gain variations then correction is very straightforward and low-cost. If on the other hand the actual beam shapes distort, correction could be more expensive and similar to that for SKA1-low.

10 Data Transport from CSP to SDP Centres

10.1 SKA1-low and SKA1-survey – Australian site

The Australian government and CSIRO have installed a fibre link from the ASKAP correlator centre on Boolardy station to the Pawsey supercomputing facility in Perth. It is operated by AarNET. The SKA have reserved 24 optical fibre cores in this cable link.

Table 18 Data Transport: Boolardy Correlation Centre to Perth

| | | |
|---|----------|--|
| Bit rate output of the SKA1-survey correlator | ~39 Tbps | Including 4670 GByte/s max raw data output from the correlator, transient and pulsar candidates and meta-data distribution to the SDP. No provision has been made in this budget for concurrent VLBI transmission. |
| Bit rate output of the SKA1-low correlator | ~11 Tbps | Including 842 Gbytes/s max raw data output from the correlator for SKA1-low. |
| Distance Correlator to HPC in Perth | ~820 km | 370 km MRO to Geraldton and 450 km Geraldton to Perth. |

10.2 SKA1-mid – South African site

The response from the site bids suggested placing the HPC at the array site, whereas this baseline design calls for the Science Data Processing centre to be in Cape Town, similar to the case for the Australian site. Data transport links exist from the Northern Cape to the Western Cape. Table 19 contains the basic parameters.

Table 19 Data Transport: Karoo Correlation Centre to Cape Town

| | | |
|--|----------|--|
| Bit rate output of the SKA1_mid correlator | ~27 Tbps | Including 3250 Gbyte/s max raw data output from the correlator, transient and pulsar candidates and meta-data distribution to the SDP. No provision has been made in this budget for concurrent VLBI transmission. |
| Distance Correlator to HPC in Cape Town | ~670 km | Along transport corridors. |

11 Synchronisation

It is the function of the synchronisation sub-system within the SKA to provide the frequency reference signals required, over the required bandwidths and link distances. Whilst SKA1-low, SKA1-survey and SKA1-mid may have different synchronisation requirements, a common approach to design may lead to a single site-wide, or even SKA1-wide synchronisation system design. Similarly the needs of SKA2 will be kept in mind in the design phase of this subsystem, in order to avoid unnecessary replacement costs and to avoid substantial changes in this critical sub-system between SKA1 and SKA2. For this reason the synchronisation system described here is based upon the potential top operating frequency of the SKA1-mid antenna, 20 GHz. At these frequencies it should be possible to limit coherence losses to ~2% for the 20 GHz case, and much less for lower frequencies.

Coherence can be maintained through the use of accurate independent clocks or by a frequency reference distribution from a central reference clock. At every antenna or station, the synchronisation system will provide a standard reference sine wave from which clocks for digitisation and/or local oscillator signals can be derived (if needed), and a pulse-per-second (1-PPS) signal (or similar) from which time-tags can be derived.

The existence of a coherent signal at every antenna could generate correlated radio interference (RFI). The impact on all the telescopes on the site will have to be assessed to ensure that such interference, if present, is not harmful. If so, appropriate shielding measures will be needed.

The status of the synchronisation system as a single point of failure means that the provision of redundant clock sources and equipment may be required.

11.1 Timing

Sufficiently accurate Coordinated Universal Time (UTC), converted to sidereal time using regularly published Earth-rotation data (UT1 – UTC and higher order corrections), is fundamental on each site for absolute pointing of antennas and array beams (beamformers of all types). Time servers will be needed for these devices, providing for example, synchronised sine-wave and 1 pulse-per-second (PPS) signals with UTC time-tags. These will be required also for the Telescope Managers and anything else in the systems that create time-tags.

High-precision, reference to International Atomic Time (IAT) timing of the data streams is not strictly required for imaging observations, once delays or clock offsets from the synchronisation system have been determined for each antenna. However, astrometry and VLBI observations may require high-precision reference to IAT.

VLBI and transient detection equipment, where present, will have access to time services to which output data can be tagged in the appropriate way for those types of observations.

Each site will require as a minimum, an active hydrogen maser clock, synchronised to IAT using GPS signals. Reliability and continuity may require redundant clocks at the array centre, possibly incorporating existing clocks, if available. Time-tagging of events must be traceable ultimately to Julian Day Number IAT through an archive of drifts between the local clocks and GPS signals.

An initial analysis of time requirements that will be able to support decade-long tracking of pulse arrival times for gravitational wave detector experiments indicates that accuracy of 10 ns will be needed over 10 years, equivalent to Allan variance of 3×10^{-16} [28].

12 Telescope Manager

The SKA telescope manager is responsible for three distinct aspects of the operations: first, the management of an astronomical observation; second the management of the telescope hardware and software subsystems in order to perform that astronomical observation and third general purpose communications for operators, maintainers and other users of the array. The Telescope Management is also focused on ensuring safety at all times.

The Observation Management subsystem ingests high-level descriptions of observations, as scheduling blocks or higher-level form. These descriptions are then scheduled. As observations are made, the scientific data, visibilities or time series, are matched with the corresponding telescope configuration meta-data and then dispatched for processing within Scientific Data Processing.

The Telescope Management subsystem controls the appropriate subsystems and collects monitor data that is used to track the entire status of the telescope including subsystem status, site security, weather monitoring, site power supply, etc. The collection of monitor data is part of the system model that describes the status of the telescope at any one time.

This entity, the system model, will contain the state-of-the-system as a function of time. A sub-set of the contents will be provided to users as meta-data. System information extracted from scientific data, such as calibrations, will also form part of the system model. The required functionality, contents, time resolution, monitoring cadence, access, and throughput requirements will be analysed as a system-wide task. Many of these requirements will be informed by a concept of operations for each site and telescope. Physically this information may be distributed across the system, but ultimately it must be archived at the super-computing center.

As noted in Section 11.1, time-tagging of events or changes in system state must be traceable ultimately to Julian Day Number IAT.

13 Data Products

Defining specific data products is beyond the scope of this document. However we can sketch a possible approach to the classification of data products. Such classification is helpful for delineating responsibilities for the production of data products.

One possible classification scheme is shown in Figure 27 and Figure 28. The SKA Observatory will be responsible for all data products up to and including level 5. Science Teams are responsible for the validation of level 5 products. Upon validation the products become level 6. It is expected that the enhanced data products in level 7 are the responsibility of the science teams.

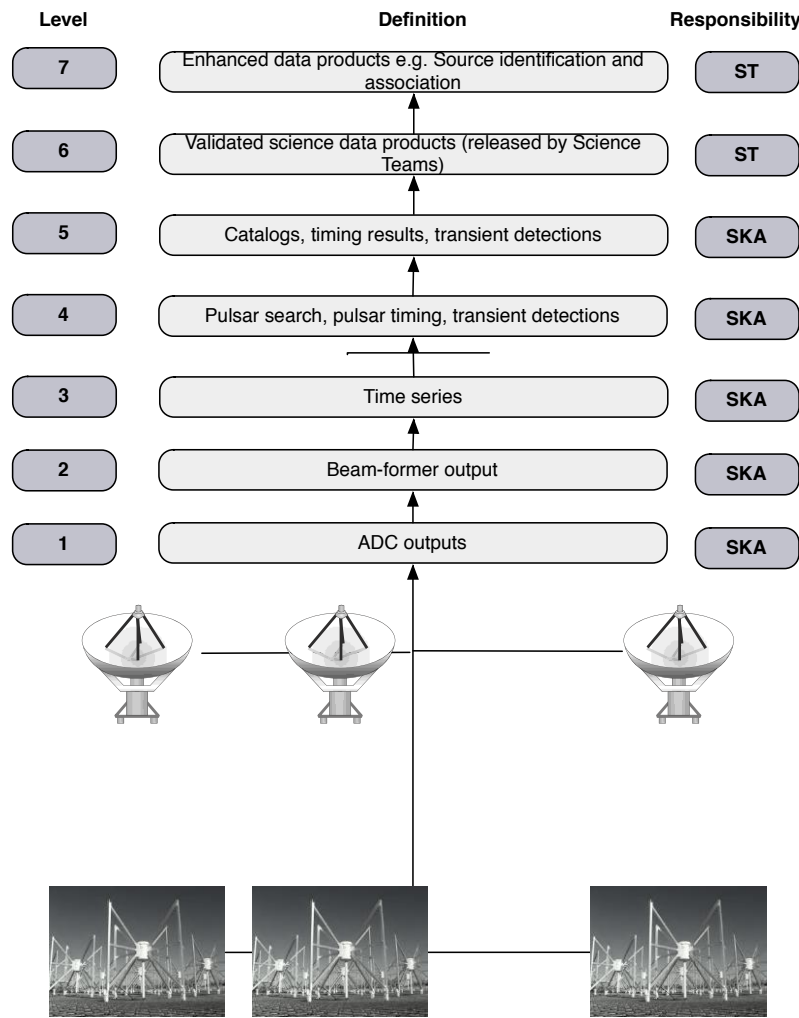


Figure 27 Classification of data levels for time-series processing.

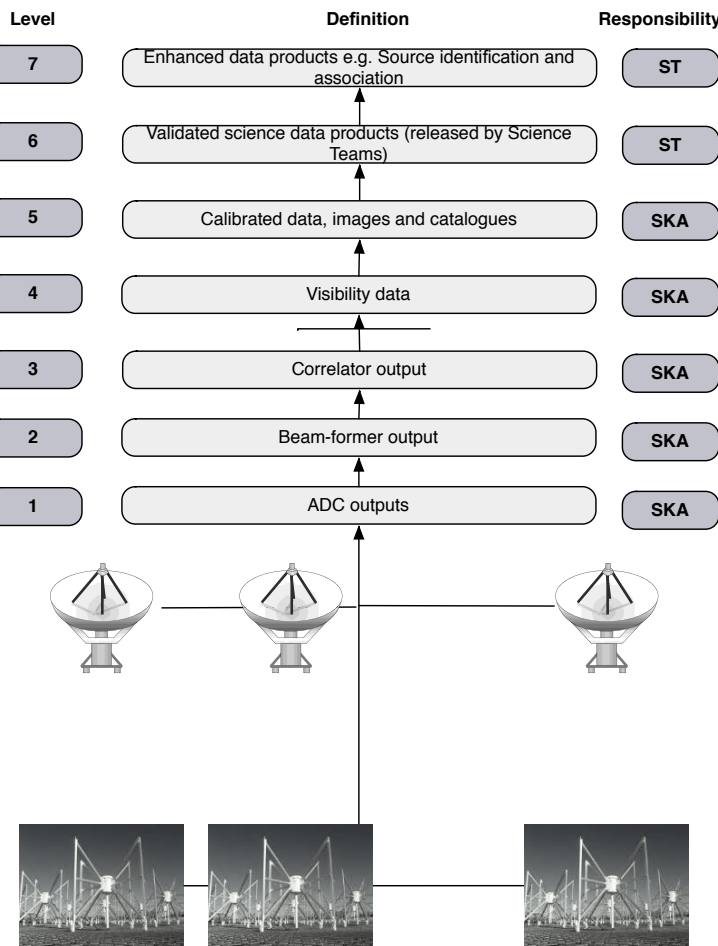


Figure 28 Classification of data levels for imaging

With this classification established, we can discuss how and where which class of product is constructed. Each telescope has a computer dedicated to processing, and there will be Regional Science and Engineering Centres (RSECs). In principle, the visibility data output by the correlator could be made available to Science Teams at the RSECs. To see if this is viable, we need to examine the telescope data rates. Table 20 shows typical data rates for the telescopes, calculated for a 12 hour observing run. Note that these are the maximum allowed by the telescope and would not necessarily be observed. The continuum visibility data sets are only a few times smaller because of the large number of channels needed to avoid bandwidth smearing on these long baselines. Clearly, moving the visibility data around long distances will require very large bandwidth. The data product images, though, are much smaller and easier to move. Hence, the default expectation is that visibility-based processing occurs at the telescope computer, and image- or catalogue-based processing can occur elsewhere. Note that this need not be a blanket proscription. The DRM chapter on EoR specifies that the prime data product is the calibrated and edited visibility data cube at 0.1 MHz frequency resolution and temporal resolution sufficient to track the ionosphere. This would be 10 – 100 times smaller than the full data set and could therefore be copied to a RSEC.

Table 20 Data Rates (In and Out) for a Typical 12 Hour Observation

| | Data in (GB/s) | Integration Time (s) | Data set (PB) | Continuum image (GB) | Spectral Line Image (GB) | Transient Images (GB) |
|--|----------------|----------------------|---------------|----------------------|--------------------------|-----------------------|
| | | | | | | |

| | | | | | | |
|--------|-----|-----|-----|----|-----|-----|
| Low | 420 | 1.8 | 36 | 17 | 180 | 400 |
| Survey | 42 | 1.8 | 3.5 | 23 | 250 | 530 |
| Mid | 8.5 | 1.4 | 0.7 | 29 | 320 | 930 |

If we now restrict the discussion to level 5 data products, all of these will have to be generated in a carefully controlled environment in which the algorithms are well understood, highly tested, and the implementations work at high efficiency on the distributed/parallel computing platforms available. The algorithms, software, and computing platform are very much an intrinsic part of the telescopes. However, this natural concern and caution does not rule out the execution of processing code that is developed by science teams on the telescope computer. It does mean that a rigorous certification process must be followed.

14 RFI Management on Both Telescope Sites

A vital aspect of the design of the telescope is ensuring that devices that produce radio frequency interference (RFI) are suppressed or shielded. There are RFI standards for the sites already, administered by the host countries. The huge increase in electrical equipment will pose a major RFI challenge that must be met.

15 Infrastructure in Australia

Operations in Australia will share ASKAP infrastructure at several locations: on/near the site, which will contain SKA1-survey and SKA1-low and nearby maintenance and living facilities, in Geraldton where the MRO Support Facility is being constructed, Perth where the Pawsey Computing Centre is located, and the location of the Host Country Headquarters, most likely in Sydney. The Pawsey Computing Centre is shared with other projects, though it is likely that, as with ASKAP, SKA1 facilities would not be shared.

15.1 On-or-Near Site

Merging site infrastructure that services SKA1-survey and SKA1-low with existing infrastructure when construction starts is primarily a matter of investigating the following:

- Increases in power provision,
- Routing of fibre and power to new antennas,
- Options for adding roads,
- Re-use of buildings and expansion, if needed,
- Other site infrastructure, such as water treatment.

Planning will require an operational plan for the site, especially facilities that are required for maintenance. Preliminary maintenance estimates will use information from existing radio telescope facilities.

Careful planning of the SKA1 dish positions in relation to the ASKAP dishes and existing infrastructure is a balance between configuration (science) and engineering aspects (roads and reticulation of power and fibre). The positions of antennas in this document are indicative only of density on the ground. Considerable latitude is available to place them in positions to minimize infrastructure and servicing costs as much as possible.

Changes or additions to infrastructure must be designed, planned and built according to a time schedule commensurate with the arrival of major components of telescopes and equipment. In addition changes to the infrastructure will need to be made so as to minimise disruption to ASKAP operations.

On-site ASKAP infrastructure is indicated in Figure 29. It includes tracks for roads, the Control Compound Building, airstrip and the location of a proposed Power Station.

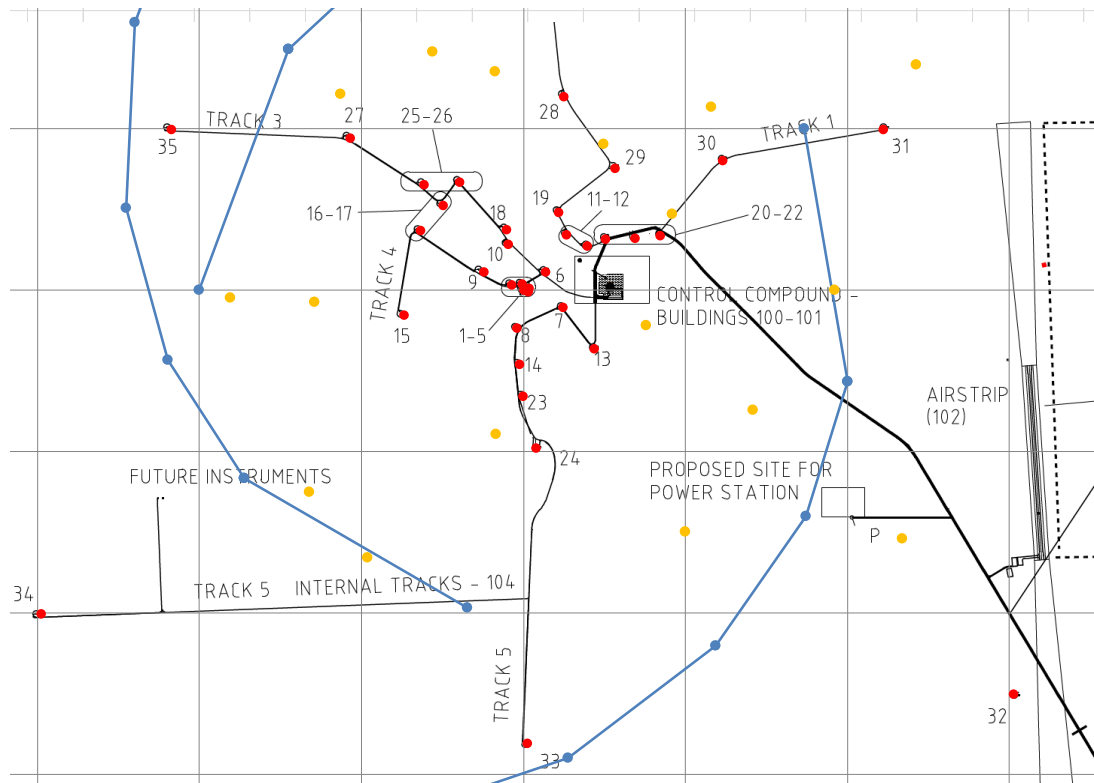


Figure 29 : SKA1/ASKAP site infrastructure shown in relationship to the SKA1-survey and ASKAP antennas.
The yellow dots are additional core antennas in a quasi-random array. The blue dots connected by lines are the SKA1 antenna spiral arms. Grid lines are centred on ASKAP antenna 1, and are at 1000-m intervals.

15.1.1 Power

15.1.1.1 Power reticulation Infrastructure

Figure 29 shows the central part of the ASKAP configuration with its dishes in red and additional SKA1 dishes in yellow. The distribution of these latter dishes is random, but has the required density. An improved final placement of these dishes, merging with the ASKAP infrastructure is required and does appear feasible.

Cables of the type that supports the power requirements for the SKA1 dishes must be routed, even while there may be some of the existing cables for ASKAP that could serve additional antennas as well.

From this figure it appears that that, while not straightforward, the merging of the two infrastructural services is feasible. Under and over-passes for cable routes will be unavoidable, and this should be done so as to leave existing reticulation infrastructure unaffected.

In addition, the issue of providing power to the additional antennas along the spiral arms, plus SKA1-low must be investigated. For the latter the reticulation of power (and fibre) will virtually not interfere with any existing infrastructure in the ground.

15.1.1.2 Provision of power

It is expected that the proposed power station, indicated in Figure 29, will have the capacity to power the entire ASKAP array with all its PAFs installed, including a complete data processing chain. The capacity will be about 1.1MW, mainly limited by the step-up transformer that feeds the main supply to the control building. The proposed power station will initially provide 2 MW of installed diesel power for redundancy purposes and about 500kW of photovoltaic power. Power is generated at 415V and is stepped up to 6.6kV for distribution to antennas and the control building.

In a second phase 1 to 1.5MW photovoltaic system will be added in a renewable expansion project. Regardless of the generation options the power entering the control building remains limited in capacity by the step up transformer mentioned earlier. This power cap applies to the entire site, including the MWA.

Given these circumstances the additional demand of the complete SKA1-survey in terms of required additional power generation must be worked out. The power requirements for SKA1-low must be investigated. Because of the relatively large separation between the two instruments it is likely that a separate power station for SKA1-low will be optimal.

15.1.2 Data Transport

The situation with regards to the fibre reticulation infrastructure is very similar to that of the reticulation of power (see Figure 29). Although there may be issues of cross-overs of routes, there should be no fundamental problem with supplying fibre to each of the SKA1 dishes interspersed with ASKAP. For SKA1-low the situation is even more straightforward as there is no existing fibre infrastructure in the ground to deal with.

It is expected that there will be a large bandwidth fibre interconnection between a concentrator facility near the centre of SKA1-low to the control/signal processing facility close to the SKA1-survey/ASKAP core.

15.1.3 Buildings

It is anticipated that for SKA1-survey, and less applicable for SKA1-low, much of the existing building infrastructure can be used. The on-site building infrastructure near the ASKAP core includes:

Central signal processing facility/Control Building – This RFI shielded facility will contain the SKA1-survey and SKA1-low signal processing hardware, a maser room and data handling equipment. Additional space is available for SKA1 data processing and support hardware. The cooling and power infrastructure should support this. Appendix B provides a rough analysis of the space needed to house the Central Signal Processing equipment for SKA1-survey and SKA1-low.

Power Station – This is a planned facility servicing ASKAP.

Staff accommodation – A small number of units can be shared. These are located at Boolardy Station.

'Near'-site facilities are those in Geraldton, the MRO Support Facility. The amount and nature of space that can be shared must be evaluated.

15.1.4 Roads

The ASKAP on-site road system can be used and extended using the same classes of roads, including the types of drainage culverts and erosion protection. Temporary roads may be needed during construction of the SKA1-survey. Access to the ASKAP antennas will have to be maintained.

An additional road system will have to be designed for SKA1-low.

15.1.5 Other Infrastructure

15.1.5.1 Water and Waste Management

Existing ASKAP water supply and waste management must be examined for extensibility to SKA1 demands. These fall into two categories:

Temporary – During SKA1 construction sufficient water capacity must be available at the construction camp(s) and at foundation concrete plants.

Permanent – In the operations phase sufficient water capacity must be available to support the expected number of staff on-site and the required cooling water.

Both instruments, SKA1-survey and –low, must be provided for.

15.1.5.2 Air Transport

Figure 29 indicates the location of the airstrip close the centre of the MRO. A second airstrip is available at Boolardy Station.

15.2 Off-site Infrastructure

- Offices for HCHQ, possibly rental accommodation.
- Supercomputing centre, Pawsey center.
- Data connectivity from Central Signal Processing building on site to the supercomputing centre. See tables for volume.

16 Infrastructure in South Africa

Operations in South Africa will require infrastructure in at least two places: on/near the site, which will contain SKA1-mid, itself, and nearby maintenance and living facilities, and Cape Town, the location of the Host Country Headquarters and an associated SKA1-mid Computing Centre. The Computing Centre may not be in the same location as the Host Country Headquarters but they will be in the same region. The Computing Centre may be a facility shared with other projects.

16.1 On-or-Near Site

Merging site infrastructure that services SKA1-mid with existing infrastructure when construction starts is primarily a matter of investigating the following:

- Increases in power provision,

- Routing of fibre and power to new antennas,
- Options for adding roads,
- Re-use of buildings and expansion, if needed,
- Other site infrastructure, such as water treatment.

Planning will require an operational plan for the site, especially facilities that are required for maintenance. Preliminary maintenance estimates will use information from existing radio telescope facilities. For example, the MeerKAT project has assembled historical figures from NRAO on maintenance of cryogenic receivers.

Careful planning of the antenna positions is a balance between configuration (science) and engineering aspects (roads and reticulation of power, fibre and roads). The positions of antennas in this document are indicative only of density on the ground. Considerable latitude is available to place them in positions to minimize infrastructure and servicing costs as much as possible.

Changes or additions to infrastructure must be designed, planned and built according to a time schedule commensurate with the arrival of major components of telescopes and equipment. In addition changes to the infrastructure will need to be made so as to minimise disruption to MeerKAT operations.

16.1.1 Power

16.1.1.1 Power reticulation Infrastructure

Figure 30 shows the central part of the MeerKAT configuration with the dishes in blue and additional SKA1-mid dishes in RED. The distribution of these latter dishes is random, but has the required density. A better final placement of these dishes, merging with the MeerKAT infrastructure is required and does appear feasible.

Cables of the type that supports the power requirements for the SKA1 dishes must be routed, even while there may be some of the existing cables for MeerKAT that could serve additional antennas as well. The MeerKAT power infrastructure uses miniature substations that feed multiple antennas.

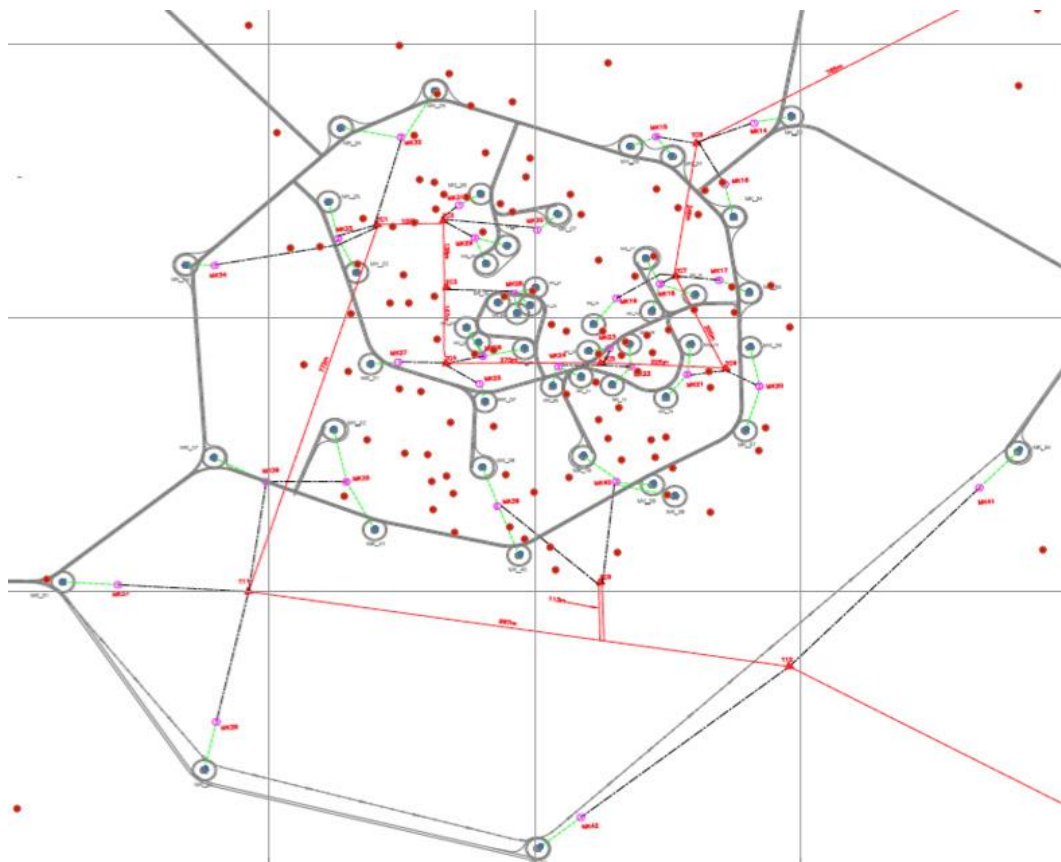


Figure 30 MeerKAT power distribution network, showing potential positions of SKA1-mid antennas, shown as red dots. Miniature sub-stations are depicted as red triangles, and power lines are red and green lines. Roads are indicated by grey lines.

Investigating how much and what kind of substations to add to the existing ones is an important aspect. Figure 30 gives the impression that, while not straightforward, this is feasible. Under and over-passes for cable routes will be unavoidable, and this should be done so as to leave existing reticulation infrastructure unaffected.

16.1.1.2 Provision of power

Power to the MeerKAT site is currently provided by an overhead 33 kV line, designed for low RFI (minimized sparking, no corona). The power line runs from a new substation near Carnarvon to the Power Facility building. From there, power is distributed by sub-surface 400-V lines to the antenna foundations. The total maximum capacity is currently 5 MVA, of which 2.5 MVA would be available for SKA1.

It is unlikely that the SKA1 power requirements would fit this budget and therefore extension of current power provision must be examined. A possible source of power is a large sub-station to the north of the site from which a high-voltage power line could link up either with the substation serving the 33 kV line or with a new one. This source of power would be sufficient to carry the project through to SKA2.

16.1.2 Data transport reticulation infrastructure

Figure 31 shows the layout of the fibre MeerKAT fibre network. The situation with fibre is very similar to that for reticulation of power to the antennas. Although there may be issues of cross-overs of routes, there should be no fundamental problem with supplying fibre to each of the SKA1 antennas interspersed with MeerKAT antennas.



Figure 31 Routing of fiber of the MeerKAT site

16.1.3 Buildings

It is anticipated that for SKA1-mid much of the existing building infrastructure can be used. The on-site building infrastructure in the Karoo includes:

Central signal processing facility (Karoo Array Processor building) – This bunkered and RFI shielded facility will contain the MeerKAT correlator hardware, a maser room and data handling equipment. Additional space of 77 racks is available for SKA1-mid data processing and support hardware. The cooling and power infrastructure should support this. Appendix B provides a very rough analysis of the space needed to house the Central Signal Processing equipment for SKA1-mid.

Power Facility – This is an existing building servicing MeerKAT, buried and RFI shielded. It contains a switching room, transformers, UPS units and distribution panels. There will be two transformers dedicated for SKA1: 33/22kV and 22kV/400V. It is stated that the total maximum capacity of the Power Facility is 5 MVA, of which 2.5 MVA would be available for SKA1.

Staff accommodation – A small number of units can be shared.

Dish assembly hall – Will be vacant by the time SKA1 dishes arrive on site.

Pedestal integration building – Can be reused as such or find other use.

Construction camps (Losberg and Meys Dam) – These exist, can be used and adapted for SKA1-specific requirements.

Near-site facilities are those at Klerefontein, close to Carnarvon. These include:

Workshops and offices – These are of sufficient size for MeerKAT operations. Co-use for SKA1 should be possible to some degree.

Staff accommodation – A small number of units can be shared.

16.1.4 Roads

The MeerKAT on-site road system can be used and extended using the same classes of roads, including the types of drainage culverts and erosion protection. Temporary roads may be needed during construction of the SKA1 array. Access to the MeerKAT antennas will have to be maintained. Figure 30 and Figure 31 provide a first order idea of the complications in providing access to all telescopes in the core region.

16.1.5 Other Infrastructure

16.1.5.1 Water and Waste Management

Existing MeerKAT water supply and waste management must be examined for extensibility to SKA1 demands. These fall into two categories:

Temporary – During SKA1 construction sufficient water capacity must be available at the construction camp(s) and at foundation concrete plants.

Permanent – In the operations phase sufficient water capacity must be available to support the expected number of staff on-site and the required cooling water.

16.1.5.2 Air Transport

The existing airstrip at Carnarvon can be used for most cases, while the newly constructed all-weather airstrip at the site is available as well. It must be noted however that the positioning of the new airstrip close to the MeerKAT core will interfere with the freedom of placement of SKA1 dishes.

16.1.5.3 Weather stations

Existing weather stations will be incorporated into SKA1 infrastructure.

16.2 Off-site Infrastructure

- Offices for HCHQ, possibly rental accommodation.
- Supercomputing centre, analogous to the Pawsey center. Infrastructure possibly shared with other projects and growing over time.
- Data connectivity from Central Signal Processing building on site to the supercomputing centre. See tables for volume.

17 References

- [1] SKA Memo 100, "Preliminary Specifications for the Square Kilometre Array", R. T. Schilizzi, P. Alexander, J. M. Cordes, P. E. Dewdney, R. D. Ekers, A. J. Faulkner, B. M. Gaensler, P. J. Hall, J. L. Jonas, K. I. Kellermann, dated December 2007.
- [2] "High-Level SKA System Description", P. E. Dewdney et al, document WP2-005.030.010-TD-001, Rev A, dated 2010-02-15.
- [3] SKA Memo 125, "Concept Design for SKA Phase 1 (SKA₁)", M.A. Garrett, J.M. Cordes, D. De Boer, J.L. Jonas, S. Rawlings, and R. T. Schilizzi (SSEC SKA Phase 1 Sub-committee), dated August 2010.
- [4] SKA Memo 130, "SKA Phase 1: Preliminary System Description", P. E. Dewdney, J-G bij de Vaate, K. Cloete, A. Gunst, D. Hall, R. McCool, N. Roddis, and W. Turner, dated November 2010.
- [5] "SKA1: High-Level SKA System Description", P. E. Dewdney et al, document WP2-005.030.010-TD-002, Rev A, dated 2011-02-14.
- [6] "Report and Recommendation of the SKA Site Advisory Committee (SSAC)", J.M. Moran et al, dated Feb. 16, 2012.
- [7] "Report of the SKA Siting Options Working Group", P. Alexander et al, dated May 2012.
- [8] "The Square Kilometre Array Design Reference Mission: SKA Phase 1", SKA Science Working Group led by T. J. W. Lazio, date May 28, 2012.
- [9] "Realigned Approach Following Site Agreement", K. Cloete, dated Aug. 15, 2012.
- [10] "SKA System Engineering Review Panel Report", J. Spyromilio et al., dated Dec. 7, 2012.
- [11] "Pre-Construction Phase, Stage 1 Work Breakdown Structure and Statement of Work", K. Cloete et al, dated Sep. 20 2012
- [12] "Interferometry and Aperture Synthesis in Radio Astronomy", A. R. Thompson, J. M. Moran, and G. W. Swenson, (second edition), Wiley, 1986.
- [13] R.P. Millenaar and R. Bolton, "Array Configurations for Candidate SKA Sites: Design and Analysis", document WP3-050.020.010-TR-001 (Rev C), R.P. Millenaar, R. C. Bolton, and J. Lazio, dated Nov. 4, 2011.
- [14] G. Mallema, L. Koopmans (eds), European SKA EoR Working Group, White Paper on "Reionization and the Cosmic Dawn with the Square Kilometre Array", Version 1 (Sept. 13, 2012).
- [15] W.A van Cappellen, M. Ruiter, G.W Kant, "Low Band Antenna; Architectural Design Document", LOFAR-ASTRON-ADD-009, Mar 21, 2007.
- [16] E. de Lera Acedo, N. Razavi-Ghods, L.E. Garcia, P. Duffet-Smith, P. Alexander, "Ultra-Wideband Aperture Array Element Design for Low Frequency Radio Astronomy", IEEE Transactions on Antennas and Propagation, Vol. 59, Issue 6, dated June 2011.
- [17] R. Smits, M. Kramer, B. Stappers, D.R. Lorimer, J. Cordes, A. Faulkner, "Pulsar searches and timing with the SKA ", Memo 105, (2008)
- [18] J. Lazio, M. Huynh, "On The Configuration of SKA Phase 1", 2012.
- [19] M. Huynh et al., "Is there an Optimum Frequency Range for Phased Array Feeds? Question 2 of the Magnificent Memoranda II", SKA Memo 142, Aug. 2012.
- [20] N. Roddis, R. Rayet, "Design approaches for cryogenically cooling receiver front ends for the SKA Dish Array", REP/1304/2774, Callisto Limited, Mar 7, 2012.

- [21] G. Cortes, W. Imbriale, L. Baker, "DVA1 Optics Design and Analysis", DVA1 CDR document, June 17, 2012.
- [22] W. A. Imbriale, L. Baker, G. Cortes-Medellin, "Optics Design for the U.S. SKA Technology Development Project Design Verification Antenna", Antennas and Propagation (EUCAP), 2012 6th European Conference, 2012.
- [23] Bhatnagar, S., Cornwell,T.J., Golap,K., & Uson,J.M., "Correcting direction-dependent gains in the deconvolution of radio interferometric images", A&A 487, 419-429 (2008)
- [24] Cornwell, T.J., "SKA1 Calibration And Imaging Cost Model", SKA memo, (2013)
- [25] Mellema. G., et al, "The European SKA EoR Science Working Group White Paper on Reionization and the Cosmic Dawn with the Square Kilometre Array", arxiv:1210.0197v1, (2012)
- [26] Tasse, C., van der Tol, B., van Zwieten, J., van Diepen, G., & Bhatnagar, S., "Applying full polarization A-Projection to very wide field of view instruments: An imager for LOFAR", arXiv:1212.6178, (2012)
- [27] S. Yatawatta et al., "Initial deep LOFAR observations of Epoch of Reionization windows: I. The North Celestial Pole", arXiv:1301.1630v2
- [28] SKA PrepSKA WP2: LO and Timing Requirements, S. Garrington and R.Spencer, JBCA The University of Manchester, 13 June 2011.
- [29] Carilli, C. L., & Rawlings, S. 2004, *Science with the Square Kilometer Array*, New Astron. Rev. (Elsevier: Amsterdam)
- [30] Gaensler, B.M. 2004, "Key Science Projects for the SKA" SKA Memorandum #44; http://www.skatelescope.org/documents/Gaensler_key_science_projects_0402.pdf
- [31] Garrett, M. A., et al. 2010, "Concept Design for SKA Phase 1 (SKA₁)," SKA Memorandum #125; http://www.skatelescope.org/PDF/memos/125_Memo_Garrett.pdf
- [32] Schilizzi, R. T., et al. 2007, "Preliminary Specifications for the Square Kilometre Array," SKA Memorandum #100; <http://www.skatelescope.org/PDF/memos/100MemoSchilizzi.pdf>
- [33] J. Lazio, M. Huynh, "On The Configuration of SKA Phase 1", private communication, 2012.
- [34] Condon, J. J. 1974, "Confusion and Flux-Density Error Distributions," ApJ, 188, 279
- [35] Condon, J. J., Cotton, W. D., Fomalont, E. B., et al. 2012, "Resolving the Radio Source Background: Deeper Understanding Through Confusion," ApJ, submitted; arXiv:1207.2439
- [36] Kellermann, K. I., Fomalont, E. B., Mainieri, V., et al. 2008, "The VLA Survey of the Chandra Deep Field-South. I. Overview and the Radio Data," ApJS, 179, 71
- [37] Owen, F. N., & Morrison, G. E. 2008, "The Deep SWIRE Field I. 20cm Continuum Radio Observations: A Crowded Sky," AJ, 136, 1889
- [38] Windhorst, R. A., Cohen, S. H., Hathi, N. P., Jansen, R. A., & Ryan, R. E. 2008, "'GiGa': The Billion Galaxy H I Survey-Tracing Galaxy Assembly from Reionization to the Present," in The Evolution of Galaxies Through the Neutral Hydrogen Window, eds. R. Minchin & E. Momjian (AIP) vol. 1035, p. 318
- [39] SKA Science Working Group, "The Square Kilometre Array Design Reference Mission: SKA-mid and SKA-lo", report, v1.0, February 2010.
- [40] SKA Memo 113, "LOFAR imaging capabilities and system sensitivity", www.skatelescope.org, R.J. Nijboer, M. Pandey-Pommier, A.G. de Bruyn, July 2009.

- [41] “*Science Technology Trade-off Process*”, SPDO Released Document, WP2-005.010.030-MP-004, P. Dewdney.
- [42] “*Observing Time Performance Factors in Carrying Out SKA Trade-offs*”, SSEC4 Discussion Document, WP2-005.010.030-PR-001, P. Dewdney.
- [43] “*Development of SKA Phases 1 and 2. Discussion Paper*”, P. Dewdney, R. Schilizzi, K. Cloete, v7 dated 15 August 2010.
- [44] “*Low Frequency Antenna Options for SKA Phase 1*”, Jaap D. Bregman, ASTRON internal document, 2010-06-23.
- [45] Norris, R.P., Hopkins, A.M., Afonso, J., et al. (2011), Publications of the Astronomical Society of Australia, 28, 215
- [46] WALLABY Web Site, <http://www.atnf.csiro.au/research/WALLABY/>
- [47] Private communication, N. Razavi-Ghods, University of Cambridge, 2012.
- [48] S. Padhi, “*Antenna Standardization Report*”, Ver: 2.0, Aug. 1, 2012.
- [49] M. Pantaleev, J. Yin, M. Ivashina, J. Conway, “*Final Report of the Eleven Feed Project: Development of Broadband Cryogenic Frontend Prototype for the SKA*”, SKA Memo 144, May 2012.
- [50] G.W. Kant, P. D. Patel, “*EMBRACE: A Multi-beam 20,000-Element Radio Astronomical Phased Array Demonstrator*”, IEEE Transactions on Antennas and Propagation, Vol 59, Issue 6, Part 1, 2001.
- [51] J. M. Cordes and T. J. W. Lazio, “*NE2001.I., A New Model for the Galactic Distribution of Free Electrons and its Fluctuations*”, arXiv:astro-ph/0207156, Jan 2003.

Appendix A: Design formulae

17.1 Log-Periodic Array Design Relationships

The following relations have been used to relate the properties of array elements with those of stations and the entire array:

- Element size:
 - Log Periodic antennas: L_e is determined by the length of the longest dipole element, which in turn determines the lowest frequency.
- Element Effective Area:
 - Sparse regime: $A_{\text{eff_element}} = (\lambda^2/4\pi) (\eta D_{\text{element}})$, where λ is the wavelength, η is the radiation efficiency of the antenna element, and D_{element} is the directivity of the antenna element, which is assumed to be approximately constant over its useful range of frequencies.
 - Dense regime: $A_{\text{eff_element}} = L_e^2$
- Element Physical Area: $A_{\text{element}} = L_e^2$, where A_{element} is the physical area of an element.
- Station Diameter: $d_{\text{station}} = \lambda_{\text{FoV}} / \theta_{\text{station}}$, where d_{station} is the station diameter and θ_{station} is the specified diameter of the station beam at a frequency of f_{FoV} ($f_{\text{FoV}} = c/\lambda_{\text{FoV}}$).⁴ The factor of 1.3 was not used here so that station size is as compact as possible. This has the effect of decreasing the crowding in the centre of the array, but increasing the number of stations. The result is that the station FoVs are larger than necessary.
- Number of Elements per Station: $N_{\text{el_station}} = f_f A_{\text{station}} / A_{\text{element}}$, where $N_{\text{el_station}}$ is the number of elements per station, f_f is the antenna element aerial filling factor, and $A_{\text{station}} = \pi d_{\text{station}}^2/4$.
- Number of Stations: $N_{\text{station}} = N_{\text{el_total}} / N_{\text{el_station}}$, where $N_{\text{el_total}}$ is the total number of elements.
- Total Effective Area:
 - Sparse regime: $A_{\text{eff_total}} = N_{\text{el_total}} (\lambda^2/4\pi) (\eta D_{\text{element}})$
 - Dense regime: $A_{\text{eff_total}} = N_{\text{el_total}} L_e^2$
- Total Physical Area: $A_{\text{total}} = A_{\text{station}} N_{\text{station}}$, where A_{total} is the total physical area.

17.2 Log-Periodic Array Tradeoffs

Using the relations in Section 9.4 and the standard radio astronomy sensitivity relations (see footnotes to performance tables), one can derive the following in terms of quantities determined either by key science inputs or by the properties of the elements:

- *Dense-sparse Transition Frequency*: $f_t = \frac{c}{L_e} \sqrt{\frac{f_f \eta D_{\text{element}}}{4\pi}}$ where c is the speed of light and the other variables are defined above.

⁴ A factor of 1.3 is often used to determine a beamwidth from an aperture diameter. For a given beamsize, the calculated diameter may be smaller than actually needed. The details depend on the degree of tapering and sparseness of the outer elements in the array. A detailed design is likely to yield somewhat different station sizes.

- *Number of Stations:* Putting N_{station} into terms of given inputs,

$$N_{\text{station}} = \frac{4}{\pi} \frac{L_e^2 N_{\text{el_total}}}{f_f} \left(\frac{f_{\text{FoV}} \theta_{\text{station}}}{c} \right)^2 \text{ where all terms on the right side are given.}$$

- *Core Brightness Temperature Sensitivity:*

- In the dense regime is given by $T_{b_{\text{min}}} = \frac{4\pi 60 \lambda^{4.55}}{\eta \eta_s L_e^2 \theta_{\text{res}}^2 N_{\text{el_total}} \sqrt{2\Delta\nu\tau}}$ where η_s is the system efficiency, $\Delta\nu$ is the channel bandwidth, τ is the total integration time, and θ_{res} is the resolution of the core array.

- In the sparse regime, $T_{b_{\text{min}}} = \frac{4\pi 60 \lambda^{2.55}}{\eta \eta_s D_{\text{element}} \theta_{\text{res}}^2 N_{\text{el_total}} \sqrt{2\Delta\nu\tau}}$ where D_{element} is the directivity of the element.
- Note that in a maximally compact array, increasing the number of elements reduces the array resolution at the same time, leaving $T_{b_{\text{min}}}$ unchanged (i.e., $\theta_{\text{res}}^2 N_{\text{el_total}}$ is constant).

- *Elevation Limit:* given by the directivity of the element and the array foreshortening factor when the array is in the dense regime. If the half-power element pattern occurs at 50 degree elevation, the effective area will be further diminished by the array foreshortening factor, ~23%. (TBC – need a simple expression for polar diagram)

The following describes the origin of the quantities on the right sides of the above equations:

- *Filling factor (f_f):* Tests on log-period arrays indicate that a filling factor greater than 70% results in unacceptable changes to the station beam.
- *Element Length (L_e):* This is determined by the lowest operational frequency of the elements, nominally $\lambda/2$.
- *Station beam size (θ_{station}):* The EoR observations are very sensitive to spatial frequency artefacts that might result from stitching multiple beams to cover the field of view. A single smooth beam covering a specified field-of-view results in a specification for θ_{station} . This must be specified at a particular frequency, f_{FoV} . The values developed in [14] are 5 degrees and ~100 MHz, respectively.⁵
- *Efficiencies (η and η_s):* These are the radiation and system efficiencies, respectively. They have been estimated to be ~90% in both cases (rather optimistically). In principle they can be functions of frequency.
- *Array Resolution (θ_{res}):* Ideally this is as high as possible. However, it trades directly against brightness temperature sensitivity. For EoR observations, this has been taken as secondary to achieving sufficient brightness temperature sensitivity.
- *Channel Bandwidth ($\Delta\nu$):* This is determined by the required resolution in redshift space (~100 kHz). Higher resolution will be needed to deal with interference and potentially other effects, but for sensitivity channels can ultimately be averaged.

⁵ Smoothness in both spatial and spectral dimensions is a major design criterion for all of the SKA telescopes.

- *Total Observing Time (τ):* A nominal 1000 hours for each field observed has been used in sensitivity estimates.
- *Element Directivity ($D_{element}$):* Log periodic antenna elements can be designed for a specific directivity within limits, although it tends to be higher than dipoles. Thus it is possible to trade the number of array elements against sky coverage (ie less sky coverage implies fewer elements). Since the number of elements drives total cost, this is an important trade.
- *Total Number of Elements (N_{el_total}):* This is both a major determinant of sensitivity and system cost.

Examining the above relations reveals that there is not much trade space available if the science goals are to be met. The minimum cost array compatible with EoR-observation derived requirements is the most compact array possible, combined into beams that “illuminate” sufficiently large fields to meet the lowest required spatial frequencies. Directivity is maximized so as to be able to reach the declinations of the candidate observing fields. The number of elements is increased to reach the required brightness sensitivity. Note that high element directivity is superior to increased tracking time (sky coverage) per day, since increased tracking time improves sensitivity per day by a square root factor.

Note that the power of λ is 4.55 in the dense regime, but only 2.55 in the sparse regime. This means that it is important to decrease the filling factor (lower f_t) as much as possible; however, for a given total number of elements, the number of stations must rise, leading to a more expensive correlator system.

17.2.1 PAF parameters

The methods used in this document to calculate the PAF performance are approximate. This is necessary because there are many options available for PAF beamforming and assembly of the beams on the sky. Given the PAF physical diameter, d_{PAF} , the upper frequency/wavelength in the band, λ_{min} , the beam deviation factor for the dish optics in FWHM/wavelength, f_{bd} , and the dish diameter D_{dish} , the number of elements, beams, and FoV can be estimated. Elements are separated

by $\lambda_{min}/2$, so the PAF diameter in elements is $2d_{PAF}/\lambda_{min}$, and $N_{el} = \text{floor}\left[\frac{\pi}{4}\left(\frac{2d_{PAF}}{\lambda_{min}}\right)^2\right]$, where N_{el}

is the number of elements. The diameter in beams is

$$\left[\frac{d_{beam}}{beams}\right] = \left[\frac{d_\lambda}{wavelengths}\right]\left[\frac{f_{bd}}{beams / wavelength}\right], \text{ and the maximum number of beams is}$$

$$N_{beam} = \text{floor}\left[\frac{\pi}{4}d_{beam}^2\right]. \text{ The number of beams will decrease in proportion to frequency. The}$$

beam area of single beam at highest frequency is $\Omega_{beam,\lambda min} = \frac{\pi}{4}\left(\frac{66\lambda_{min}}{D_{dish}}\right)^2 \text{ deg}^2$. Thus the field-of-

view of the PAF on dish is $FoV_{PAF} = N_{beam}\Omega_{beam,\lambda min} \text{ deg}^2$, independent of frequency in the band.

The FoV_{PAF} is approximate, depending on how many beams are actually formed and their pattern on the sky. They are assumed to be at half-beam spacings. Thus the signal-to-noise across the entire

pattern will be lower at the crossing points because overlapped noise adds in quadrature. At the crossing points it will be $\sqrt{2}$ higher than on beam centres. A smoother signal-to-noise pattern would be obtained by observing for half the time with the beam peaks on the previous beam centres.

Appendix B: CSP Equipment Size and Power Dissipation

In this appendix, we provide rudimentary estimates for equipment rack space and thermal dissipation for the CSP equipment located in the CSP facilities at both sites. This is to facilitate initial and approximate indication on compatibility with existing infrastructure.

Several candidate technology options are open for the processing implementation at SKA1 including architectures based on the following technologies:

- ASIC
- FPGA
- GPU
- MIC
- Hybrid

The suitability of each technology type will be ascertained by subsequent cost-benefit trade off analysis that is beyond the scope or needs of this section. Consequently, a couple of example technologies have been utilised in providing the estimates below. The choice is arbitrary and is not intended to reflect in any way the preference on the technical solution.

Although estimates are sized and described separately, they could potentially co-exist on the same processing platform. Alternatively, specific technology can be directed to specific areas where its characteristics are at best advantage in terms of power consumption, equipment space or flexibility in programming.

Table 21 SKA1-low Central Beamformer Equipment Estimates

| FPGA | | |
|--|--------------------|---|
| Number of hardware multipliers 2016 | | |
| Top end device | ~15,000 | |
| Mid range device | ~7,500 | |
| Clock rate | ~350 MHz | |
| Processing capability | 2.6 T mult/s | |
| FPGA Dissipation (estimated) | 60W | |
| FPGAs per board | 4 | Assume board dissipation ~ 360 W Allowing 50% power for other components |
| Assumed processing efficiency | 80% | |
| Typical processing capability per board | 8.3 T multiplies/s | |
| Number boards per 1 U rack space | 0.5 to 2 | Assume 2U |
| Available space per rack | 40 U | Assumes 48U rack with 6U for switches/ breaker units etc. |
| Cabinet footprint | 1000 x 650mm | Estimate TBC |
| Rack Dissipation maximum | 20kW | Assumed |
| Processing per rack | ~ 330 T Multiplies | ~ 7.2 kW per rack* |
| Correlator SKA1-Low Log Periodic Option | | |
| Channeliser processing load** | 60 T Mult/s | |
| Correlator load | 1660 T mult/s | Total channeliser + correlator = 1720 T mult/s |

| | | |
|---|--------|--------|
| Number of cabinets | ~ 10.8 | 80 kW* |
| *Excluding PSU efficiency and Cooling | | |
| ** (Ntaps + 3 log ₂ (Nchan)) x BW x 2ny x Nstat * Npol x Nbms ; Ntaps ~12 cf ASKAP | | |

Table 22 SKA1-mid Correlator Projected Equipment Estimates

| FPGA | Capability given in SKA-1 Low CSP table | |
|-----------------------------------|---|--|
| Processing per rack | ~ 160 T Multiplies | ~ 7.2 kW per rack* |
| Channeliser processing load** | 250 + 34 T Mult/s | SKA1-Mid + MeerKat = 284 T mult/s |
| Combined correlator SKA1-Mid load | 2003 T Mult/s | Total channeliser + correlator = 2287 T mult/s |
| Number of cabinets | ~ 14.3 | 100 kW* |

*Excluding PSU efficiency and Cooling

** (Ntaps + 3 log₂(Nchan)) x BW x 2ny x Ndish * Npol x Nbms ; Ntaps ~12 cf ASKAP

Table 23 SKA1-mid Central Beamformer Equipment Estimates

| FPGA | Capability given in SKA-1 Low CSP table | |
|--------------------------------|---|---------------------|
| Processing capability per rack | ~ 160 T Multiplies | ~ 7.2 kW per rack** |
| SKA Central Beamformer load | 50 T Mult/s | |
| Number of cabinets | ~ 0.3 | 2 kW** |

* Based on information in SKA Memo 136 section 6.

**Excluding PSU efficiency and Cooling

Table 24 SKA1-Mid Non-Imaging Survey Equipment Estimates

| GPU | | |
|--|-------------------|--------------------------------|
| Projection to 2016***** | | |
| Peak processing (Single Precision) | ~10 T Flops | |
| Assumed processing efficiency | 10% | Conservative estimate |
| GPU processing | 1 T Flops | |
| PCIe v 3 | ~10 Gby/s | |
| GPU Dissipation (estimated) | 250W | |
| GPUs hosted per server | 2 | |
| Hosting server | | |
| No processors per hosting Server | 2 | multi-core x86 (~ 8 cores) |
| Rack size | 2U | |
| No supported GPU cards | 2 | |
| Estimated dissipation per server + 2GPUs | 750W | |
| Rack power limitation | ~ 20 kW | Assumed |
| Number of servers per rack | ~20 | |
| Communication fabric | | |
| Switch aggregate bandwidth | ~75 T b/s | Non blocking |
| No. ports | 648 | 56 Gbps ports |
| Switch size | 29U | |
| Switch Dissipation | 10kW | |
| Cabinet footprint | 1000 x 650mm | Estimate TBC |
| Processing per rack | ~ 40 T Multiplies | ~ 20 kW per rack** |
| Beamformer | | |
| Beamformer load 835 beams* | 254 T Ops/s | Greater than 5° of GP |
| Beamformer O/P rate 835 beams ** | 4 T bits/s | |
| Beamformer load 2222 beams* | 680 T Ops/s | Less than 5° of GP |
| Beamformer O/P rate 2222 beams ** | 11Tbits/s | |
| Dedispersion | | |
| Max Number of Dispersion Measures | ~16113 | See Pulsar search region table |

| | | |
|---|---------------|---------------------------------------|
| Dedispersion load** | 4 T Ops/s | Optimized dedispersion |
| Dedispersion O/P rate | 2 T bits/s | 4 bit assumed |
| Binary Search | | |
| Number trial accelerations | 120 | For +/- 100 m s ⁻² |
| Binary search load*** | ~ 9.6 P Ops/s | |
| Binary search O/P rate | 130 T bits/s | 4 bit assumed |
| Pre-Whitening & Normalisation**** | | |
| Peak load | TBD Tops/s | |
| Average O/P rate | 130 T bits/s | |
| Harmonic sum | | |
| Number of harmonics | 8 | |
| Processing load**** | TBD T Ops/s | |
| Average O/P rate | 16 T bits/s | |
| Threshold Detection | | |
| S/N ratio | 7 | |
| Detections | TBD | |
| Processing load | 25 T Ops/s | TBC |
| Average O/P rate | TBD | Depends on S/N and RFI |
| Candidate Detection | | |
| Normal Pulsars | 9800 | TBC |
| MSPs | 1240 | TBC |
| Processing load TBD | TBD | |
| SKA survey processing load peak | ~10 P Mult/s | Based on acceleration processing load |
| Number of processing cabinets (peak option) | ~ 250 | ~5 MW** |

*Nbms * Ndish * B * 2ny *2pol

** (Nbms* Ndm *log₂(Ndm)*1/tsamp optimised (Taylor tree piecewise linear in ~ 64 sub-bands.(max Nbms* Ndm * Nchan)*1/tsamp

***Ndm*Nbms*Nacc*Nsamp*log₂(Nsamp)*1/tobs

**** running mean and rms across blocks of frequency cells subtracted from each cell

*****Nbms*Nbms*Nacc * 1/t_{obs} * log₂(nh) * N_{samp}

*****Ndm*Nbms*Nacc * 1/t_{obs} * N_{samp}

*****Based on road map from Nvidia & Real-time, fast radio transient searches with GPU de-dispersion paper

*****Excluding PSU efficiency and Cooling

Table 25 SKA1 Pulsar Timing Parameters

| | | |
|------------------------------------|--------------|------------------------------------|
| Timing Beamformer | | |
| Number of simultaneous beams | 10 | |
| Beamformer load | ~5 T ops/s | |
| Beamformer O/P rate | 225 T bits/s | Assuming 8 bit beam data |
| Coherent Dedispersion | | |
| Dmmax | 3000 | |
| Number of simultaneous beams | 10 | |
| Time resolution | 100ns | |
| Band 2 t _{dm} *** | 8.9s | For band 2 0.95 to 1.67 GHz |
| Nsamp | 89,494,598 | Band 2 |
| FFT size | 134,217,728 | |
| Band 3 t _{dm} *** | 2.78 s | For band 3 1.65 to 3 GHz |
| Nsamp | 27,800,000 | Band 2 |
| Band 3 FFT size | 33,554,432 | Rate = 1 per 3.4 seconds |
| FFT overlap | 50% | Band 3 |
| FFT ops/s 10 beams **** | 20 G Flops/s | Band 2 |
| FFT ops/s 10 beams **** | 25 G Flops/s | Band 3 |
| Dedispersion multiplication | negligible | Band 2 & 3 |
| IFFT ops/s 10 beams **** | 20 G Flops/s | Band 2 |
| IFFT ops/s 10 beams **** | 25 G Flops/s | Band 3 |
| Total simultaneous processing load | ~ 50 G Flops | Assumes folding load is negligible |
| No Servers | 1 | |
| No. Cabinets | 0.2 | |
| Dissipation | 1.5kW | |

*doesn't take into account pulse jitter noise

**derived from radiometer equation with correction using spectral index assumption S_v proportional to v^α with $\alpha = -1.41$

****tdm= $8.3 \times 10^6 \times \text{DM} \times \Delta f \times f^3$ in ms (with frequencies in MHz)

**** FFT ops/s = Nbms x 5 x Nsamp x $\log_2(\text{Nsamp})$ x overlap x FFT rate

Table 26 SKA1-survey Central Beamformer Equipment Estimates

| FPGA | | Capability given in SKA-1 Low CSP table |
|--------------------------------|--------------------|--|
| Processing capability per rack | ~ 160 T Multiplies | ~ 7.2 kW per rack** |
| Channeliser processing load*** | 440 T Mult/s | 96 dishes, 35 beams |
| SKA-Survey load | 1313 T Mult/s | Total channeliser + correlator = 1753 T mult/s |
| Number of cabinets | ~ 11 | 80 kW** |

* Based on information in SKA Memo 136 section 6.

**Excluding PSU efficiency and Cooling

*** (Ntaps + 3 $\log_2(\text{Nchan})$) x BW x 2ny x Ndish * Npol x Nbms ; Ntaps ~12 cf ASKAP